(12)

RD&E

CENTER

Technical Report

No. 13131

AGGLOMERATING SELF-CLEANING AIR CLEANER

CONTRACT NO. DAAE07-83-C-RO24

OCTOBER 1985

By Martin B. Treuhaft
Department of Engine and Vehicle Research
Southwest Research Institute
6220 Culebra Road
San Antonio, TX 78284

U.S. ARMY TANK-AUTOMOTIVE COMMAND
RESEARCH, DEVELOPMENT & ENGINEERING CENTER
Warren, Michigan 48397-5000

NOTICES

This report is not to be construed as an official Department of the Army position.

Mention of any trade names or manufacturers in this report shall not be construed as an official indorsement or approval of such products or companies by the U.S. Government.

Destroy this report when it is no longer needed. Do not return it to the originator.

UNCLASSIFIED
SECURITY CLASSIFICATION OF THIS PAGE

AD-A167 629

REPORT DOCUMENTATION PAGE

1a. REPORT SECURITY CLASSIFICATION Unclassified	1b. RESTRICTIVE MARKINGS
2a. SECURITY CLASSIFICATION AUTHORITY	3. DISTRIBUTION / AVAILABILITY OF REPORT Approved for public release; Distribution Unlimited
2b. DECLASSIFICATION / DOWNGRADING SCHEDULE	
4. PERFORMING ORGANIZATION REPORT NUMBER(S) 03-7442	5. MONITORING ORGANIZATION REPORT NUMBER(S) TACOM T.R: 13131
6a. NAME OF PERFORMING ORGANIZATION Southwest Research Institute 6b. OFFICE SYMBOL (If applicable)	7a. NAME OF MONITORING ORGANIZATION
6c. ADDRESS (City, State, and ZIP Code) 6220 Culebra San Antonio, Texas 78284	7b. ADDRESS (City, State, and ZIP Code)
8a. NAME OF FUNDING / SPONSORING ORGANIZATION U.S. Army Tank-Automotive Command 8b. OFFICE SYMBOL (If applicable) AMSTA-RTG	9. PROCUREMENT INSTRUMENT IDENTIFICATION NUMBER
8c. ADDRESS (City, State, and ZIP Code) Warren, Michigan 48397-5000	10. SOURCE OF FUNDING NUMBERS PROGRAM ELEMENT NO. / PROJECT NO. / TASK NO. / WORK UNIT ACCESSION NO.

11. TITLE (Include Security Classification)
Agglomerating Self-Cleaning Air Cleaner

12. PERSONAL AUTHOR(S)
Martin B. Treuhaft

13a. TYPE OF REPORT	13b. TIME COVERED	14. DATE OF REPORT (Year, Month, Day)	15. PAGE COUNT
Final	FROM _____ TO _____	1985, October	

16. SUPPLEMENTARY NOTATION

17. COSATI CODES			18. SUBJECT TERMS (Continue on reverse if necessary and identify by block number)
FIELD	GROUP	SUB-GROUP	

19. ABSTRACT (Continue on reverse if necessary and identify by block number)

This report describes an experimental program to evaluate an agglomerating self-cleaning air cleaner concept for application to diesel-powered tactical trucks and combat vehicles. Technical feasibility was evaluated through laboratory testing of candidate agglomerating media and through a design parameter component study of the agglomerator, inertial separator, and final filter integration and system operation. Several factors were used to evaluate media potential; namely, initial resistance as a function of airflow, dust loading and pressure drop recovery; the improvement in inertial separator efficiency (an indirect measure of agglomerate transport); overall operating efficiency; and consideration of the physical characteristics of the media with respect to their likely influence on design. Both surface loading and depth-type media were considered, and successful results were obtained with each. Overall, results clearly show that the agglomerating self-cleaning air cleaner concept can provide a significant improvement over standard systems with respect to service life. As a result, an air cleaner system based on this concept would fill the void

20. DISTRIBUTION / AVAILABILITY OF ABSTRACT	21. ABSTRACT SECURITY CLASSIFICATION	
☒ UNCLASSIFIED/UNLIMITED ☐ SAME AS RPT. ☐ DTIC USERS	Unclassified	
22a. NAME OF RESPONSIBLE INDIVIDUAL Gus Khalil	22b. TELEPHONE (Include Area Code) 313/574-5189	22c. OFFICE SYMBOL AMSTA-RTG

DD FORM 1473, 84 MAR — 83 APR edition may be used until exhausted. All other editions are obsolete.

SECURITY CLASSIFICATION OF THIS PAGE
UNCLASSIFIED

19. between larger self-cleaning air filter (SCAF) units and the smaller cylindrical units currently used on many tactical trucks and small combat vehicles. This will allow the smaller vehicles, which cannot readily accept extended-life units, to function satisfactorily in a combat mission role.

PREFACE

The author wishes to thank Tim Duncan, Daryl Schuchart and Maurice York for their contributions during testing and Terry Edwards for her help in preparing this report.

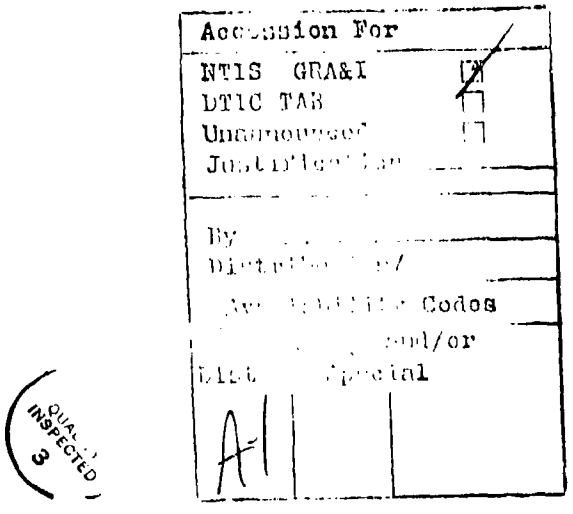

THIS PAGE LEFT BLANK INTENTIONALLY

TABLE OF CONTENTS

TABLE OF CONTENTS (Continued)

LIST OF ILLUSTRATIONS

LIST OF ILLUSTRATIONS (Continued)

LIST OF ILLUSTRATIONS (Continued)

LIST OF ILLUSTRATIONS (Continued)

LIST OF TABLES

THIS PAGE LEFT BLANK INTENTIONALLY

1.0. INTRODUCTION

This final report, prepared by Southwest Research Institute (SwRI), for the U.S. Army Tank-Automotive Command (TACOM) under Contract DAA07-83-R024, describes an experimental program to evaluate an agglomerating self-cleaning air cleaner concept for application to diesel-powered tactical trucks and combat vehicles. Technical feasibility was evaluated through laboratory testing of candidate agglomerating media and through a design parameter component study of the agglomerator, inertial separator, and final filter integration and system operation. Several factors were used to evaluate media potential; namely, initial resistance as a function of airflow, dust loading and pressure drop recovery, the improvement in inertial separator efficiency (an indirect measure of agglomerate transport), overall operating efficiency, and, to some extent, consideration of the physical characteristics of the media with respect to their likely influence on design. Both surface loading and depth-type media were considered, and successful results were obtained with each. Overall, results clearly show that the agglomerating self-cleaning air cleaner concept can provide a significant improvement over standard systems with respect to service life. As a result, an air cleaner system based on this concept could fill the void between larger self-cleaning air filter (SCAF) units and the smaller cylindrical units currently used on many tactical trucks and small combat vehicles. This will allow the smaller vehicles, which cannot readily accept extended-life units, to function satisfactorily in a combat mission role.

2.0. OBJECTIVES

The primary objectives of this program were to study, analyze, and conduct laboratory tests to determine the feasibility and applicability of the agglomerating self-cleaning air cleaner concept to diesel-powered tactical trucks and combat vehicles.

3.0. CONCLUSIONS

3.1. Agglomerating Self-Cleaning Air Cleaner Feasibility

The agglomerating self-cleaning air cleaner concept is technically feasible, and when fully developed, should be applicable to several classes of military vehicles.

3.2. Service Life

The agglomerating self-cleaning air cleaner can provide a significant improvement in air filter capacity for Army vehicles operating in highly dusty environments. Overall, dust capacities in excess of five to ten times those for standard systems seem probable.

3.3. Agglomerator Type

Both surface loading and depth-type media show potential as agglomerating materials. While surface loading media require reverse airflow for regeneration and agglomerate release, most depth-type media (meshes, foams, or packed beds) allow

straight-through operation, which greatly simplifies design and component integration requirements.

3.4. Precleaner Operation

The performance of conventional inertial separators is greatly improved by dust agglomeration. The degree of improvement depends on the extent to which the particle size distribution is shifted above the cut point.

3.5. Impact of Precleaner on Overall Service Life

Overall service life is very sensitive to precleaner efficiency provided the pressure drop penalty for incorporating the precleaner is not severe. Dust loading for the final filter with respect to the new particle size distribution exiting the precleaner must be considered and some redesign is likely for system optimization.

3.6. Cost Considerations

The straight-through agglomerator design should offer cost advantages over a surface loading-reverse flow design.

3.7. Vehicle Integration

The straight-through design concept should be easier to package and install because its design requirements and method of operation are simpler than those of a surface loading-reverse flow type agglomerator. Control system technology should also be less complex for the straight-through unit. At this point however, both concepts should be considered for further development, at least until sufficient data are available to demonstrate a clear superiority.

3.8. Reliability

Because it is less complex and will have fewer working parts, the straight-through agglomerator should prove more reliable than a reverse flow unit.

4.0. RECOMMENDATIONS

4.1. Development and Testing

Further development and testing should be conducted to define performance over longer term operation. This effort should be directed toward development of half- and full-scale units for evaluation and demonstration. Both surface loading and depth-type agglomerators should be pursued.

4.2. Prototype Design Verification

Once the laboratory prototype (either half- or full-scale) has been developed and tested, some degree of optimization should be accomplished, followed by engineering evaluation tests for design verification.

4.3. Control System Development

Concepts and designs for an actuating mechanism for agglomerator regeneration (for surface loading units) should be pursued and a pressure drop control activation circuit should be developed and evaluated.

4.4. Vehicle Integration

A full-scale Agglomerator Air Cleaner System (AACS) for a particular family of vehicles should be designed, fabricated, and tested to demonstrate AACS capability.

5.0. DISCUSSION

5.1. Introduction

An agglomerating self-cleaning air cleaner system can provide a significant improvement in air filter capacity for Army vehicles operating in highly dusty environments. This system would be especially useful for smaller vehicles which cannot readily accept larger self-cleaning air filter (SCAF) systems. As such, it could help fill the void between larger SCAF units and the smaller cylindrical units currently used on many tactical trucks and smaller combat vehicles, thereby enabling these vehicles to keep up with combat vehicles equipped with extended life systems. For example, the service life of a SCAF system on the M60 and M1 is 200 hours. This can be compared to the static system which has a 20-hour nominal life, or perhaps an 80-hour life when an extended life element is used. The service life of air cleaners on smaller vehicles, which cannot accept regular SCAF units because of packaging restraints, is near the lower end of this range. Therefore, a major goal of this program was to consider a system that would provide a service life of at least five times that of the present static system when operating in zero visibility dust. For a full-scale system, this requirement meant a minimum service life of approximately 100 hours.

The agglomerating self-cleaning air cleaner concept is illustrated in Figure 5-1. Here, dusty air enters the agglomerator where particles are temporarily collected and agglomerated, that is, they are physically brought together to form larger particle masses. At some predetermined level of agglomerator loading (pressure drop), the agglomerates are made to release into an optimized second-stage inertial separator, where they are removed from the airstream. Because the inertial separator now operates on particles having a distribution that is much larger than that of the original dust stream, its overall efficiency is significantly improved. This greatly reduces the dust burden on the final filter. Furthermore, when the agglomerates are periodically removed from the agglomerating media, its pressure drop approaches the initial level so that, to a large extent, the system is self-cleaning.

This concept was initially studied by SwRI in the early 1970's.[1] The major effort was directed toward investigating methods for increasing the size and mass of the average dust particle prior to its entry into the initial separator. Purposely, the approach bypassed the intricacies involved in improving the separator itself, and instead concentrated on improving overall separation efficiency strictly by altering

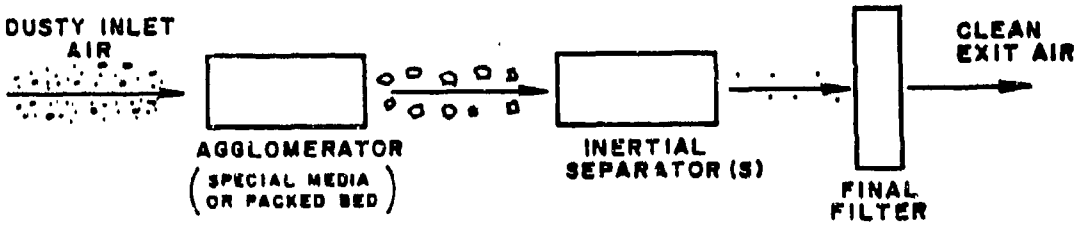

Figure 5-1. Illustration of Agglomerating Self-Cleaning Air Cleaner Concept

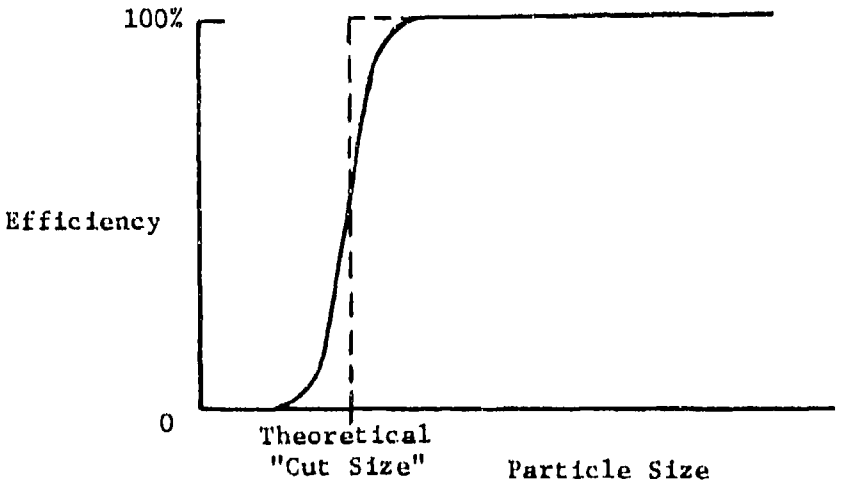

Figure 5-2. Typical Performance Curve for an Inertial Separator as a Function of Particle Size

the particle size distribution of the incoming dust. (As shown in Figure 5-2, the separation efficiency of an inertial separator increases rapidly as particle size approaches and exceeds a critical value, often termed the "cut size"). This approach was taken because over the years many investigators have tried to improve inertial separator performance, generally by making changes in some way or another to the unit's geometry in an attempt to lower its "cut size". As a result, design norms have been established so that further design changes only tend to produce marginal improvements at best.

Results from the earlier program, which used surface loading media, showed that particles could be removed from the air stream and readily agglomerated by developing a filter cake on the surface of an upstream barrier media, as illustrated in Figure 5-3. The massing together of smaller particles to form agglomerates resulted from particle proximity in the filter cake and from surface forces associated with the dust particles themselves. Once a sufficient quantity of dust was collected to cause a predetermined pressure drop across the media, a reverse flow technique was used to suddenly release the dust in large agglomerate masses into a conventional inertial separator. Significant improvements in separator efficiency verified the agglomeration principle and demonstrated the availability of suitable surface collection media. In several cases, separator efficiency was increased from 80 percent to 96 percent on fine test dust. Furthermore, the surface collector proved to be self-cleaning to a high degree indicating that a reliable and long-life system should be feasible. And, since the agglomeration concept is applicable to all classes of inertial separators whose efficiency primarily depends on particle size, considerable flexibility should exist in tailoring components to meet specific installation and operating requirements.

Results of a life test on one sample media are shown in Figure 5-4. In this test the media operated for over 70 hours, at which time testing was terminated not because collector life was expended, but because program priorities precluded further testing of that particular media. During the test, 7,600 grains of dust were fed and 74 cleaning cycles were performed. The pressure drop after cleaning ranged from 0.15 to 0.30 inches of water and was 0.2 inches after the final cleaning cycle. Overall efficiency for the agglomerator and inertial separator was 91.8 percent, giving an average improvement of 16.2 percent over the inertial separator alone.* Absolute efficiency for the combined system increased 12.8 percentage points. Furthermore, these values were quite conservative. This was because the test airflow was only 39.4 percent of the rated separator airflow, thus its efficiency during the cleaning cycle was lower than normal and would be expected to improve when operating at rated airflow. Operation on coarse dust should provide even higher overall efficiency values.

These data can be used to illustrate possible performance characteristics for potential agglomerating air cleaner configurations. For example, for a high efficiency system, the agglomerator/separator could be used as a precleaner followed by a final filter, as previously illustrated in Figure 5-1. In this configuration, overall system efficiency will improve, but life will now depend on the life of the final filter. Of course the final filter will see a much lower dust load than that entering the agglomerator unit or that which would be encountered if only

*Percent improvement = $\frac{12.8}{(91.8 - 12.8)} \times 100$

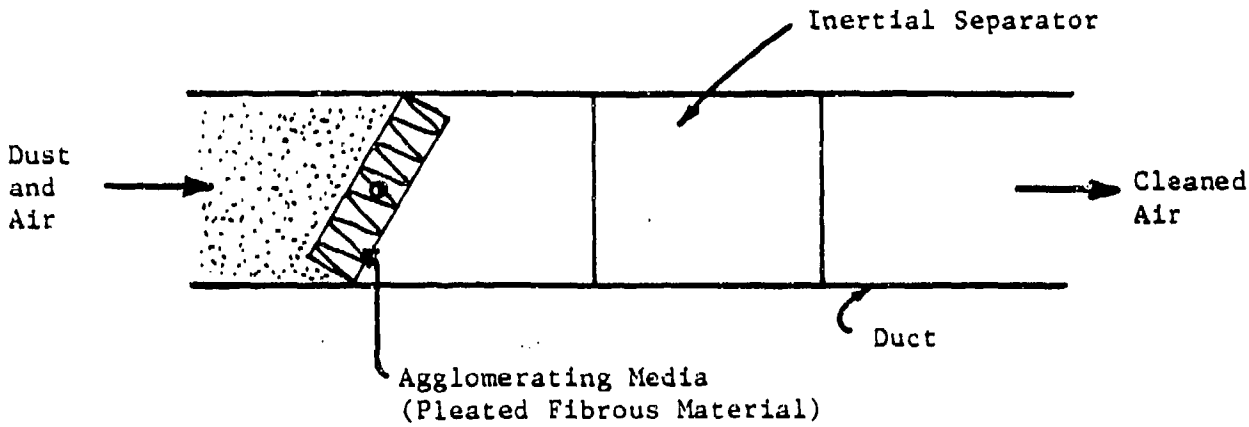

a) Dust collecting and agglomerating on fibrous media

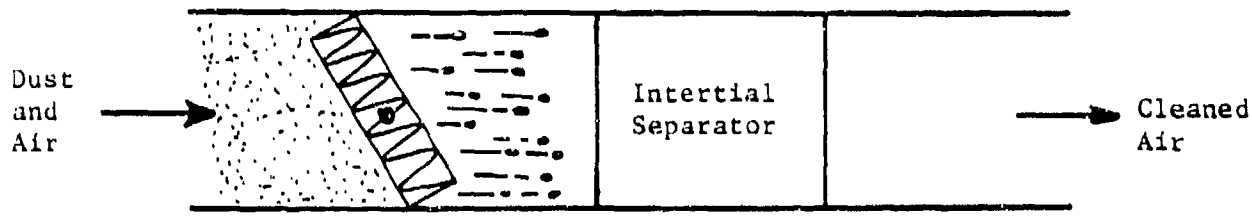

b) Fibrous media quickly reversed, releasing agglomerated dust into inertial separator

Figure 5-3. Illustration of Agglomerator Test Stand

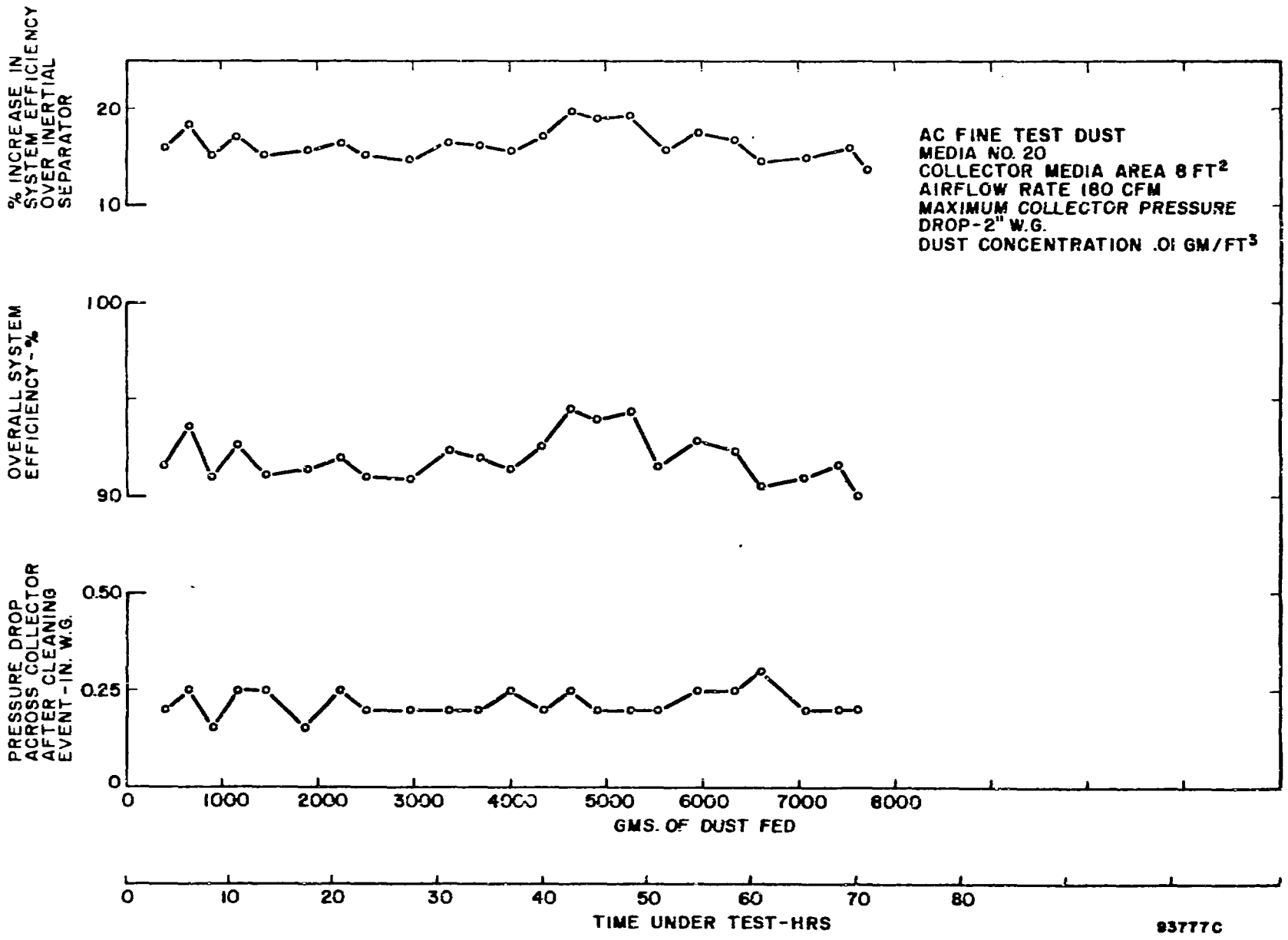

Figure 5-4. Results of Life Test from Earlier Program

a precleaner were used. For the test shown in Figure 5-4, about 92 percent of the dust was removed upstream of the final filter, compared to 80 percent for the conventional system (on fine dust) using only the inertial separator. Comparing these penetrations shows that the life of existing filter systems could theoretically be increased 2-1/2 times by incorporating an agglomerator unit. This is conservative because efficiency values on the order of 96 percent were typically obtained prior to this particular life test. For this range, the factor of improvement becomes 5:1 and with coarse dust, should increase further.

Additional improvements may be likely when higher restriction levels between cleanings are allowed, since this will prolong the dust loading interval. In the earlier program, the maximum pressure drop contribution of the agglomerator was limited to two inches of water because the intended use was for a gas turbine engine. In the current program, allowable restriction could be several times this value, depending on overall component and system design.

When all of the data from the earlier program were considered, it was clear that a method existed to significantly improve the performance of conventional inertial separators by dust agglomeration. The price required for this improvement would be the added pressure drop for the agglomerating collector, the requirement to sense and monitor collector pressure drop, and the mechanical means needed to dislodge the agglomerates once a predetermined pressure drop was reached. These requirements did not reduce the usefulness of the concept.

5.2. Current Program - Agglomerator Concepts

Although several surface loading media were identified in the earlier program as being good candidates for an agglomerating air cleaner system, it was likely that other media had since become available that could offer improved performance and cost advantages. In addition, the requirements had changed, providing for a wider range of operation with more likelihood of success. Also, experience had been gained with another agglomeration concept that showed significant potential for this application; namely, agglomeration in packed beds or depth-type media. As a result, the current program was designed to investigate the surface and depth loading concepts and to update the state-of-the-art with respect to available and appropriate agglomerating media.

Basically, the agglomerating media in either concept must exhibit three qualities. It must capture and retain dust with reasonable efficiency so that particle agglomeration can take place with minimal non-agglomerate penetration. Next, it must be regenerable, capable of operating over many cycles without detrimental restriction and without frequent cleaning. Finally, it must develop sufficient agglomerates to improve precleaner efficiency so as to provide a significant increase in overall system life.

Theoretical operation of the surface loading agglomerator has already been discussed. Dust particles are collected and agglomerated on a rather high efficiency, first-stage barrier, and then dumped into to a second-stage inertial separator during regeneration. Since the inertial separator now sees particles which are aerodynamically larger than those in the original dust stream, overall precleaner efficiency is improved, lowering the relative dust burden of the final filter, if used. This

concept, identified as a Type I agglomerator, is illustrated in Figure 5-5. Potential component integration is shown in Figure 5-6.

Along with the general properties of efficiency and initial restriction, the loading characteristics of the agglomerating media are significant because they directly affect its useful life, and as such, the cleaning cycle frequency of the system. Ideally, the agglomerating media should build a filter cake over a rather long period of time, with only a moderate rate of restriction increase. Then, during regeneration the media should approach its initial state so that the loading cycle can be repeated. For most conventional filter media, however, loading is an irreversible process in that once loading has reached a certain point, the media must be discarded and replaced. For these media, cleaning is ineffective, primarily because initial restriction cannot be satisfactorily restored. Naturally, these media are not appropriate for use as agglomerators.

For a given media, loading as a function of time is influenced by a large number of parameters, for instance, the size, concentration, and nature of the incoming dust particles, the operating face velocity, and the type and rate of cake build-up, to name a few. Media loading as evidenced by the backpressure history of the agglomerator will dictate when cleaning must be accomplished in order to maintain satisfactory engine operation. This will establish the normal operating cycle or cleaning frequency requirement for the system, which in turn will affect system size and method of operation.

Two other factors dealing with loading must also be considered, namely, the effects of loading on collection efficiency and the impact loading may have on particle reentrainment during backflushing. In the first case, it is likely that loading will increase the collection efficiency so that ultimately smaller and smaller particles will be removed during the loading cycle. It is clear that single fiber collection efficiencies will change as will effective porosity and fiber diameter. Of these, the change in effective porosity should be most significant, with the decrease in porosity providing an overall increase in collection efficiency.

The impact of loading on reentrainment is more complex. In almost all automotive applications, direct reentrainment is undesirable because it increases particle penetration, thereby reducing overall system efficiency. As a result, most automotive-type media are designed to minimize direct reentrainment.* In the agglomerating self-cleaning air cleaner concept, however, effective reentrainment is essential. During regeneration, particles must be reentrained from the agglomerating barrier to restore system restriction. The success of this operation depends on the extent that separation forces can be generated in excess of particle adhesion forces within the media. In addition to any direct mechanical forces that might be involved, movement of the gas stream in the immediate vicinity of the collected particles is a significant factor. In most cases, to gain initial movement, a particle must receive energy from an external source; for instance, form the impact of

* There are many filtration processes where reentrainment is required; for instance, bag houses for powerplants or filters for product recovery. Although these media typically have properties that are different from typical automotive type media, several have been evaluated in this program, many with encouraging results.

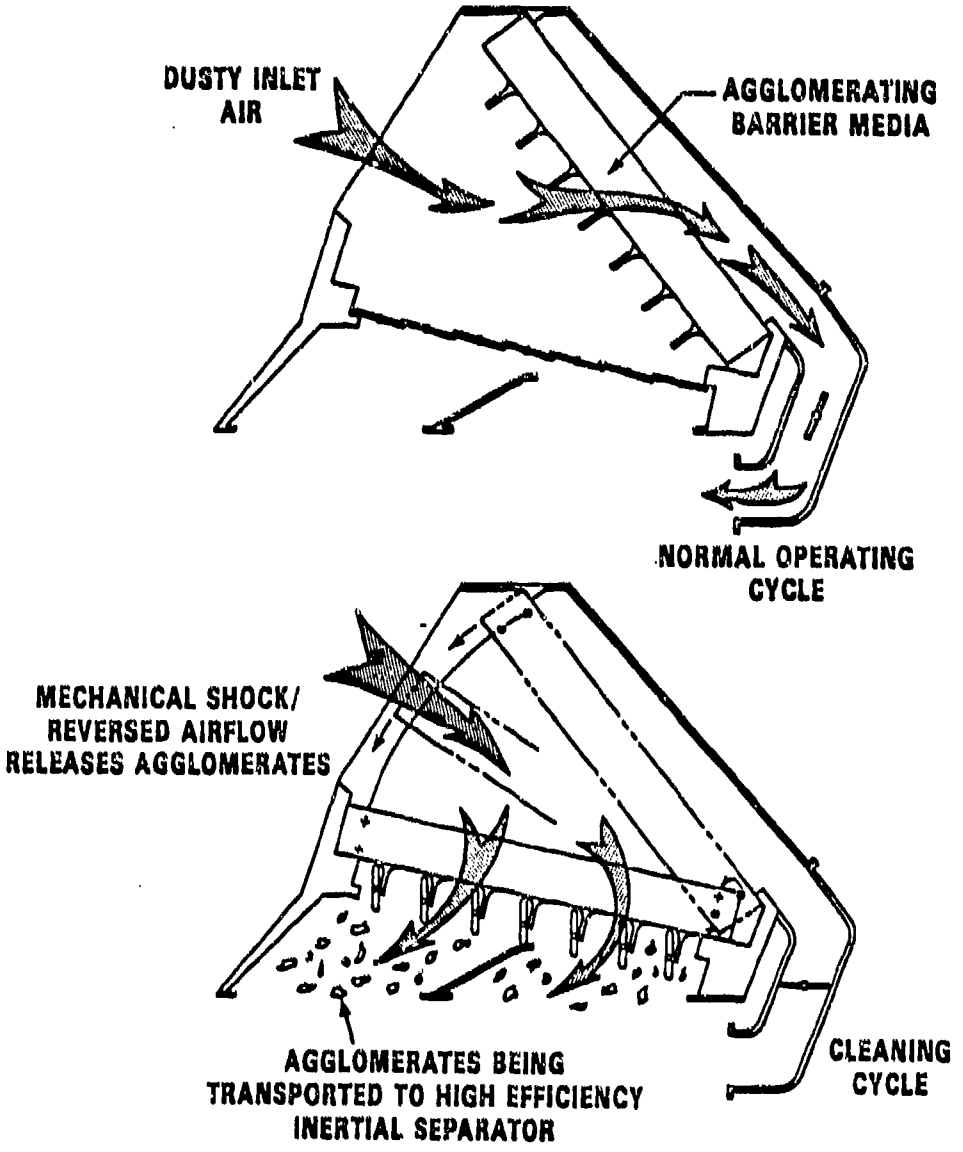

Figure 5-5. Illustration of Type I Self-Cleaning Agglomerator Concept

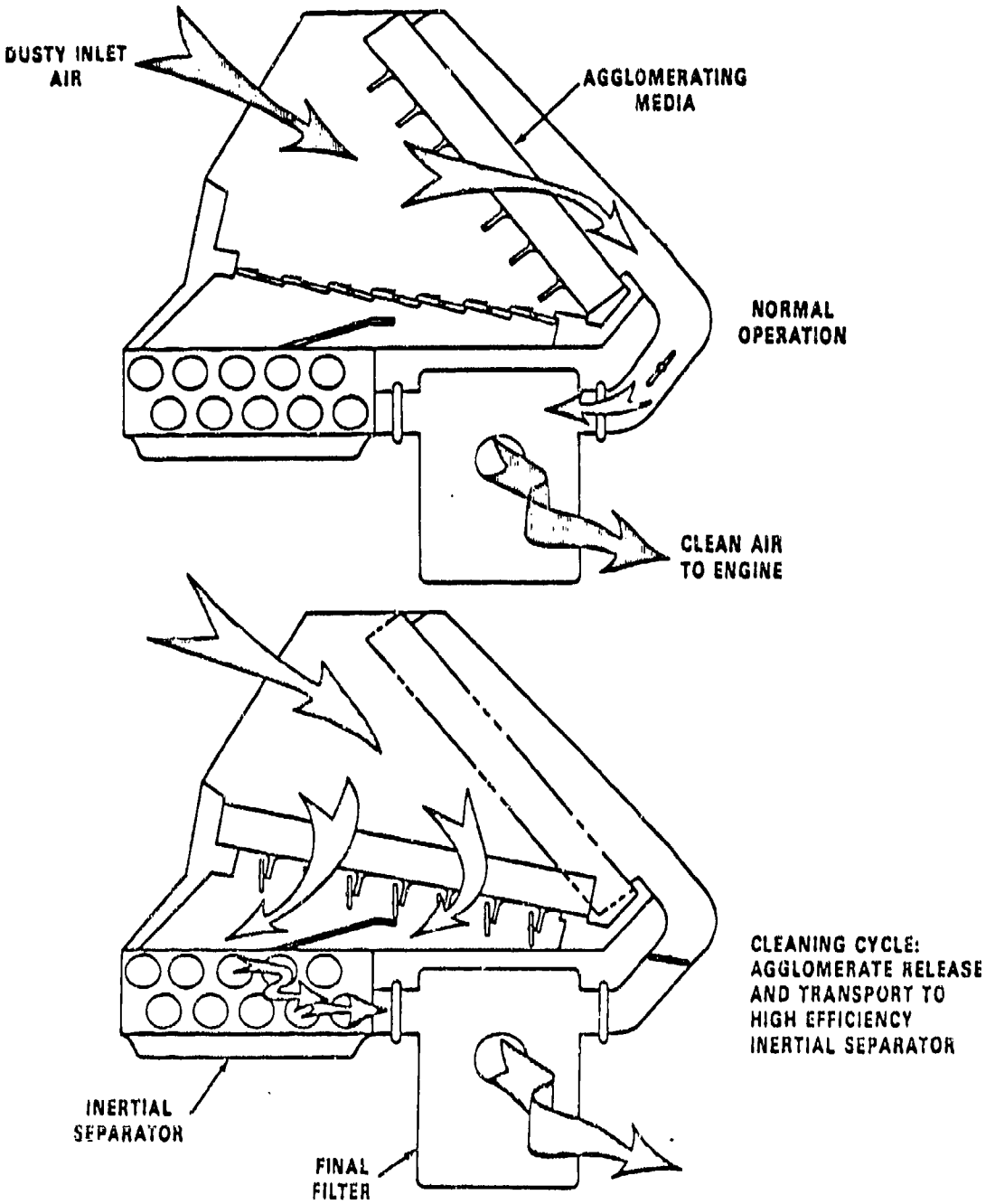

Figure 5-6. Potential Component Integration for Type I Agglomerator

another particle or object or from the drag forces of the moving gas stream about the exposed profile of the particle. While other supplementary factors may cause initial particle movement, these are the major forces so far as potential reentrainment is concerned. Schematically, the force relationship for initial movement of a particle resting on a surface can be illustrated in Figure 5-7. From this schematic, the theoretical forces accounting for the combined effects of friction and cohesion can be given as:

$$F = W \tan\phi + K_c A_c \tag{1}$$

where:
- W = Weight of particle
- ϕ = Angle of friction
- K_c = Coefficient of cohesion
- A_c = Contact area.

The external force acting on a particle at rest, or airborne, by a moving airstream can be given by aerodynamic drag considerations. In classical aerodynamic theory, the drag force acting on a surface A is given by:

$$F_D = C_D\, q\, A \tag{2}$$

where:
- C_D = Drag coefficient
- q = Dynamic pressure, $1/2\rho v^2$

For a spherical particle of radius r,

$$F_D = C_D\, 1/2\rho v r^2 \tag{3}$$

and C_D becomes a unique function of the particle Reynolds number, $2rv\rho/\mu$. For instance, for Reynolds number (N_R) less than about 1:

$$C_D \cong \frac{24}{N_R} \tag{4}$$

giving laminar relative motion between particle and the airstream, with a drag force equal to:

$$F_D = 6\mu\pi v r \tag{5}$$

As N_R increases, a transition region is reached representing the gradual development of turbulence in the motion. Here an empirical relationship for C_D (for N_R in the range $1<N_R<1000$) seems to hold fairly well, namely:

$$C_D = 30/N_R^{5/8} \tag{6}$$

For fully developed turbulence (for N_R of about 1000 to 2×10^5) C_D is merely approximated by a value of 0.44, whereas for high turbulence, even in the boundary layer ($N_R > 2 \times 10^5$), C_D is approximately 0.10. From these expressions it is obvious that the drag coefficient and the drag force on the particle fall off rapidly as Reynolds number increases. For agglomerates, the situation is more complex, but the trend should be similar, with the irregularly-shaped particles tending to have

$$F = W\tan\phi + K_c A_c$$

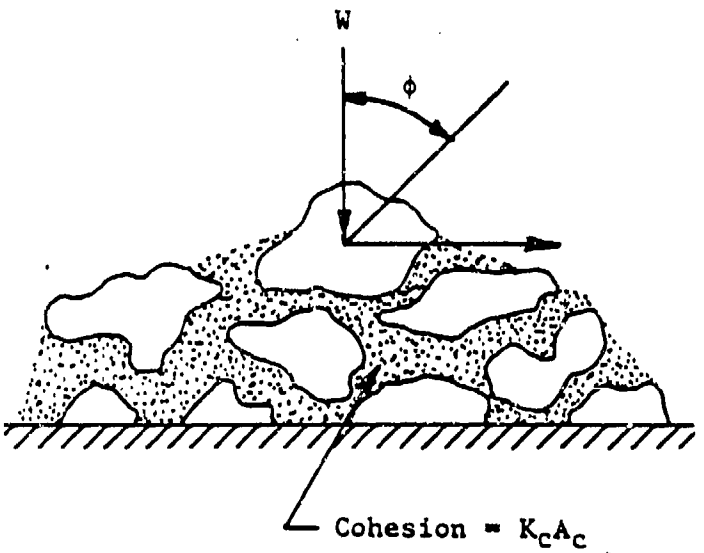

W = Weight of particle

ϕ = Angle of Friction

K_c = Coefficient of Cohesion

A_c = Contact Area

Figure 5-7. Schematic Representation of Theoretical Friction and Cohesive Forces Acting on Particles at Rest

higher drag coefficients than spheres of the same volume. During any given operation, local Reynolds number, and hence C_D, will be highly dependent on engine operation (gas flow velocity) and agglomerator design.

If aerodynamic forces alone are the source of reentrainment, then F_D must be greater than F for each particle unit. Particle shape, especially the shape of the combined agglomerate, will directly influence reentrainment potential because of its effect on exposed surface area and on the arrangement of the particle with respect to adjacent particles. Differences in behavior between the airborne particles and the bulk dust, for instance, the collected particles, will also influence the agglomerator design, which must now accommodate both collection and reentrainment.

While initial particle movement (initial reentrainment) may be the result of both air drag and perhaps mechanical forces, after very short travel the particles will be controlled by the ensuring airflow pattern. This is important because the flow must be sufficient to maintain "flotation" until the agglomerates are totally free of the filter media. Failure to do so would result in recapture, lowering the overall regeneration factor during the cleaning cycle. It is also necessary to control the release process, as much as possible, so that the agglomerates are not broken into small units, thereby reducing separator efficiency by making the inertial separator operate on a smaller than optimal particle size distribution. As the previous equations show, the dependence of the drag coefficient on Reynolds number is significant, with values of C_D at low Reynolds number ranging at least a few orders of magnitude greater than for those at higher Reynolds number (representing fully developed turbulent flow). Furthermore, turbulent motion enhances random collisions and increases shear stress on the particles. As a result, agglomerates that are stable under relatively quiet conditions (laminar flow) often tend to break up under turbulent flow conditions.

The increase in particle concentration in the airstream at the outset of the cleaning cycle also raises questions of aerodynamic interference and particle collision. In laminar motion, interparticle collisions for uniformly-sized particles are not expected although aerodynamic interference may result even at relatively low concentrations. In turbulent motion, random collisions are to be expected, with the number of collisions increasing with increasing particle concentration. For multidisperse suspensions, collisions are expected because of velocity differences that result from particle size.

The important point is that the agglomerator unit must first of all provide suitable particle trapping, then effective particle release within the unit, on demand, and finally, efficient transport of the particles to the inertial separator. Failure in either of these latter two stages will result in a net loading of the agglomerator media or increased loading of the final filter, ultimately reducing service life.

Much of the above discussion also applies to the second agglomerator concept that was investigated. In this concept, the Type II agglomerator, dusty air is directed through a "depth type" media, for instance, a granular bed, mesh or foam, and then to an inertial separator and final filter, as illustrated in Figure 5-8. Alternatively, the media can be backflushed during cleaning, as shown in Figure 5-9.

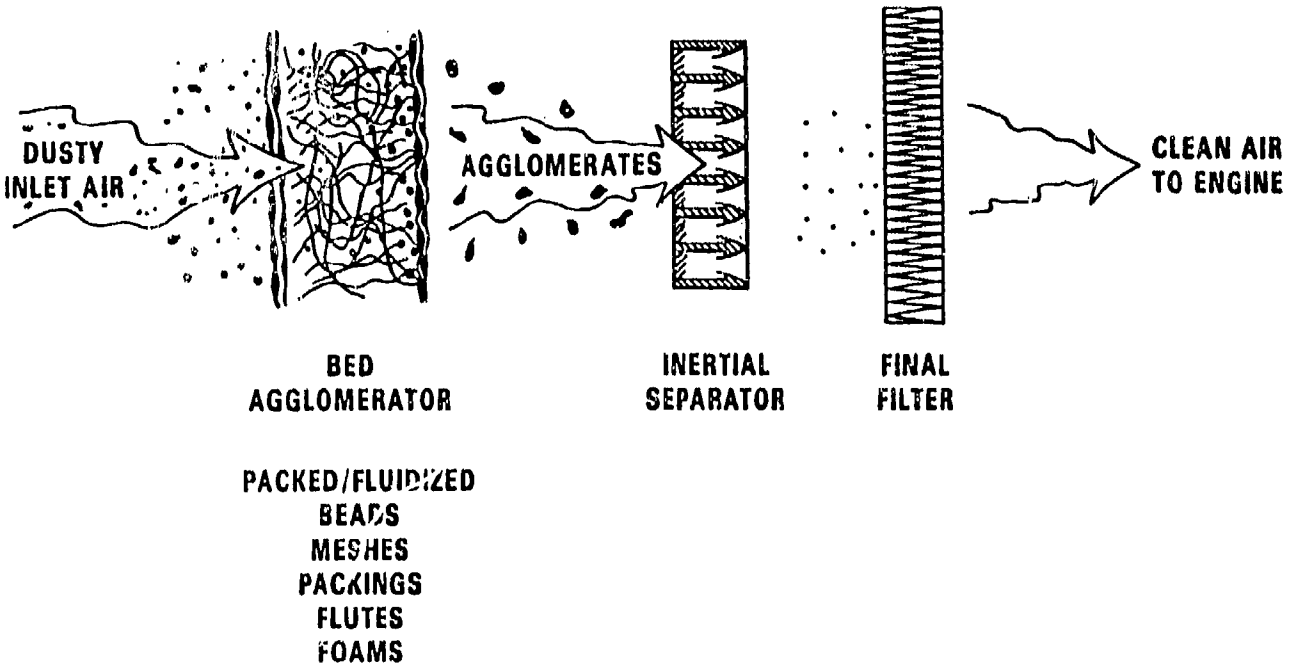

Figure 5-8. Illustration of Type II Agglomerator with Straight-Through Continuous Operation

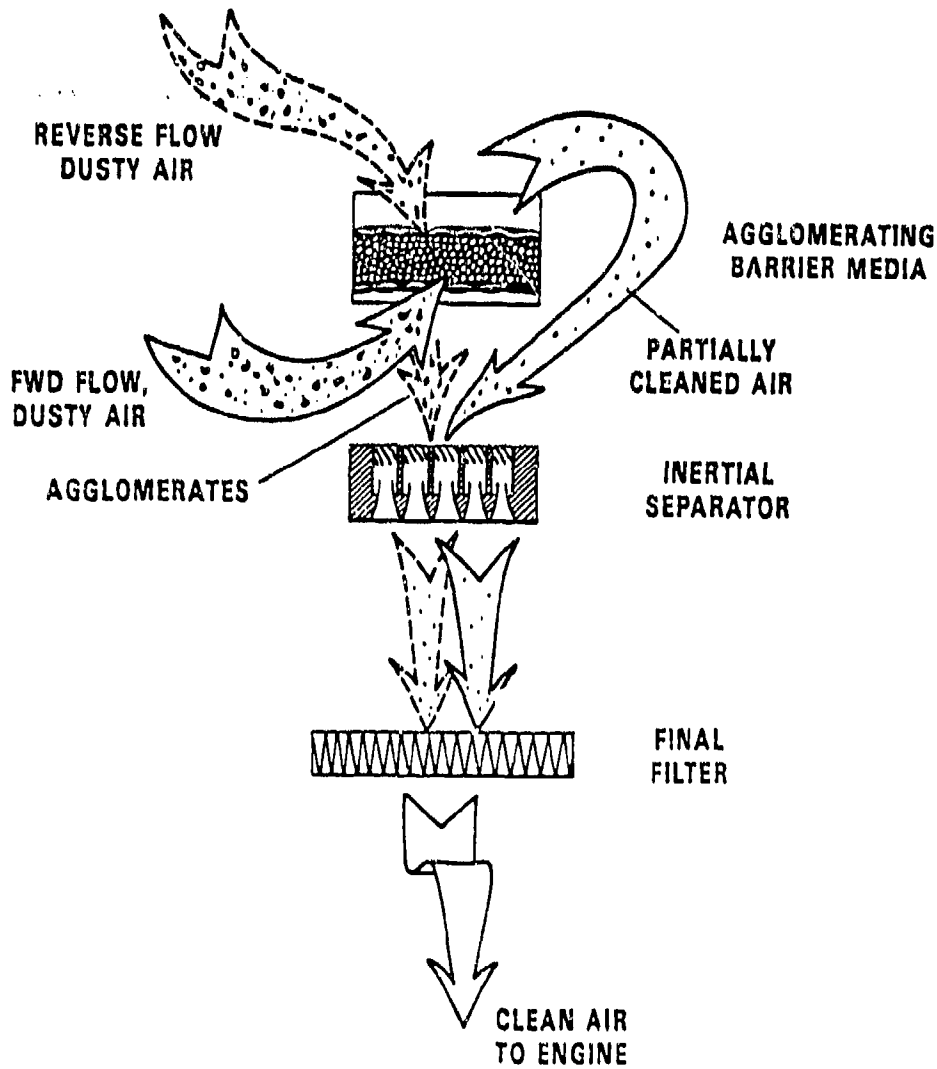

Figure 5-9. Illustration of Type II Agglomerator with Reverse Flow Operation

In these illustrations the agglomerator section generally functions as a depth filter where, as the name implies, particle capture is not limited to the surface, but is continuous throughout part or all of the media's thickness. Whether or not particles are trapped in a normal fashion depends on the collection efficiency with respect to individual particles and on the ability of the media to hold or store particles without reentrainment back into the airstream. The collection efficiency of a depth-type filter is enhanced by interspacial deposits, hence a depth filter can be made to operate as a graded media filter where larger particles are typically collected closer to the surface while smaller particles are collected within the bed by an increasingly dense particulate deposit. This effect is desirable for collecting smaller particles that would otherwise penetrate, although an excessively deep filter would probably only increase backpressure, with little additional benefit in overall particle removal.

Theoretically, reentrainment within granular beds (or other types of depth filters) depends upon the ratio of the separation forces to the adhesion forces for particle-to-granule and particle-to-particle interactions. While these forces, for other than very simple configurations, cannot be easily or accurately predicted, adhesion forces generally include Van der Waal's, electrostatic, and surface tension capillary forces that usually increase in proportion to particle diameter. Separation forces, on the other hand are mostly related to air drag and mechanical shear, the latter caused for instance, by granule slippage or in the case of a fibrous media, by fiber movement.

For small particles suspended in air, drag forces are proportional to particle diameter. The ratio, therefore, of separation force to adhesion force, where only simple Stokes-drag applies, would be independent of particle size. However, because particles are attached to granules or to other particles, the flow field in their vicinity becomes rather complex, with substantial velocity gradients existing near the granule's surface. As a result, drag forces in this region may be proportional to the square of the particle diameter and reentrainment, as indicated by the ratio of the air drag forces to the adhesion forces, should be proportional to particle diameter. Other theoretical considerations suggest that air-induced reentrainment probably depends on particle diameter raised to some power between 0 and 1.

The pressure drop from fluid flow within the bed can produce additional body forces on the granules. Stress within the bed is distributed by granule-to-granule friction, and no equilibrium shear stress can exist that is greater than that determined by internal bed friction. If the ratio of shear to normal stress at a location becomes equal to or exceeds the coefficient of external friction, slippage will occur resulting in a new stress distribution. If, during slippage, the shear forces overcome particle adhesion forces, particles will separate and may become resuspended by interstitial gas flow. Reentrainment, therefore, would be expected to increase in conjunction with factors that increase shear stress within the bed, such as bed depth, granular bed density, bed diameter, and pressure drop from fluid flow. The maximum shear stresses that can develop will depend on the friction coefficients (both internally and with respect to boundaries, such as walls) which are in turn influenced by the particulates that have already been collected. Experimentation regarding air drag in a stationary bed loaded with dust has produced an interesting result. While no significant reentrainment was encountered in the stationary bed, when the bed was put in motion, significant reentrainment occurred. Thus, on a microscale, reentrain-

ment appears to involve shear forces associated with granular motion that overcome particle adhesion forces to facilitate resuspension of the particles by air drag.

For the "straight through" design (Figure 5-8), ideal performance would be characterized as follows: when clean, the agglomerating unit would act as a filter; however, after sufficient loading, reentrainment of the larger agglomerate masses would occur with the overall characteristic behavior changing to that of an agglomerator. If, during normal operation, sufficient agglomeration could be accomplished, resulting in both particle growth and agglomerate release, then it might be possible to reach a semi-steady-state condition whereby the inertial separator could achieve satisfactory collection efficiency to provide for a long-lived air cleaner system without mechanical complication. For example, if the agglomerator raises precleaner operating efficiency from 90 to 95 percent, the amount of dust reaching the final filter would be reduced by 50 percent.

5.3. Media Design Parameters for Particle Collection and Reentrainment

Several mechanisms affect the movement and removal of particles in gas streams. This is evident by many theoretical treatments which indicate that particle penetration through a filter should initially increase with face velocity, reach a maximum, and then decrease, the complete curve being roughly parabolic. The first part of this curve represents the diffusion zone where random Brownian motion of particles in the gas stream enhances the chance for particle capture. As the face velocity increases, the diffusion mechanism becomes less important and is replaced by inertial affects, which cause the particle to deviate from the streamlines as they bend around the fibers allowing for interception or impaction. The combined effects of diffusion and inertia on particle trajectories tend to increase the probability of deposition with the mutual effect being greater than the sum of the contributions of the separate deposition mechanisms.

The individual mechanisms of interception, diffusion and inertial impaction are illustrated in Figure 5-10, which shows the paths followed by particles approaching a typical cylindrical fiber in a filter. For pure interception (path a), the center of the particle follows a given streamline and, for a particle of finite diameter, the particle will touch the fiber when its center approaches within a distance of half the particle diameter from the collector surface.

Deposition by inertial impaction (path b) is due to a change in direction of the carrier gas as it moves around the fiber. Heavy particles, which cannot follow the motion of the fluid because of their inertia, cross the streamlines and collide with the obstruction which caused the disturbance. If the gas velocity and particle size are sufficiently small, the motion of the particle in the stream will obey Stokes' drag law and the forces acting on the particle can be inferred from knowledge of the drag coefficient.

In the absence of external forces, the accelerating force on the particle at any instant will be equal to the drag force created by the velocity difference between the particle and the gas. This leads to a mathematical expression for collection efficiency by inertial impaction which is a function of the inertial parameter ψ and Reynolds number only. There is some discussion in the literature as to what constitutes a critical value for ψ, below which there is no collection of particles

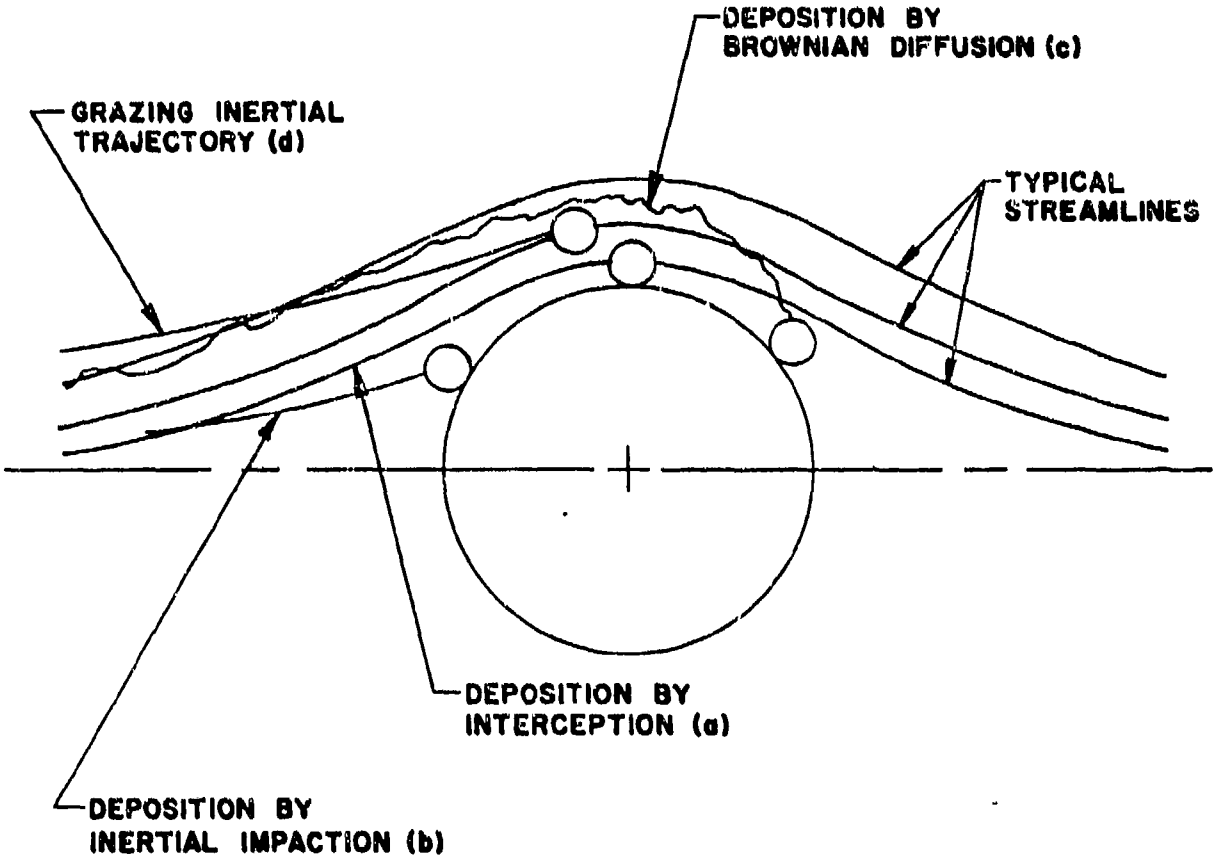

Figure 5-10. Typical Approach Trajectories Illustrating Deposition Mechanisms

due to the inertial effect. While the existence of a critical ψ may be academically interesting, it is of little practical importance since other mechanisms of collection usually enter at small values of ψ. This suggests that inertial effects are best treated by considering their combined effect with other collection mechanisms as a function of neighboring fiber interference.

It is well known that very small particles, say less than about one micron, exhibit considerable Brownian movement and therefore do not move uniformly along the gas streamlines. This movement is often sufficiently intense to produce collisions with a surface immersed in the gas, and if attractive forces at the surface are strong enough to hold the particles, a net migration of particles to the surface occurs with the continual removal of particles from the gas stream (path c). The effects of Brownian motion are most significant when the stream velocity is low because the particles remain longer in the neighborhood of the surface. As random Brownian motion carries the particle toward the surface, the overall chance for collection steadily increases because the time during which the particle stays close to the surface progressively increases.

Single fiber collection efficiency as a function of particle size for each of the above-mentioned mechanisms is shown in Figure 5-11. With respect to the dusts typically encountered by off-the-road vehicles, it is clear that interception and impaction will play a major role in collection. As will be shown later, these mechanisms will also play a major role in agglomeration.

5.3.1. Combined effects of individual filtration mechanisms. The major difficulty in developing a filtration theory lies in determining the precise nature of the interactions among the various filtration mechanisms. For this reason, many investigators have attempted to correlate theoretical and experimental data to account for the combined effects of inertia plus interception, and diffusion plus interception. The general approach is to consider the capture efficiency of a single fiber within the filter, then, under certain assumptions, expand the development to relate to overall efficiency.

The area of primary consideration is often limited to low-speed viscous flows normal to an array of fibers, each having the shape of a uniform circular cylinder. Under these conditions, the streamline pattern depends only on the configuration of the fibers in the filter and the velocity at any point in the filter is proportional to the face velocity. Although this model represents a somewhat over-simplified view, inasmuch as it permits only a partial accounting for the interaction among neighboring fibers and their random orientation within the filter mat, it does not materially change the development insofar as the individual filtration mechanisms are concerned. In most practical fibrous filters, the porosity and interfiber distance are generally large relative to particle size. Also, since all filters are composed of individual fibers, the study of collection mechanisms on isolated cylinders provides a convenient starting point for investigation into the relationships and differences between the behavior of an isolated fiber and the combined affects caused by interference of neighboring fibers in the filter mat.

5.3.2. Diffusion plus interception. The combined effects of interception and diffusion can be considered by modifying the effective distance and time equations to account for the fact that a particle will be caught if it comes within a distance of

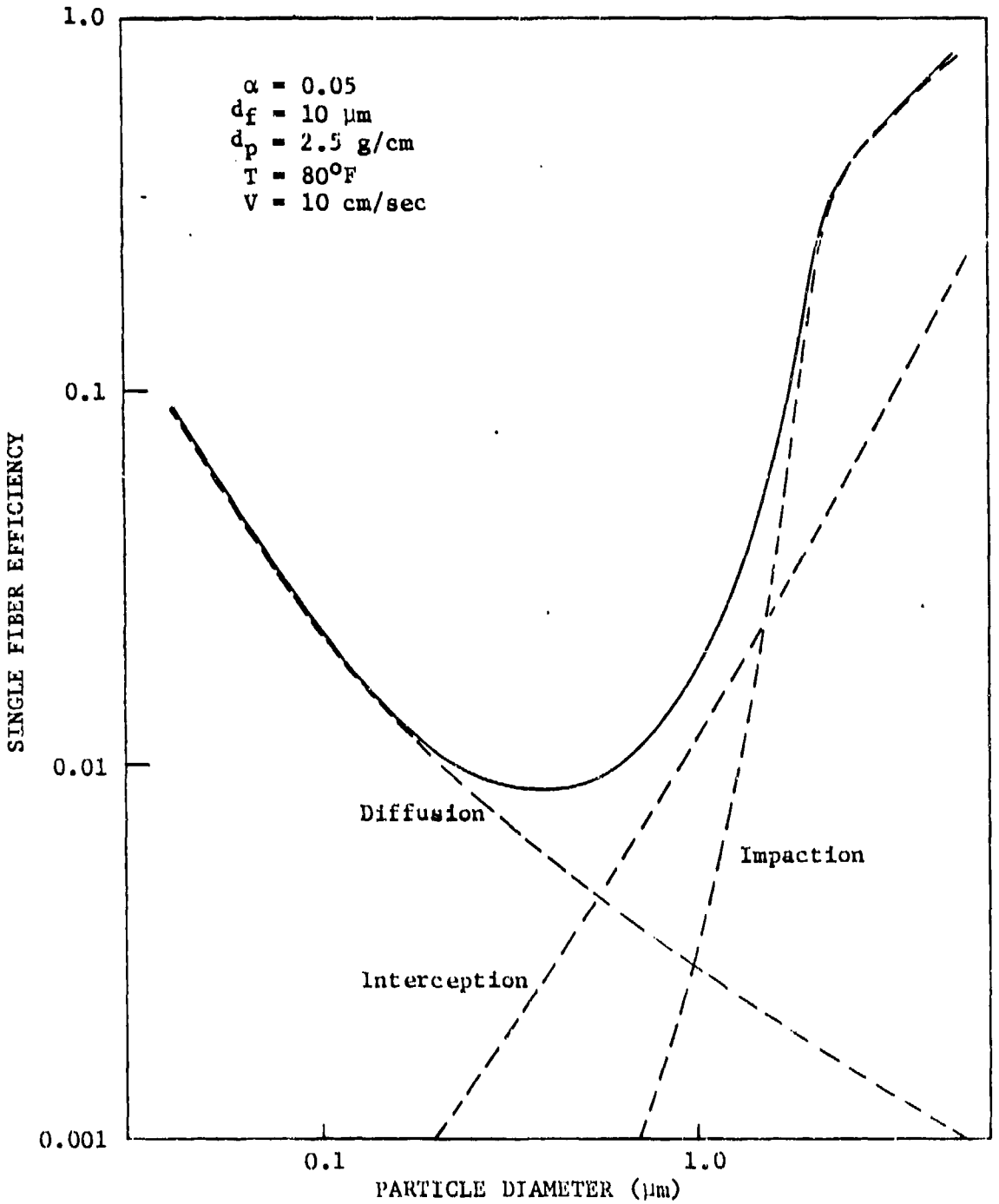

Figure 5-11. Single Fiber Collection Efficiency as a Function of Particle Size

$d_p/2$ from the surface of the collector. This treatment, which is somewhat mathematically intense, shows that in the immediate vicinity of the fiber, where large velocity gradients exist due to viscous shear, Brownian motion of the approaching particle and the effects of inertia can be expected to increase the time that the particle remains close to the cylinder, such that the probability of deposition is increased.

5.3.3. Inertia plus interception. In considering the combined effects of inertia plus interception, it is important to note that the interception effect for finite particles will change the boundary condition of the inertial impaction parameter as calculated for point masses. Finite particles are expected to be caught when their trajectories are less than $d_p/2$ away from the collector surface. When this is taken into consideration, it can be shown that the collection efficiency due to the combined effects of inertia and interception is higher than the sum of the efficiencies due to inertia and interception alone.

5.3.4. Application to a fibrous filter; interference effects. There is general agreement that the relationship between single fiber collection efficiency and overall filter efficiency, for a filter mat in which the fibers are relatively far apart and dispersed uniformly, and where neighboring fibers are staggered with respect to each other, is of the form:

$$\eta = 1 - N/N_o = 1 - \exp\left[\frac{-\alpha\beta L(d_f)_{avg}}{(d_f)_s^2}\ \eta_\alpha\right] \qquad (7)$$

where:
- N/N_o = particle penetration concentration
- α = packing density or volume of fibers in filter mat
- L = mat thickness
- $(d_f)_{avg}$ = arithmetic average fiber diameter
- $(d_f)_s$ = surface average fiber diameter
- η_α = single fiber collection efficiency based on average fiber size
- β = a constant whose value depends on the definition of η_α

When the fibers are assumed to be oriented normally to the flow direction thus $\beta = 4/\pi\ (1-\alpha)$ and the mat is assumed to be made of uniform fibers thus $(d_f)_{avg} = (d_f)_s$ this equation becomes

$$\eta = 1 - N/N_o = 1 - \exp\left[\frac{-4}{\pi}\ \frac{\alpha}{1-\alpha}\ \frac{L}{d_f}\ \eta_\alpha\right] \qquad (8)$$

where η is the ratio of the number of particles retained by the filter to the number of particles entering it. The assumption of uniform fibers, while not completely physically realistic, does not conceptually hurt the theoretical development, although it may complicate experimental verification. The arithmetic average value for d_f, which can be determined by microscopic examination, will probably be

close to the proper average size if the geometric standard deviation is not very large. Under these conditions, η can be considered as the average removal efficiency for the filter mat.

It should be noted the efficiency, when calculated in this manner, is actually a function of time, although little information on this relationship is available because the theory of time-dependent behavior of fibrous filters is not yet well developed. Inasmuch, η actually refers to the initial efficiency for a clean filter mat. (Some consideration of filter loading is presented in Section 5.3.6.)

5.3.5. Consideration of interference effects of neighboring fibers. Because the collection efficiency of a single fiber in a fibrous mat is generally greater than that for an isolated fiber at the same face velocity, it is necessary to modify the combined efficiency equations to account for the interference effect of neighboring fibers. The most significant effect is due to changes in the flow pattern and velocity distribution in the immediate vicinity of the fibers. These changes result in an increase in the collection efficiency of a single fiber, the increase being a function of the volume fraction of fibers in the filter and the Reynolds Number. Furthermore, the interference effect is generally different for each collection mechanism (inertia impaction, interception and diffusion). Experimental data for glass fiber mats $[(df_f)_{avg} = 2.5\ \mu m, (df)_s = 3.0\ \mu m$, porosities of 97 to 98%] using a homogeneous aerosol $[0.5 \leq d_p \leq .72\ \mu m]$ and velocities ranging from 0.87 to 7.0 cm/sec., showed that the collection efficiency increases as porosity decreases in accordance with the linear relationship

$$\eta_\alpha = \eta_o (1 + k\alpha) \tag{9}$$

where η_α is the collection efficiency of a single fiber in a filter with fiber volume fraction α at a superficial velocity v_s, and η_o is the collection efficiency of an isolated fiber at v_s. For these experiments, K had an average value of 4.5, with little variation even when different collection mechanisms were dominant.

5.3.6. Particulate loading. Along with the general properties of efficiency and initial restriction, the particulate loading properties of a filter media are significantly important because they directly affect the useful service life of the filter, and as such, directly influence the economics associated with the solution of a particular filtration problem. In many filter applications, particulate loading is an irreversible process in that once loading or "clogging" has reached a certain point, the element must be discarded and replaced. For these filters, cleaning is ineffective since neither the initial efficiency or the initial restriction can be restored. Often the performance of the equipment being protected by the filter is adversely affected by the increased restriction of loading as is the case, for example, of automotive engines. Of course, not all loading characteristics are necessarily detrimental. Under moderate loading there is usually an improvement in filter efficiency and it is not uncommon for some filters, for instance those used in chemical processing plants, to be pre-loaded to insure the required efficiency or to enhance a particular process. In most cases, however, loading is in one way or another an economic factor and must be considered in the design and operation of filtration system.

It has already been noted that filter loading is influenced by a large number of parameters; such as particle size and concentration, face velocity, and cake buildup, to name a few. With respect to filter cake life, a major parameter is the rate of pressure increase across the filter as a function of the amount and type of particulate being introduced to the filter. The significance of this parameter to the agglomerator concept is obvious. The backpressure history of the surface agglomerator will dictate when backflushing (cleaning) must be initiated to maintain satisfactory operation. Thus, the loading characteristics of the agglomerator, that is the backpressure rise as a function of particle removal for a given flow rate, and particle size and concentration, will establish the normal operating cycle or operating frequency for the system and influence its size and method of operation. For the straight-through type agglomerator, a "steady-state" pressure drop must be maintained where overall agglomerate reentrainment balances particle removal and buildup. Ideally, the long-term trend in pressure drop for the agglomerator, over several automatic cleaning cycles in the case of the surface agglomerator, or over extended operation for the depth agglomerator, should be such that no external maintenance is required on the agglomerator over several replacement cycles for the final filter. (Note, of course, that the operating time between filter replacements will be extended when the agglomerator is used.) In fact, if filter service life between replacements is sufficiently extended and if agglomerator maintenance is relatively simple and inexpensive, then the agglomerator is still justified in terms of its contribution to overall service life.

The effects of loading on collection efficiency and particle reentrainment must be considered. In the first case, it is likely that loading will increase the collection efficiency so that ultimately smaller and smaller particles will be removed during the loading cycle. It is clear that single fiber collection efficiencies will change as will effective porosity (thus α) and fiber diameter. Of these, the change in effective porosity should be most significant, and as can be seen by equation (8), a decrease in porosity (hence an increase in α ; $\alpha = 1 - \epsilon$) will provide an increase in η .

Irrespective of agglomerator type, dust loading on the final filter is an irreversible process such that it will eventually require replacement. It should be designed to maximize life and efficiency with respect to the size and concentration of the dust exiting the precleaner.

5.3.7. Treatment of depth-type media. Experimental data and potential-flow theory for particle impaction on cylinders in the high Reynolds number range usual agree fairly well, while theoretical efficiencies in the low Reynolds number range are considerably lower than those predicted, as indicated in Figure 5-12. This is due to the combined effects of inertial impaction and direct interception, where for low values of $\sqrt{\psi}$ (typically below 0.4) and low Reynolds number, efficiency depends principally on interception. While most fibrous filters operate in a low Reynolds number range, the depth-type agglomerator will operate at relatively high Reynolds numbers due to high design face velocities and to the relatively large collector diameter of the media. The impact of diameter and stream velocity on Reynolds number is shown in Figure 5-13.

For the depth-type unit, agglomerator design was guided most by impaction theory, with some consideration of interception, particularly for the graded mesh unit.

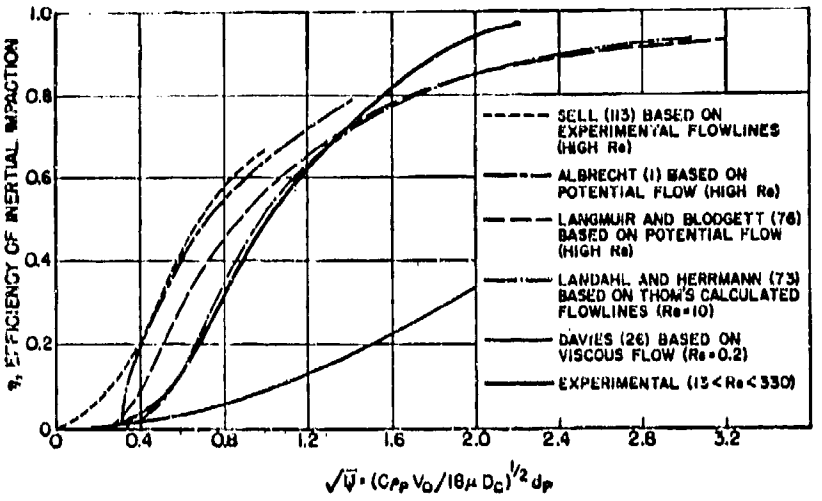

Figure 5-12. Comparison of Theoretical and Experimental Efficiencies of Inertial Impaction on Circular Cylinders (Point Masses are Assumed)[3]

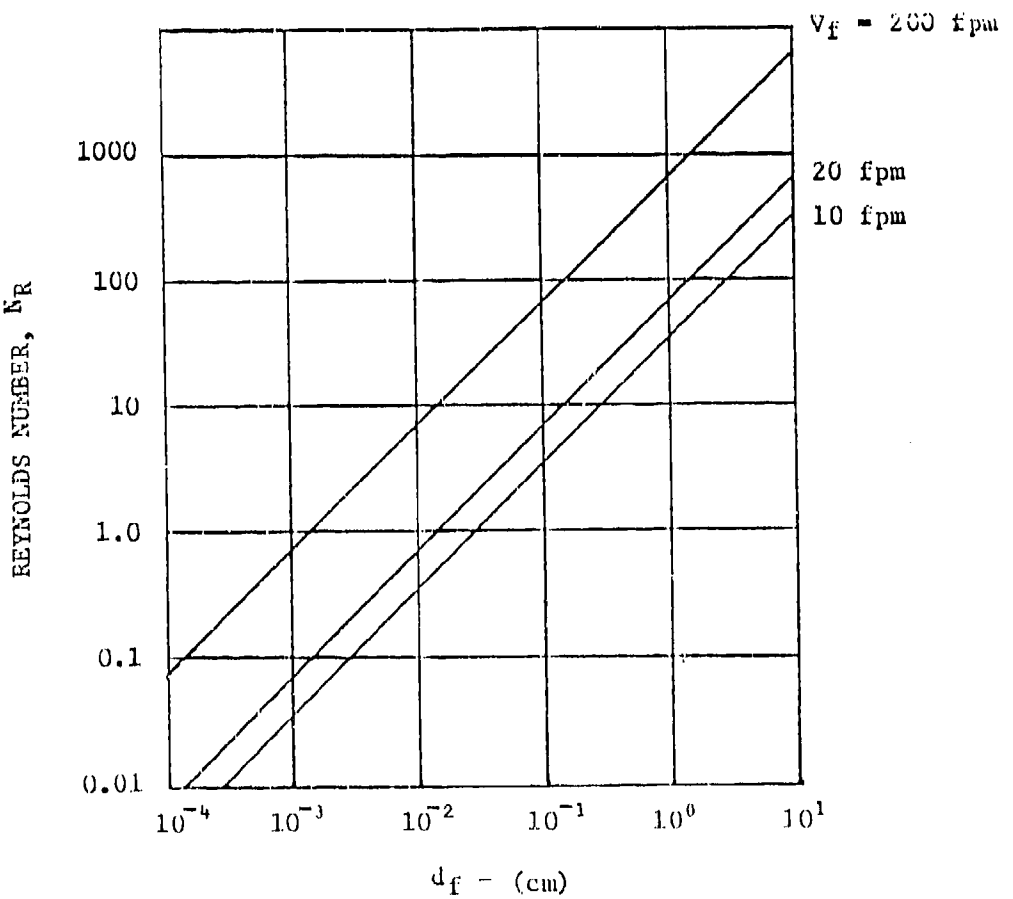

Figure 5-13. Reynolds Number as a Function of Fiber Diameter and Face Velocity

Deposition by diffusion was not considered. Gravitational collection was not considered in the initial design, although movement within the agglomerator was found to be influenced by gravity due to the high sedimentation velocity and high relaxation time for agglomerates reentrained within the bed. Gravitational collection efficiency is only a function of average fluid velocity and particle size, as contained implicitly in the definitions for sedimentation velocity, and not dependent upon granule size or the solid volume fraction of the bed.

The granular bed, and to some extent the mesh and foam type agglomerator, is an assembly of individual collectors or agglomerating surfaces, and if each collector performs nearly optimal, so should the unit. Theoretically, the granular bed can be treated as an assemblage of spheres, which is fortuitous because the treatment of impaction on spheres is analogous to the treatment in cylindrical filtration theory. In fact, for most mechanisms there is a strong similarity in the mathematical treatment between the fibrous filter model (presented earlier) and the granular filter model. Collection on an isolated collector is usually examined first because this approach shows the fundamental importance of the individual collection mechanisms (impaction, diffusion, interception, gravitational setting). The equations are then modified by functions of bed porosity to predict bed behavior more closely. Corrections for nonisolated collectors do not change the dependency on collector size for the individual collector mechanisms, although they may affect optimization when one or more mechanism is important for a given particle size.

As with filters, the pressure drop and collection efficiency of agglomerators are important parameters in their design and operation. But unlike filters, a critical parameter is their ability to promote successful agglomerate release or reentrainment. For dust collection in a packed bed, some dust accumulates on the surface in the form of a cake, the rest passing into and being collected in the interior of the bed. The surface filtration factor is inconsequential over time because holes form in the dust layer with increasing frequency as the rate of filtration is increased. Therefore, depth filtration is predominate in determining packed bed collection, primarily due to inertial collisions between the dust and the filter medium. In general, increasing the filtration rate while reducing the size of the filter medium will increase the number of inertial collisions so that collection efficiency will be higher. Above a certain velocity, however, reentrainment comes into prominence, thereby lowering the bed's efficiency. Behavior of the dust as the bed loads, depends on the state of accumulation and the operating conditions. When the bed was clean, the flow-through space between the particles corresponded to a high Reynolds number. However, as dust is deposited, the flow through the layer of dust which fills up the spaces in the medium corresponds to lower and lower Reynolds numbers, since the dust particles have dimensions of only a few microns. This enhances efficiency by bringing other collection mechanisms into play. Under high specific-deposit conditions, however, the spouting velocity increases and reentrainment becomes pronounced, limiting overall bed efficiency. If particle reentrainment can be confined to agglomerates and if a near steady-state pressure drop can be achieved, a self-regenerating (steady-state) agglomerator will result.

5.4. Testing and Evaluation of Candidate Media

Early in the program, several media manufacturers were contacted to discuss the requirements for an agglomerating media. As a result, numerous samples, mostly of

surface loading media, were obtained for initial screening and evaluation. At the outset, most of these samples were screened using the test arrangement illustrated in Figure 5-14. Air containing coarse dust, at a concentration of 0.025 grams per cubic foot air, was introduced to the test media via path A. The pressure drop across the media was monitored at constant airflow and downstream measurements were made to determine incremental and overall efficiency. At a predetermined ΔP, which depended on the media in question, the flow was instantaneously switched so as to follow path B. Dust penetration during this cycle was monitored by isokinetic sampling. Once the cleaning cycle was complete, flow was again switched to path A. This process was continued until the media's performance trends were established. The parameters of interest were ΔP increase as a function of loading, ΔP recovery, time between cleaning, incremental and overall cycle efficiency, and total dust penetration as a function of time, which indicated the amount of dust the final filter would have to accommodate for a given upstream environment.

The test apparatus was designed to accommodate depth and flat sheet media as well as packed beds, foams, and meshes. Performance for a particular flow condition and media configuration was measured by monitoring the media's impact on incremental and overall efficiency for the 2-1/2-inch swirl tube separator, relative to its baseline performance (Figure 5-15), and by the media's loading and unloading characteristics over several operating cycles. Media showing promise or some particularly interesting characteristics were identified for more extensive investigation, either in this test unit or in the unit illustrated in Figure 5-16. The major difference between these units is that in the second unit, reversed airflow during cleaning was accomplished by repositioning the media (configuration A to B) accompanied by some degree of mechanical shock. This test, while physically more severe on the media, was expected to provide maximum agglomerate release. It was also expected to indicate media performance under more realistic operating conditions, since a workable system for surface media is likely to require both reversed flow (relative to the agglomerator unit) and mechanical shock to achieve maximum effectiveness. The degree of shock imparted to the media with this setup was generally controlled by regulating the pressure and flowrate of air in the cylinders. Like the previous unit, this unit was also designed to handle flat sheet samples (up to a foot square) and some pleated and depth configurations. Airflow rates to about 200 cfm could be obtained.

As testing progressed, some modifications were made to the initial screening test rig to investigate mechanical parameters that might enhance agglomerate release from the media. For the most part, the two devices illustrated in Figure 5-17 were used. With one, the media is mechanically "thumped" by a leaf-type spring, after airflow reversal, and then the frame was wrapped. With the other, the media is "thumped" in the center by a weight attached to a pneumatic cylinder. In most cases, a considerable amount of additional dust was removed by these devices, with the leaf-spring unit generally being more effective than the pneumatic cylinder. Of course, this portion of the test was only qualitative in nature, the primary purpose being to provide a look-see at the effects of mechanical shock on regeneration.

5.4.1. Flat sheet evaluation of surface loading media. Airflow data for several candidate media are shown in Appendix A. In most cases, media were evaluated at face velocities in the 40 to 100 fpm range, even though these values are considerably higher than those usually experienced by high efficiency air filter

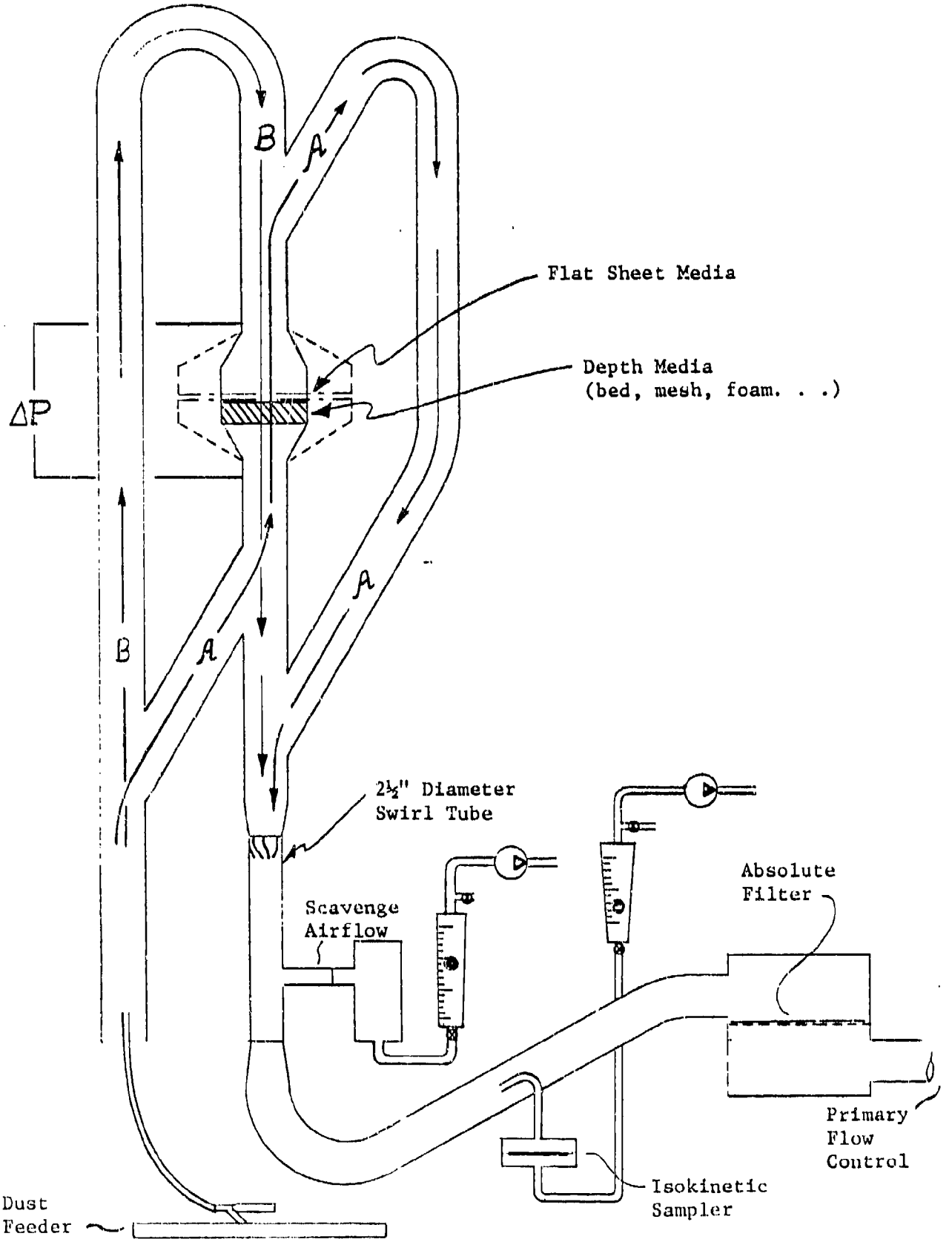

Figure 5-14. Test Arrangement for Initial Screening of Candidate Media

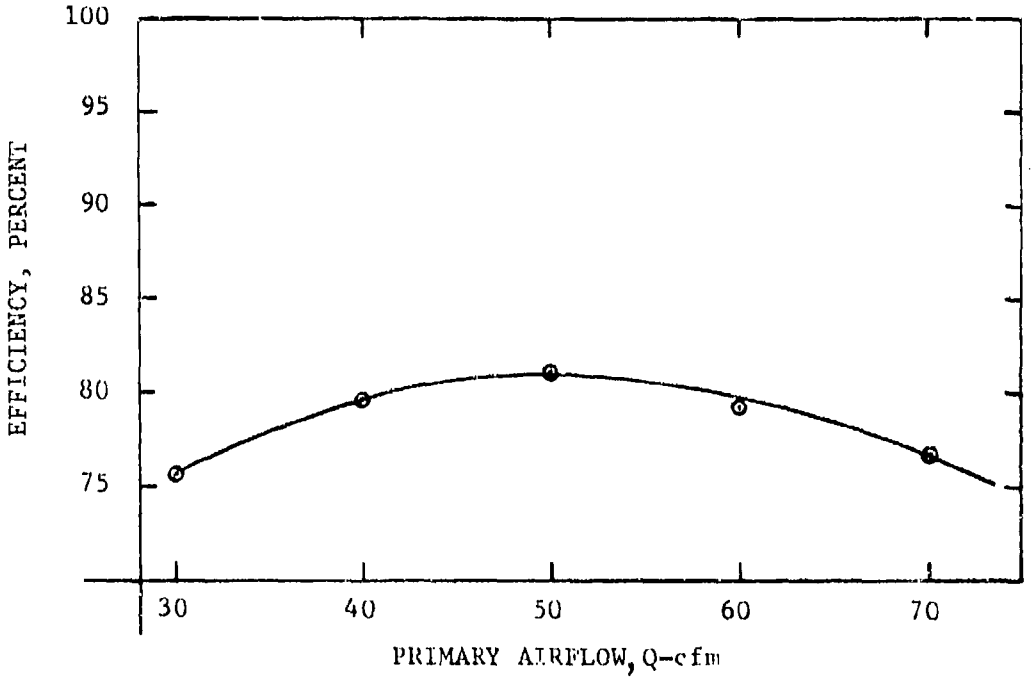

Figure 5-15. Baseline Performance of 2½-inch Swirl Tube

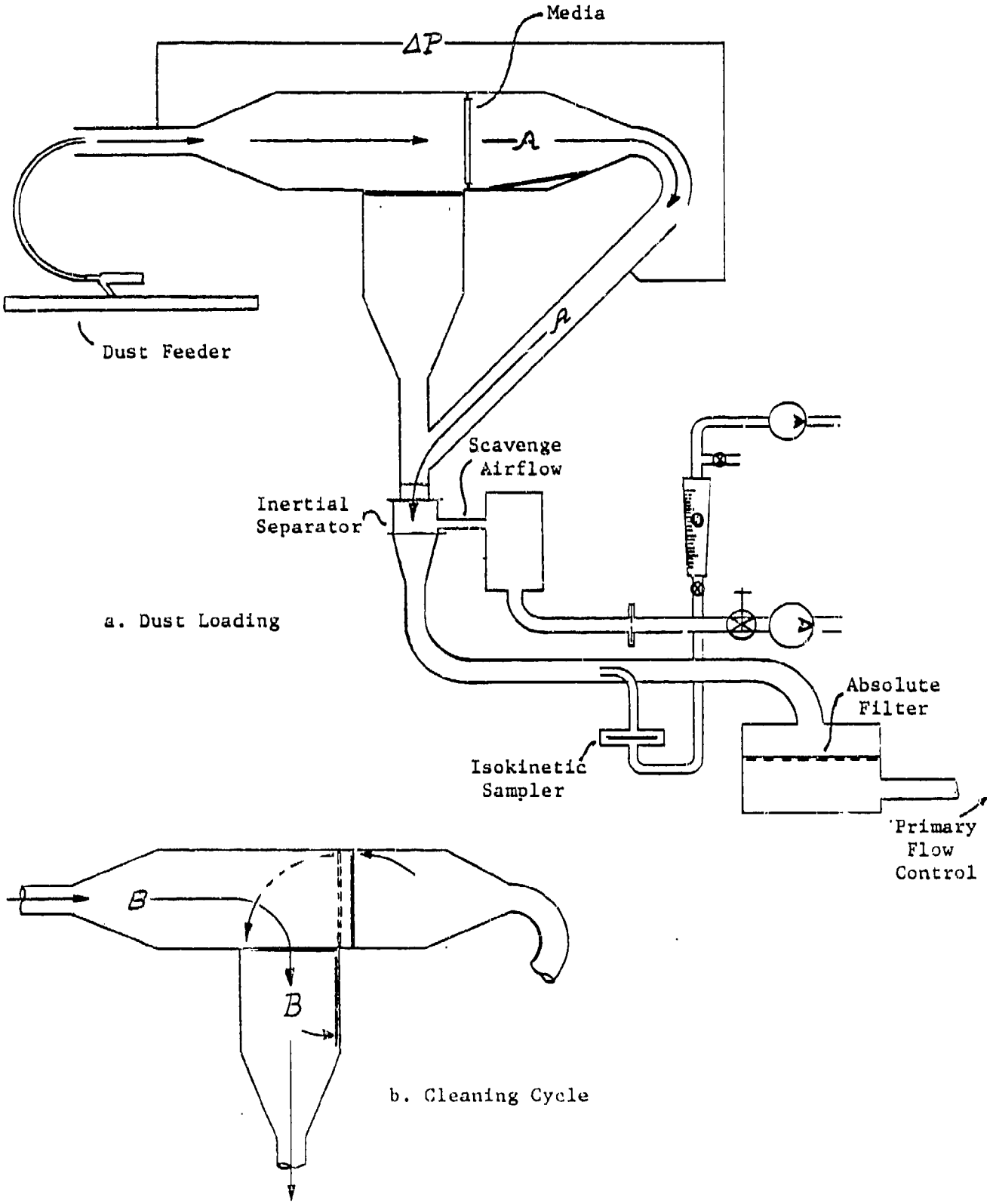

Figure 5-16. Test Arrangement for More Extensive Testing, Early in the Program

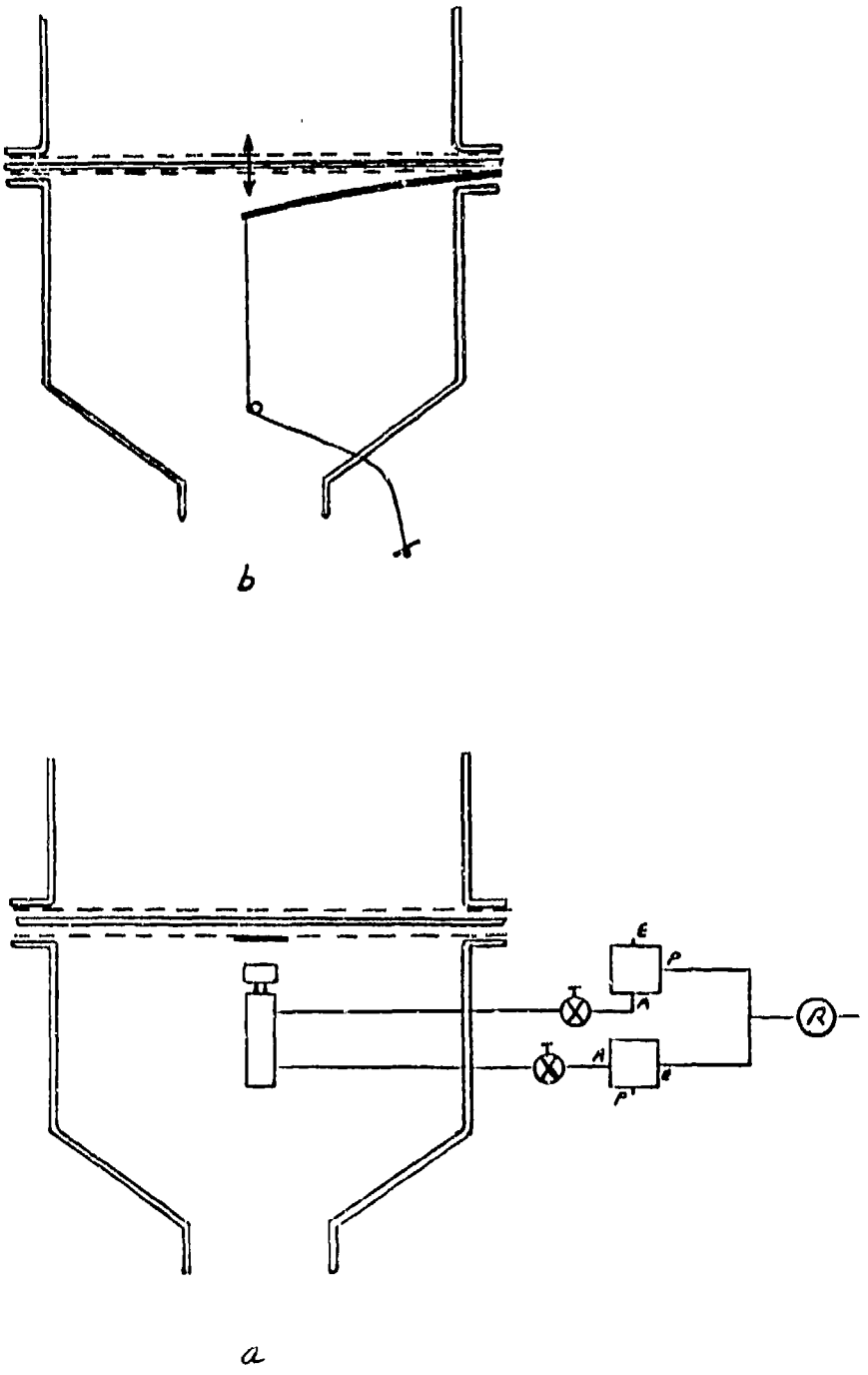

Figure 5-17. Experimental Methods of Imparting Mechanical Shock During Initial Screening of Candidate Media

media. The reason was that we were hopeful of finding a media with good agglomerating characteristics at high flow in order to facilitate agglomerator design and packaging. As will be seen, some results at the higher face velocities were encouraging. However, it was also evident that certain media warranted evaluation at lower face velocities, and in many cases this was done in the next phase of testing. Therefore, in considering the data it is important to note that a negative result does not necessarily mean that a particular media is unsuitable as an agglomerating material, but rather that it is not suitable for agglomerate development and regeneration at the higher face velocities considered desirable for this particular application.

Figures 5-18 through 5-24 illustrate data from the preliminary screening and later phases of the flat sheet evaluation program. Representative data for other media are given in Appendix B. Finally, Table 5-1 summarizes the results of the flat sheet testing in terms of efficiency during dust loading, efficiency during regeneration, and overall efficiency. The ratio of efficiency during regeneration to the efficiency of the precleaner itself is also given. This value provides a direct indication of the degree of agglomeration that was obtained during regeneration.

Figure 5-18 shows pressure drop as a function of dust loading and regeneration over five cleaning cycles for the JR-347 media during initial screening. Face velocity during this test was 101 fpm, which is more than 10 times the normal face velocity for this media. Efficiency during dust loading averaged about 99 percent, which is lower than values typically obtained when operated under normal conditions. Reasonable agglomeration was indicated and regeneration was considered somewhat successful, even though the trendline for pressure drop after cleaning is increasing. This may be due to the fact that the pressure drop levels at which cleaning was initiated were relatively high, which probably hampered cleaning by driving particles into the media. Since cleaning at lower ΔP levels is likely in practice, the media was selected for further testing later in the program. This type of reasoning was applied to several media, although many others were eliminated by these preliminary tests.

Results for the JR347 media during later testing verified this approach. As shown in Figure 5-19, loading and regeneration were significantly improved when the face velocity was reduced to 40-45 fpm, which is still quite high for this media. The data in Figures 5-20 and 5-21 provide an even better illustration of the transition as a function of face velocity. Figure 5-20 shows results from the preliminary evaluation of the KC-2 media at a face velocity of 83 fpm. Efficiency and agglomeration tendency were good, but regeneration was questionable. Testing at 36 fpm, however, produced much better results (Figure 5-21). Overall efficiency for the precleaner assembly (precleaner plus agglomerator), over 10 agglomeration cycles, was 98.3 percent, compared to approximately 83-84 percent for the precleaner unit by itself. Furthermore, when testing was arbitrarily stopped after ten (10) cycles, agglomerator recovery was intact and dust loading trends remained consistent. It should also be noted that cleaning was initiated at lower pressure drop levels, which may also have contributed to the improvement.

The data in Figure 5-21 as well as that in Figure 5-22 show results when the agglomerator is exposed to a much smaller particle size distribution, representing particles that would ordinarily penetrate the precleaner and be passed to the final

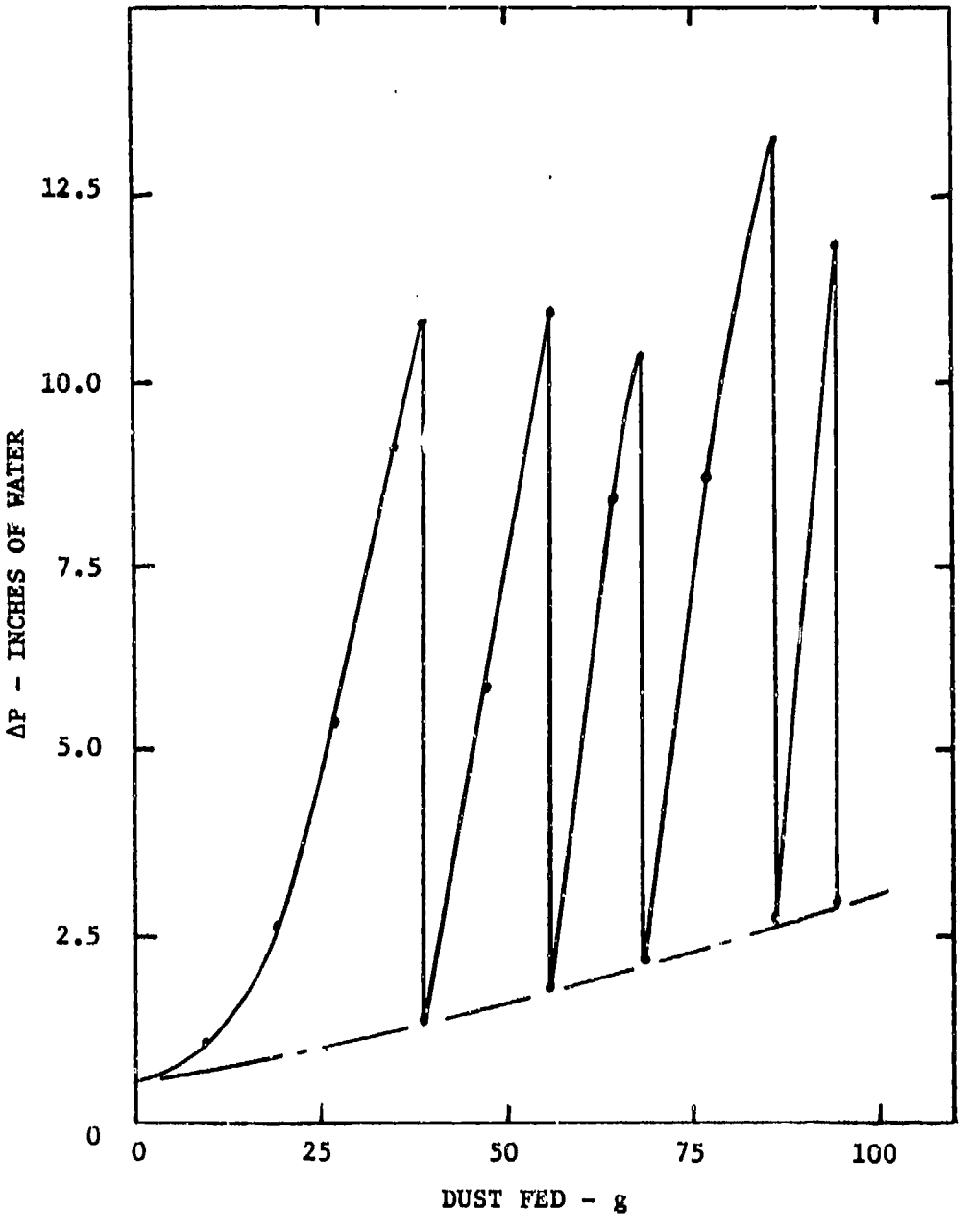

Figure 5-18. Pressure Drop Vs. Dust Fed for JR-347 Media, V_f = 101 fpm, AC Coarse Dust

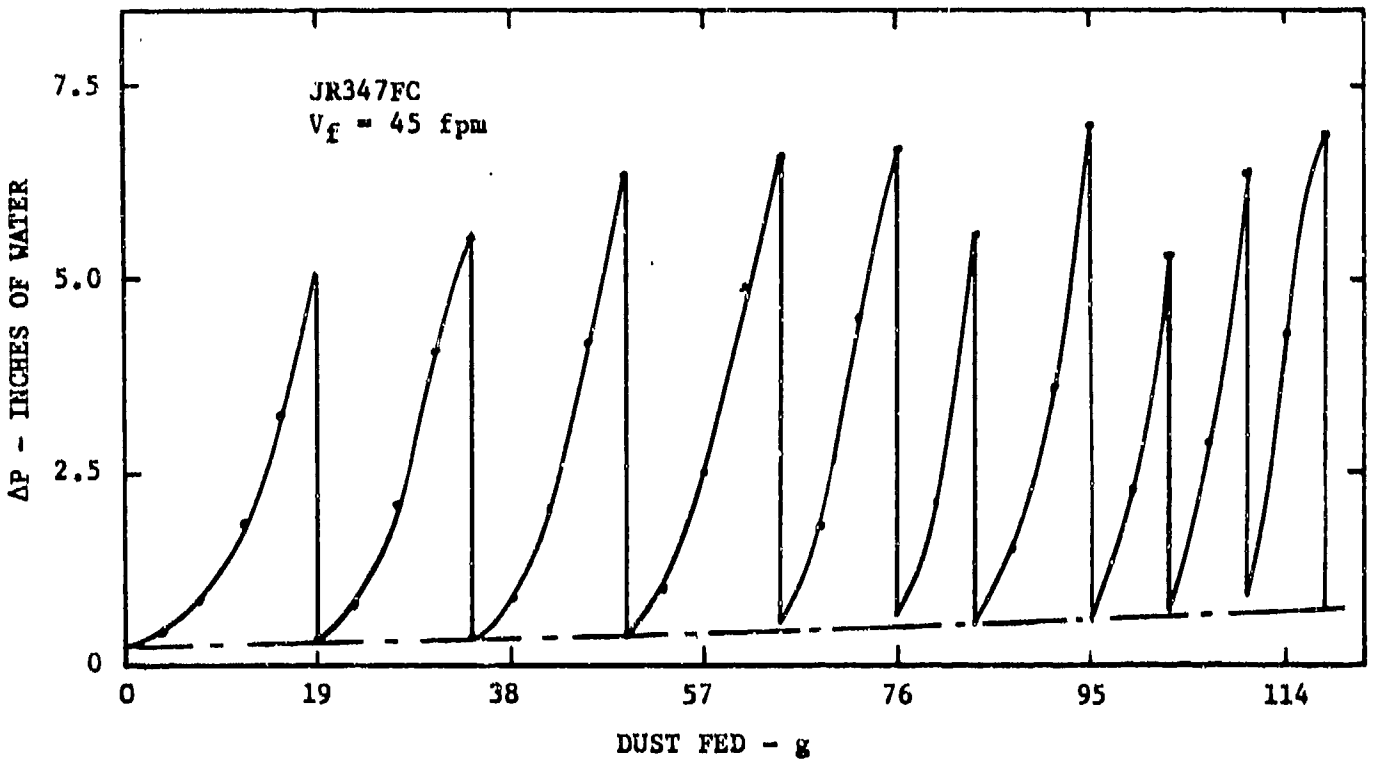

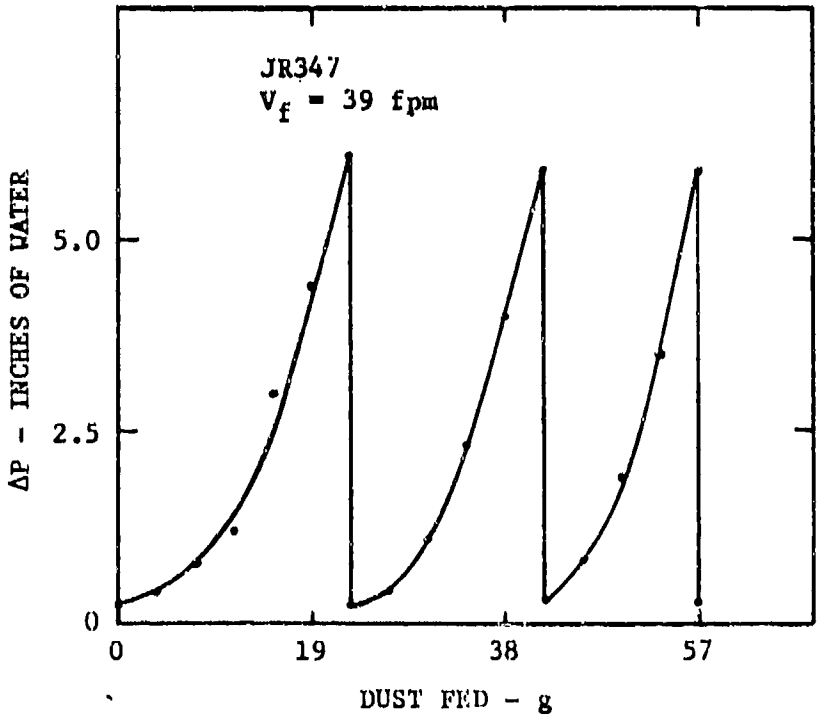

Figure 5-19. Pressure Drop Vs. Dust Fed for JR-347FC and JR-347 Media, V_f = 39 and 45 fpm, AC Coarse Dust

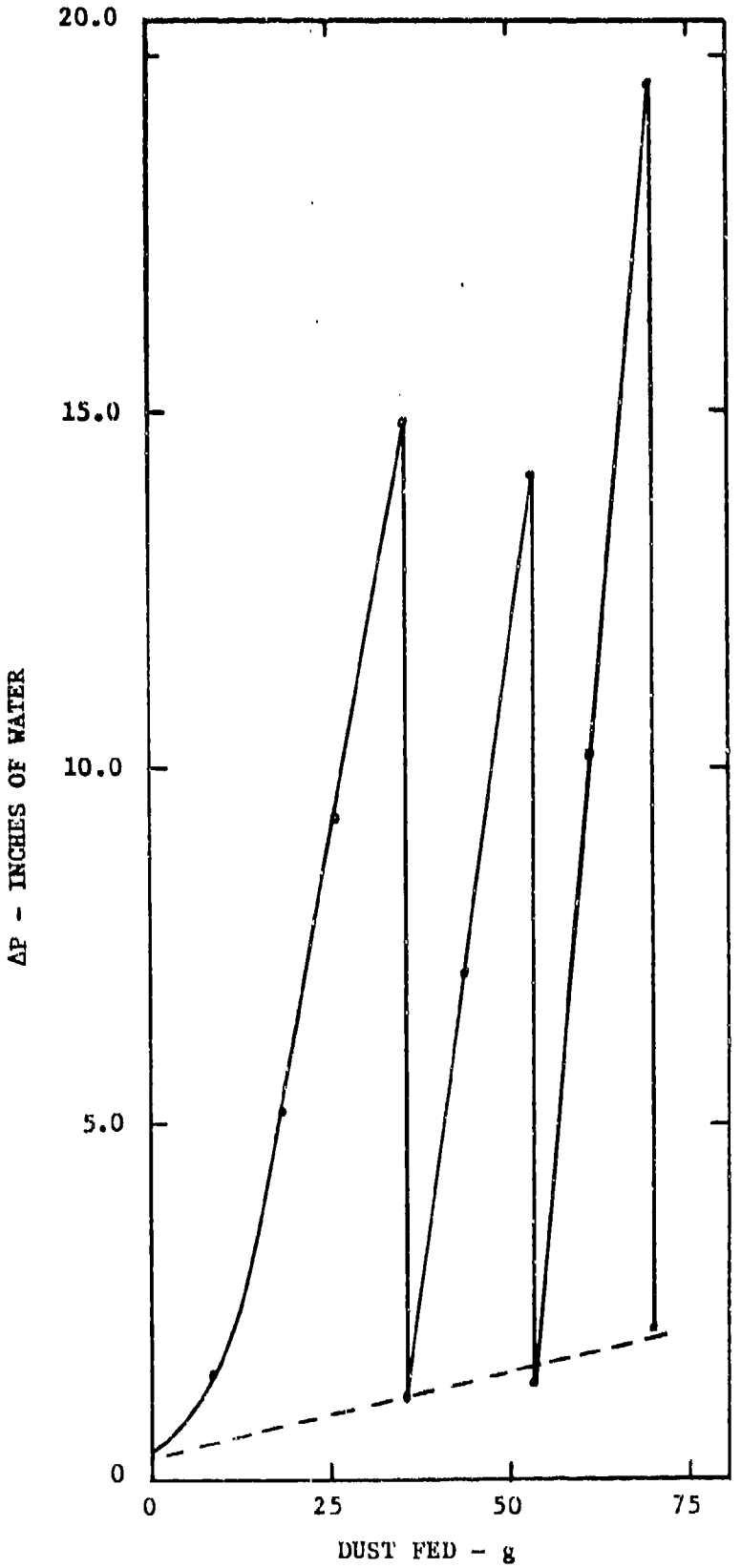

Figure 5-20. Pressure Drop Vs. Dust Fed for KC-2 Media at a Face Velocity of 83 fpm

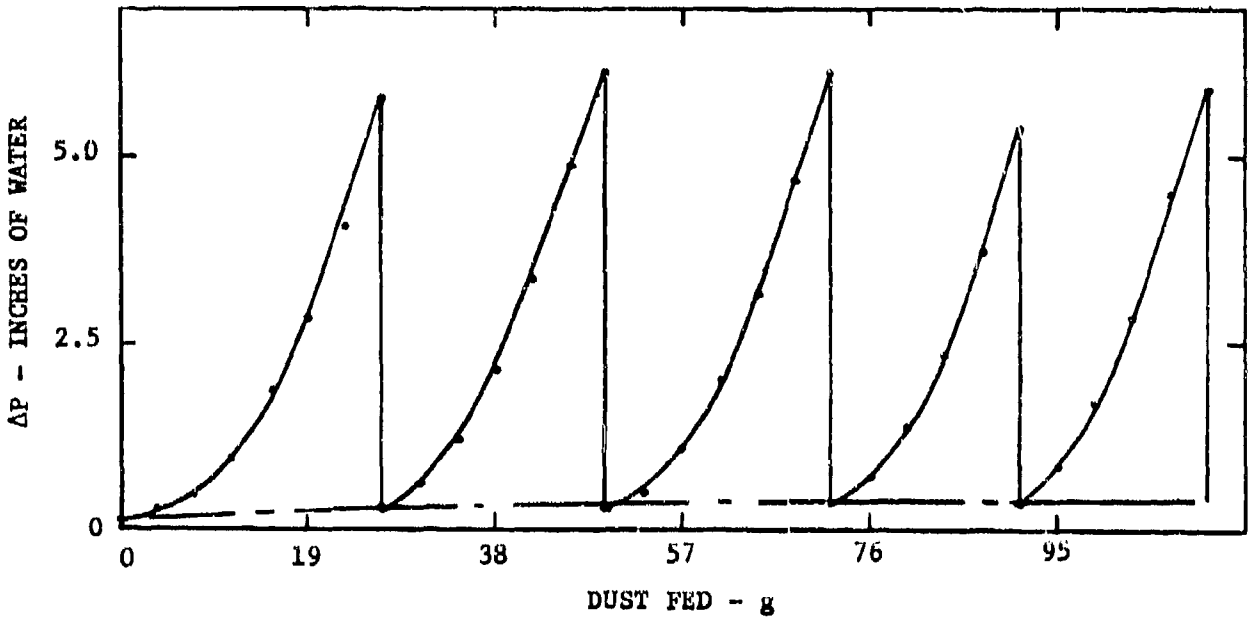

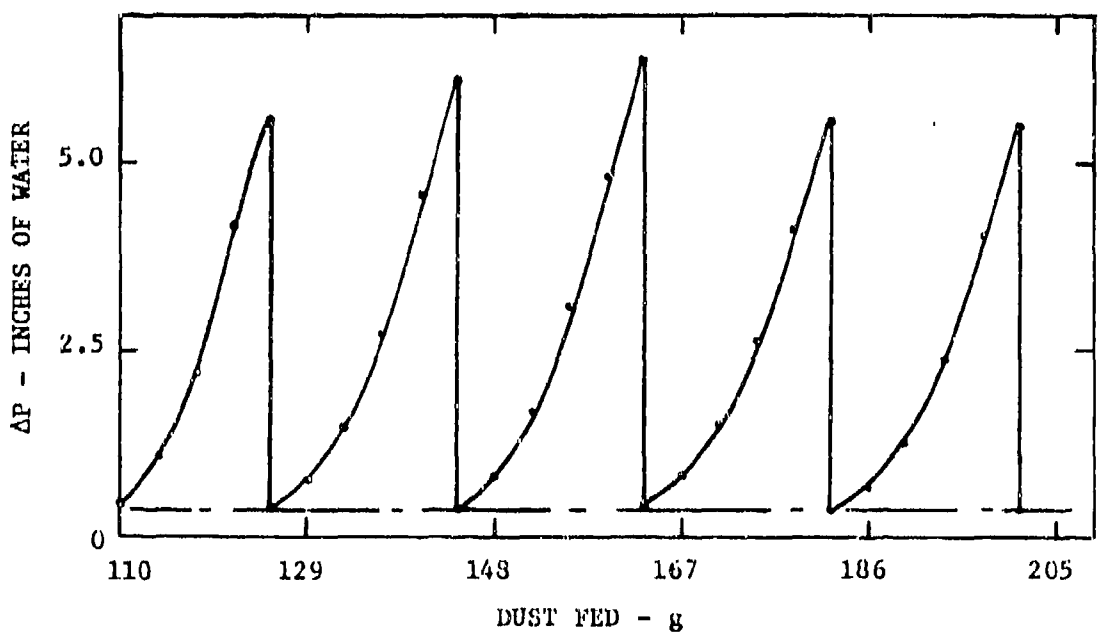

Figure 5-21. Pressure Drop Vs. Dust Fed for KC-2 Media at a Face Velocity of 36 fpm, AC Coarse Dust (Test Method 2)

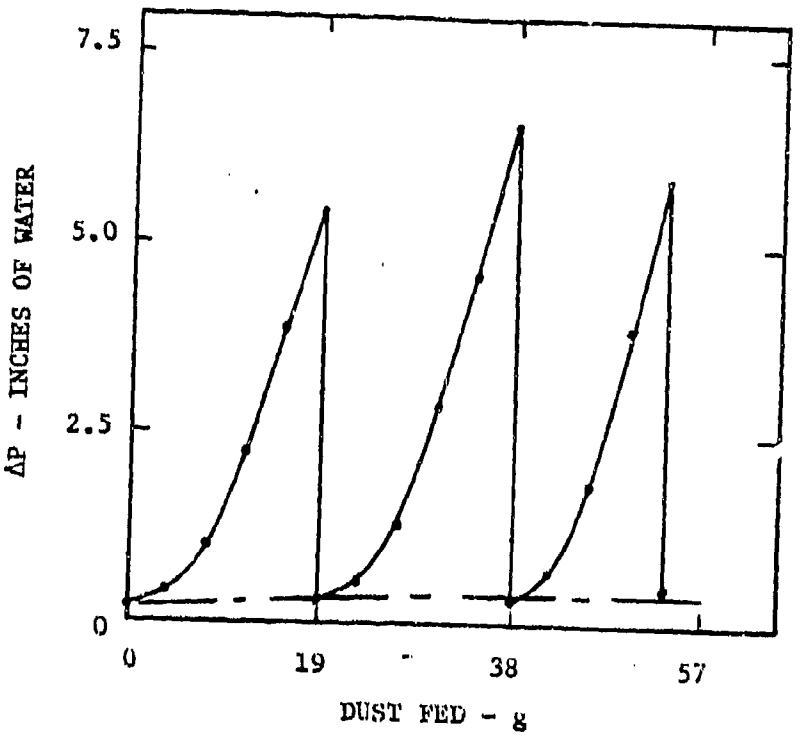

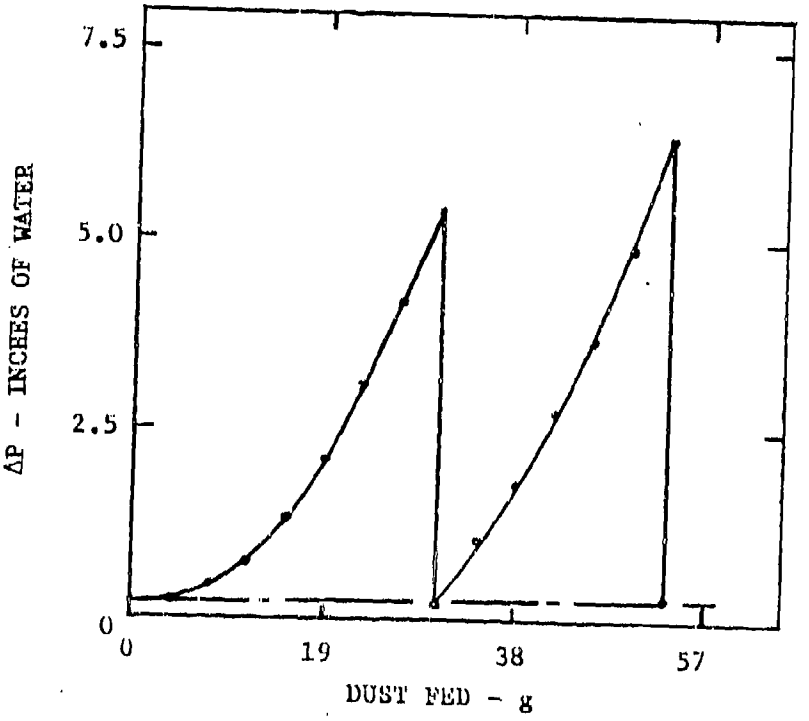

Figure 5-22. Pressure Drop Vs. Dust Fed for KC-2 Media, V_f = 36 fpm, AC Coarse Dust, Test Methods 1 and 2

TEST METHOD 1

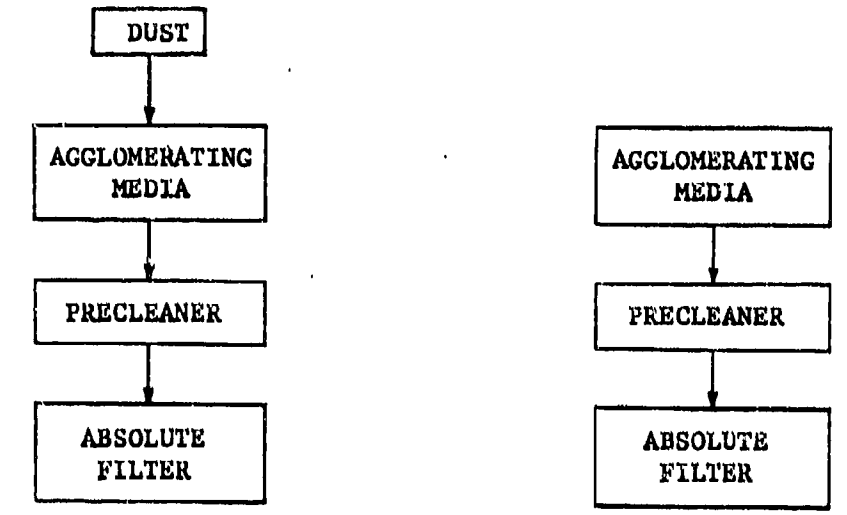

TEST METHOD 2

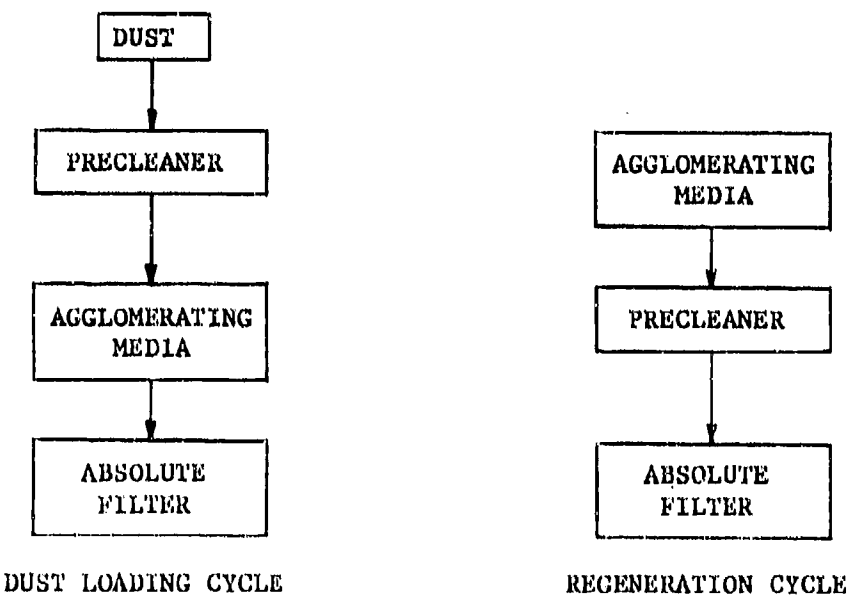

Figure 5-23. Illustration of Test Methods Used to Investigate Media Performance as a Function of Particle Size

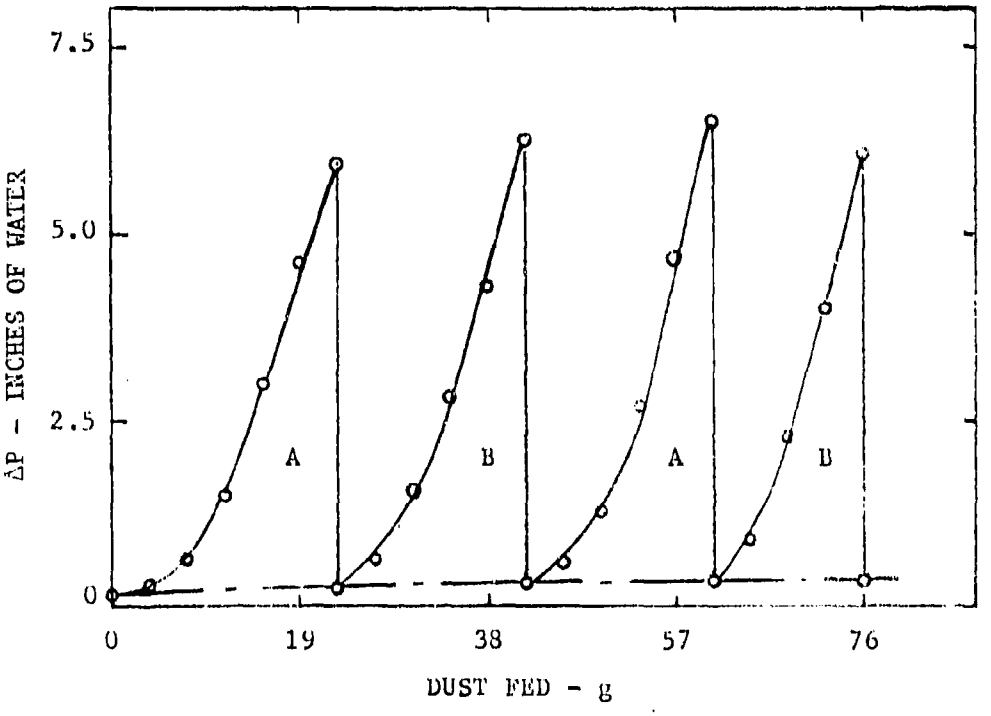

Figure 5-24. Pressure Drop Vs. Dust Fed, KC-2 Media, V_f = 36 fpm, AC Coarse Dust, Alternate Side Loading

Table 5-1. Summary of Results From Flat Sheet Testing of Candidate Media

Media* Code	Q (cfm)	V_f (fpm)	$\bar{E}_i$	$\bar{E}_\epsilon$	$\bar{E}_o$	Γ	Notes
KC-1	100	119	---	92.7	89.0	1.16	
KC-2	30	36	99.1	96.9	98.7	1.16	B
KC-2	30	36	97.4	91.6	95.7	1.10	
KC-2	30	36	99.0	97.5	98.4	1.17	B
KC-2	30	36	97.1	92.2	95.3	1.10	C
KC-2	30	36	99.1	94.9	98.3	1.14	B
KC-2	70	83	96.9	92.2	92.4	1.13	
KC-3	100	119	93.9	92.4	89.3	1.16	
KC-4	100	119	---	91.5	84.7	1.14	
KC-5	100	119	---	95.3	90.2	1.19	
KC-6	100	119	94.8	83.2	85.3	1.04	
KC-7	40	48	---	91.7	90.0	1.08	
KC-8	70	83	97.5	91.0	90.2	1.12	
KC-9	30	36	99.8	92.1	97.4	1.10	
KC-9	50	60	97.2	85.4	93.1	---	A
KC-9	70	83	97.8	91.7	91.8	1.13	
KC-10	30	36	99.9	90.5	97.0	1.08	
KC-10	40	48	---	92.6	90.0	1.10	
KC-11	30	36	99.6	90.4	97.5	1.08	
2067	45	45	94.3	90.4	---	1.06	A
2067	70	92	97.1	---	93.5	---	A
2067	70	92	96.2	87.2	92.2	1.07	A
JR-347FC	30	45	99.5	85.8	96.0	1.04	
JR-347	30	39	99.6	92.0	96.7	1.11	
JR-347	70	101	96.7	---	93.2	---	
JR-347	70	101	97.3	---	---	---	
JR-347FC	70	101	97.0	---	---	---	
JR-347	70	83	98.0	86.0	90.9	1.06	
JR-347FC	70	83	98.0	92.2	92.6	1.13	
HD-7-10S	70	144	---	---	---	---	
HD-7-10S	40	48	---	92.8	90.8	1.09	
1WT60X60	100	119	91.0	---	---	---	
1WT60X60	40	48	92.2	92.8	91.5	1.09	
1WT200X1400	40	48	95.2	---	90.7	---	
1WT165X1400	40	48	94.8	93.3	91.2	1.06	
1WT165X800	70	83	95.9	---	91.3	---	
1WT30X250	70	83	94.2	84.1	86.5	1.03	
1WT325X2300	40	55	95.1	90.1	90.0	1.02	
1WT200X1400	40	55	95.4	91.8	91.5	1.04	

Table 5-1. Summary of Results From Flat Sheet Testing of Candidate Media (Continued)

Media Code	Q (cfm)	V_f (fpm)	$\bar{E}_i$	$\bar{E}_s$	$\bar{E}_o$	Γ	Notes
T527C	40	48	95.3	92.3	92.6	1.09	
74/64PE16	40	48	94.0	91.3	91.9	1.08	
74/64PE16	40	48	95.0	86.9	88.4	1.04	
74/64PE16	40	48	95.1	---	88.8	---	
74/64PE12	70	83	98.0	91.2	91.7	1.12	
HO 1001	40	62	---	87.5	91.4	1.03	
PE 1001	40	65	---	89.6	89.8	1.06	
PE 1003	40	62	84.3	86.8	---	1.02	
S-1250-9517	30	77	98.1	84.6	95.42	1.05	
PE76K-27	100	119	95.3	92.8	90.5	1.16	
PE90K-12	40	48	---	94.0	89.1	1.07	
2F/777C	70	83	95.6	91.0	92.4	1.12	
E35	40	48	96.0	90.3	92.8	1.06	
E35	40	48	96.0	89.6	90.4	1.06	
681-C	40	48	---	90.2	89.3	1.06	
1607-S	40	48	92.9	91.2	91.6	1.08	
1607-S	40	48	---	89.2	91.6	1.05	
0805-S	40	58	97.0	81.3	93.3	---	
0805-S	70	83	96.8	90.5	90.5	1.11	
0805-S	30	39	99.9	96.0	93.9	1.19	
0805-S	70	83	99.2	89.3	92.2	1.10	
BP315	30	43	95.8	87.2	90.6	1.08	
BP315	30	43	97.9	96.7	97.0	1.19	
BP312	15	22	97.6	---	---	---	
BP312	20	29	96.0	86.3	92.6	1.08	
BP312	20	29	97.4	88.2	95.1	1.10	D
BP312	20	29	97.5	88.9	95.2	1.11	D
BP312	30	43	89.1	84.2	82.3	1.05	D
BP312	20	29	96.2	87.6	92.2	1.10	D
BP312	30	39	94.6	76.5	92.2	---	
BP312	15	22	97.1	80.4	93.7	---	D
BP312	20	29	95.9	84.4	93.7	1.06	
U2.5	30	36	99.7	84.1	98.1	1.01	

Table 5-1. Summary of Results From Flat Sheet Testing of Candidate Media (Continued)

Media* Code	Q (cfm)	V_f (fpm)	$\bar{E}_i$	$\bar{E}_e$	$\bar{E}_o$	Γ	Notes
GT3	70	92	95.0	86.4	87.9	1.06	
GT3	50	66	98.0	85.0	92.9	---	A
GT3	30	39	99.2	---	---	---	A
GT3	50	66	97.7	84.2	94.5	---	A
GT3	50	66	98.2	84.5	94.5	---	A
GT3	50	66	98.2	90.1	91.9	1.06	A
TFD272X6	40	110	91.4	94.1	90.1	1.11	
TFD272X13	100	267	---	90.6	89.1	1.13	
GR952	40	82	---	94.0	89.7	1.11	
14X14X.018	100	119	---	89.2	89.8	1.12	
18X14X.0134	100	119	94.8	89.8	89.2	1.12	
20X20X.011	100	119	---	89.6	89.6	1.12	
MM1	40	48	92.2	92.8	91.5	1.09	
110-01-100	30	36	92.6	88.7	91.3	1.10	
OS-83-91	40	82	---	89.3	91.6	1.05	
OS-83-91	70	144	---	86.7	84.0	1.07	

Table 5-1. Summary of Results From Flat Sheet Testing of Candidate Media (Continued)

* Manufacturers listed in Appendix C

Q Airflow, cfm

V_f Media face velocity, fpm

$\overline{E}_\iota$ Average efficiency during loading, percent

$\overline{E}_\epsilon$ Average efficiency during regeneration, percent

$\overline{E}_o$ Overall average efficiency for test, percent

Γ Ratio of precleaner efficiency with agglomeration to precleaner efficiency without agglomeration

A Some leakage @ filter holder or in duct upstream of precleaner

B Precleaner, then media, then precleaner during regeneration (Test method 2)

C Alternate side loading

D Double normal concentration (normal concentration: 0.025 g/ft^3 air, AC Coarse dust)

filter. In practice, these are precisely the particles that must be agglomerated and introduced to the precleaner for removal. Therefore, in the test method used to generate the data shown in Figures 5-21 and 5-22, dust was fed first to the precleaner, then the agglomerator, and then back to the precleaner during the cleaning cycle. In the conventional test method, dust was fed to the agglomerator first, then dumped into the precleaner during the agglomerator cleaning cycle. These methods are illustrated in Figure 5-23.

It is significant that operation with method 2 provided excellent performance, particularly during cleaning, even though the dust reaching the agglomerator was considerably finer than the coarse being fed to the precleaner. In fact, these data indicate that the method 2 type operation may offer excellent potential for overall system optimization. For instance, Figure 5-22 shows that method 2 provided for a 33 percent reduction in cleaning frequency, with a significant increase in overall system efficiency. Comparing media JR347 (Figure 5-19, test method 1) with KC-2 (Figure 5-21, test methods 1 and 2) further demonstrates the advantage of method 2 operation. In 10 cycles, the KC-2 media (method 2) handled nearly twice as much dust as the JF347 media, even though the performance of both media was nearly identical under test method 1. Furthermore, the length of the tenth loading cycle for the KC-2 material was characteristic of previous cycles, indicating stable performance. Overall system operating efficiency for the media/precleaner assembly was 98.3 percent versus 96.0 percent for the JR media/precleaner unit.

Figure 5-24 illustrates another interesting property of the KC-2 media, namely, that either side of this media may be suitable for the agglomerating barrier. During this brief test, dust was alternately fed to each side of the media, with reasonably good results. As can be seen, pressure drop recovery was good on each side. Of course, this test was only intended to indicate potential feasibility; a much longer test would be needed to indicate overall performance. Clearly, media that can be loaded and cleaned on either side offer maximum design flexibility.

Overall, results from the flat sheet evaluation program clearly demonstrate the advantage of the agglomeration concept. In many cases, significant improvements were made in precleaner operating performance compared to the unagglomerated case. Furthermore, several suitable agglomerating media seem to be available. In the next phase of the program, attention was directed toward depth-type media, primarily to investigate potential for the "straight through" design concept.

5.4.2. Depth-type agglomerators. Three depth-type agglomerators were investigated: meshes, foams, and packed beds. For the most part, these agglomerators were tested in their straight-through configuration, although some work was done with the meshes to investigate regeneration by reversed flow. Overall performance for these agglomerators was good, indicating feasibility for the straight-through approach and good potential for on-vehicle integration, particularly for the meshes and foams. The packed beds (beads) are less attractive because of possible attrition and settling.

5.4.2.1. Meshes. The behavior of mesh-type agglomerators was investigated by testing several configurations composed of layers having different sized polypropylene filaments. As shown in Table 5-2, filament sizes ranged from 2 to 37 mils (50 to 925 μm) and face velocities ranged from 115 to 380 feet per minute. Both

Table 5-2. Mesh Agglomerator Configurations and Test Parameters

Unit	Configuration*	Position	Test Method	V_f Range, fpm
1	1A4B4C2A4D1A	H	R	380
2	2A4B4C4D3A	H	R	380
3	7A (4" deep)	H	S	277-380
4	3A4B2C4D2C2A	H/V	S	115-380
5	3A4B4C2A	V	S	380

H - horizontal ⊥ to flow
V - vertical ⊥ to flow
R - reverse flow cleaning
S - straight-through operation

A**37/94 (925 μm)
B 8/96 (200 μm)
C 4/96 (100 μm)
D 2/96 (50 μm)

*Upstream component listed first.
**Polypropylene (filament size in mils/percentage of free void space), Kimre Inc.

horizontal and vertical orientations were used and straight-through and reversed flow regenerations were accomplished. Dust concentrations (coarse dust) ranged from 0.013 to 0.050 g/ft^3, with most testing being accomplished at 0.025 g/ft^3 air. Scavenge flows for the precleaner were set from 10 to 17 percent and different precleaner configurations (in terms of the number of swirl tubes used or the type of precleaner) were employed at various stages of testing.

Performance with the mesh agglomerators was generally good. For the most part, system efficiency increased by more than 10 percentage points compared to the unagglomerated case. Pressure drop stability and recovery were also good, in both the straight-through and reverse flow configurations. Figures 5-25 and 5-26 show system efficiency and agglomerator pressure drop as a function of dust loading for unit 4, in the straight-through configuration. The face velocity across the unit varied during testing because primary and secondary (scavenge) flows were varied. In one case, a 15 percent scavenge was set to increase precleaner efficiency slightly toward more normal levels so that better particle size data could be obtained with respect to typical precleaner operation (this particular precleaner was designed for a specific application requiring a lower efficiency, ~83-84 percent, on coarse dust). The particle size work is discussed in Section 5.4.3. In another case downstream leakage caused the primary airflow to be lower than planned, also resulting in a lower face velocity. As a result, performance represents operation over a range of face velocities, which is actually more representative of vehicle operation. The face velocity range for Mesh Agglomerator No. 4 during tests 6 to 77 is shown in Figure 5-27.

Performance data for test runs 171 to 181, for Unit 4, are given in Figures 5-28 and 5-29. Prior to these tests, the unit was cleaned and reinstalled, and the test network was checked and repaired as necessary. The pressure drop profile for the precleaner and agglomerator at the outset of these tests is given in Figure 5-30. Testing was conducted at a face velocity of 380 fpm. Overall system efficiency for the agglomerator and precleaner averaged 95.5 percent, compared to about 84 percent for the baseline case (precleaner only). On-line cleaning by mechanical shock (tapping the agglomerator housing) produced excellent pressure drop recovery. During these tests, the pressure drop peaks were allowed to reach 6-11 inches of water before regeneration was attempted. This was because one of the test objectives was to investigate whether or not steady-state conditions could be obtained for each configuration prior to reaching excessive pressure drop levels. In this case, mechanical aid was required to cause regeneration. In practice, regeneration for this particular agglomerator would likely be initiated at much lower pressure drop levels, say 4-5 inches of water, to enhance life of the overall system (note Section 5.5).

To investigate operation at a lower pressure drop levels (loaded) and to seek on-line steady-state operation, unit 4 was modified by removing the 50 μm filament package, producing configuration 5. Results for this unit are shown in Figures 5-31 and 5-32. Testing was accomplished at a fairly steady face velocity of 380 fpm. Pressure drop stabilization was obtained at about 2-inches of water and average system efficiency was 93.5 percent. These results are particularly encouraging because they indicate potential for successful, steady-state operation for the straight-through configuration. Furthermore, successful operation at high face velocity will enhance system-vehicle integration.

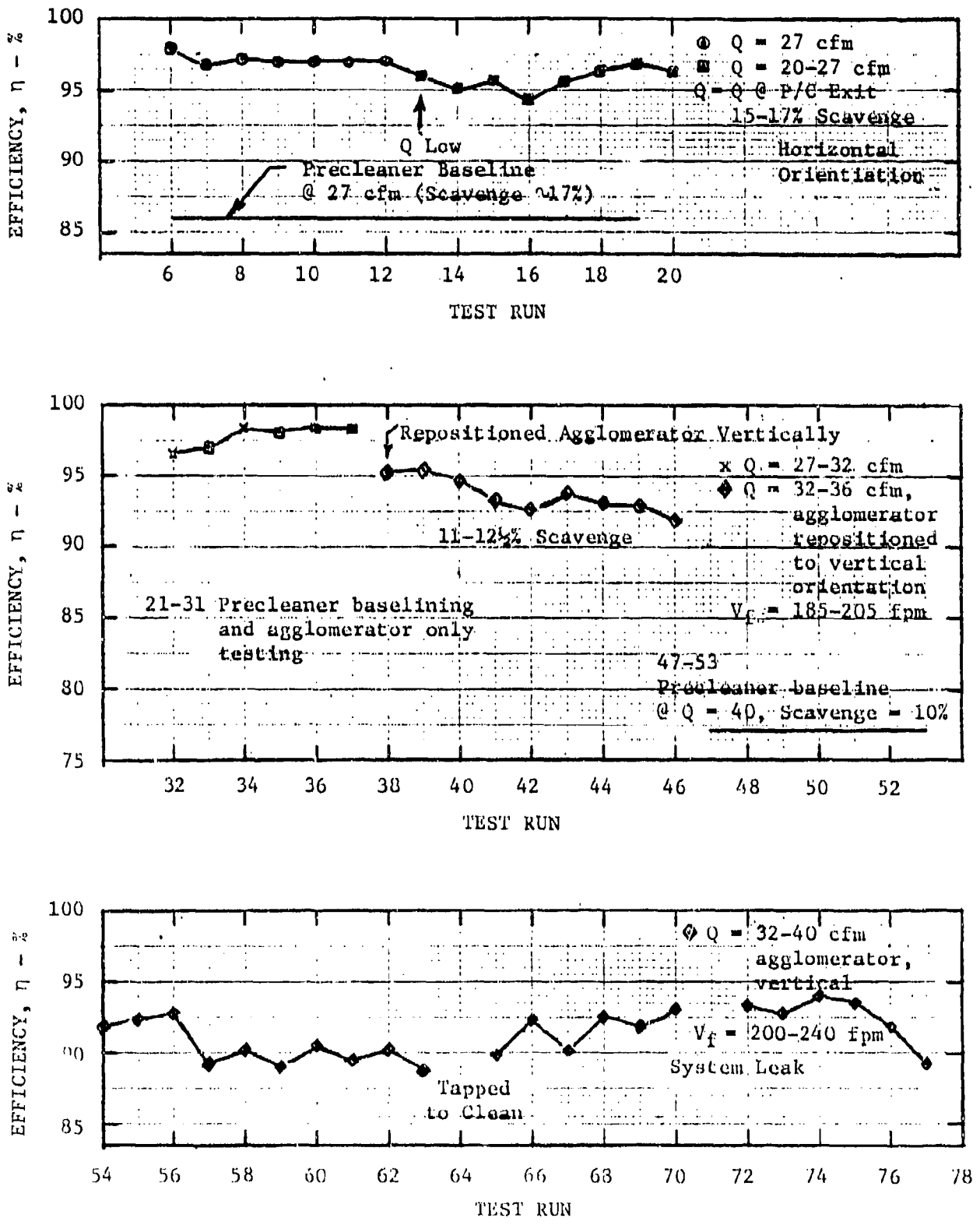

Figure 5-25. System Efficiency (precleaner and agglomerator) per Test Run, Fresh Agglomerator No. 4, V_f = 115 - 230 fpm, AC Coarse Dust, Straight-Through Configuration

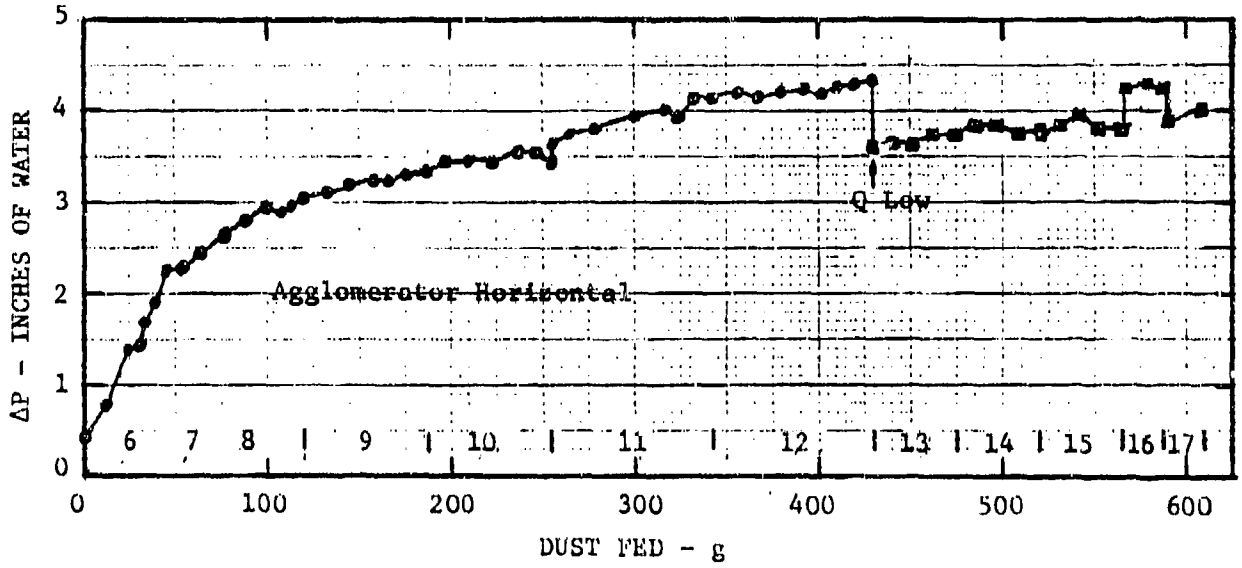

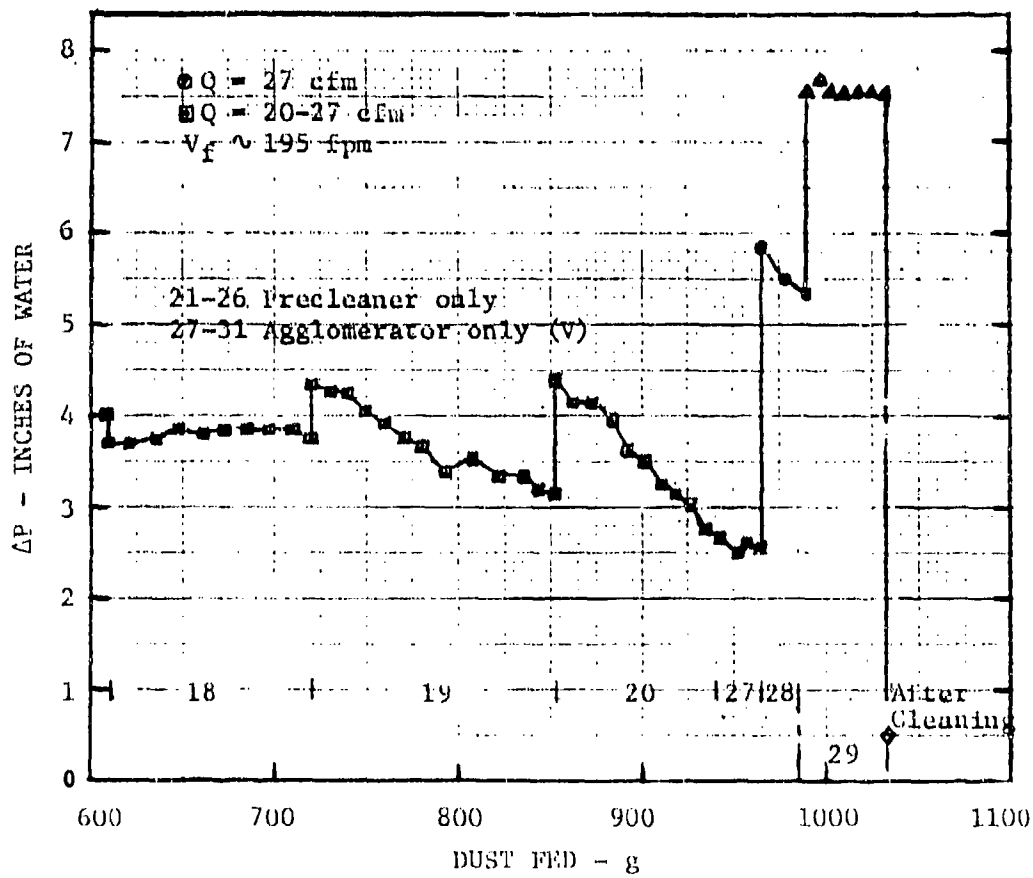

Figure 5-26. Agglomerator Pressure Drop as a Function of Dust Fed, Mesh Agglomerator NO. 4, V_f = 115 - 230 fpm, AC Coarse Dust, Straight-Through Configuration

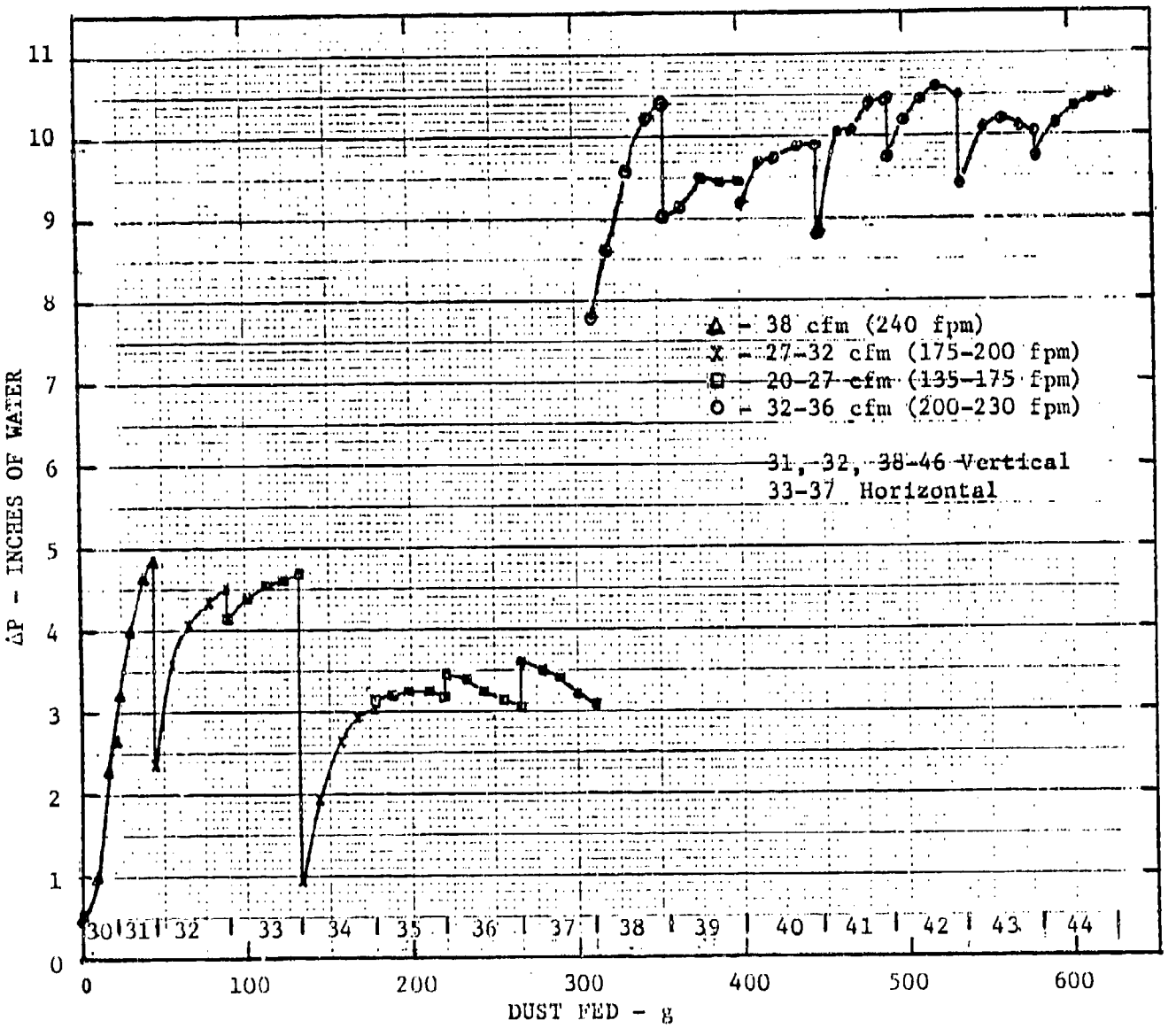

Figure 5-26. Agglomerator Pressure Drop as a Function of Dust Fed, Mesh Agglomerator No. 4, V_f = 115-230 fpm, AC Coarse Dust, Straight-Through Configuration (Continued)

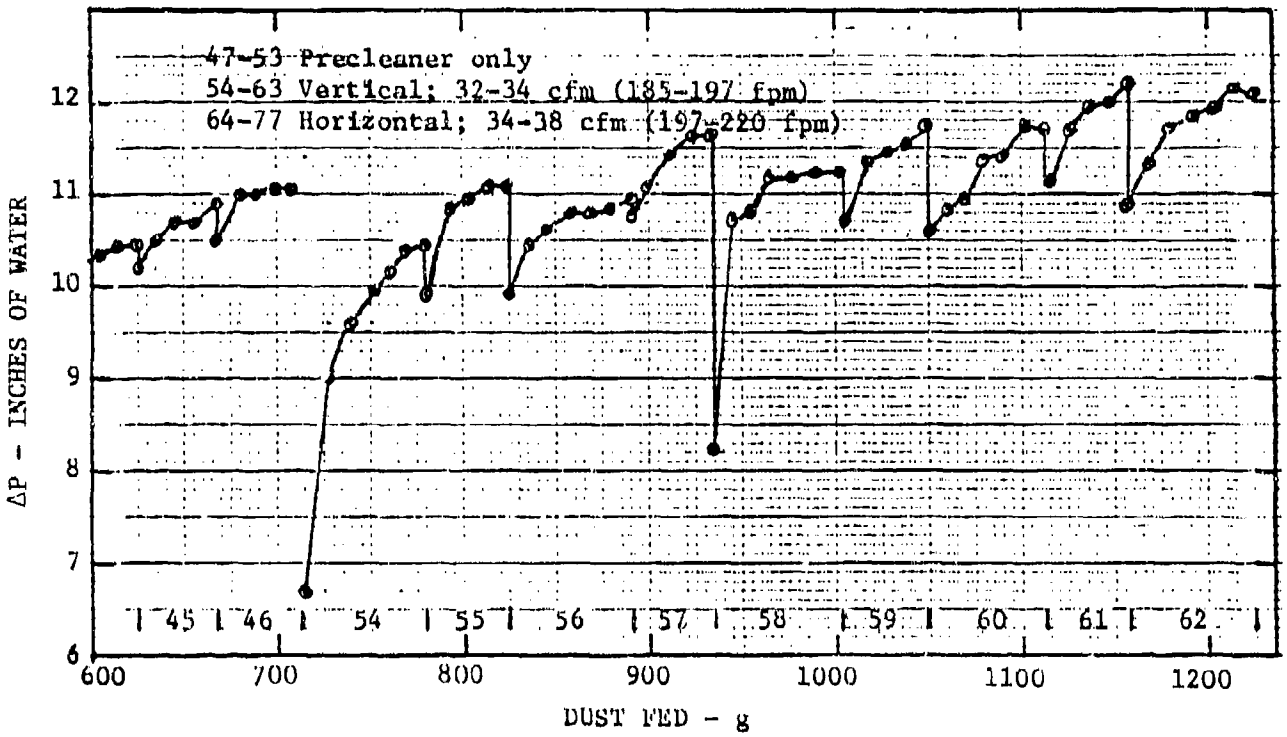

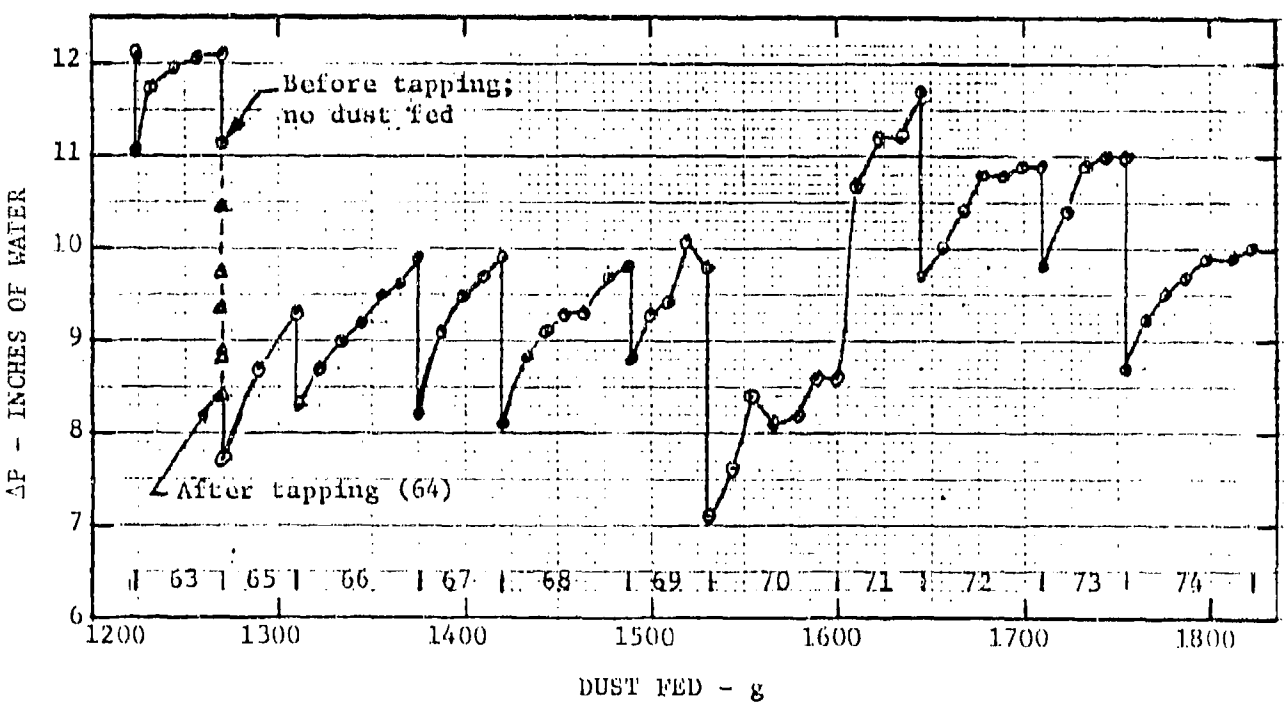

Figure 5-26. Agglomerator Pressure Drop as a Function of Dust Fed, Mesh Agglomrator No. 4, V_f = 115 - 230 fpm, AC Coarse DUST, Straight-Through Configuration (Continued)

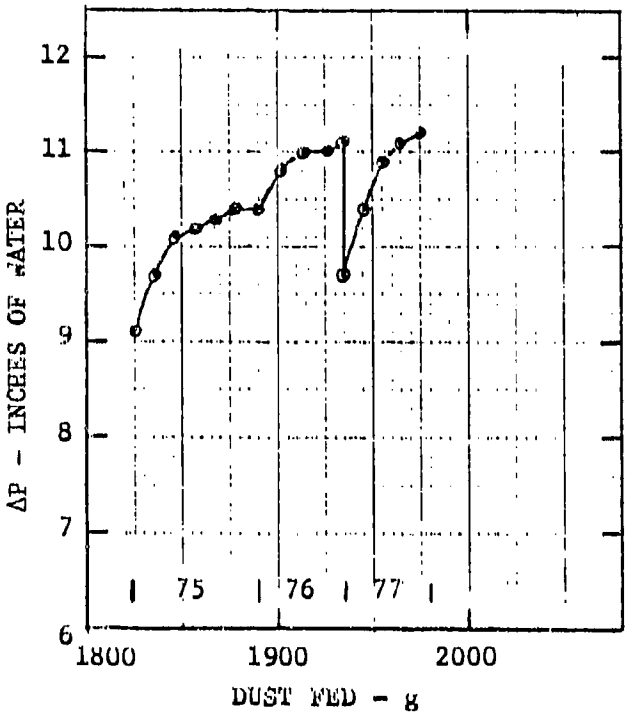

Figure 5-26. Agglomerator Pressure Drop as a Function of Dust Fed, Mesh Agglomerator No. 4, V_f = 115 - 230 fpm, AC Coarse Dust, Straight-Through Configuration (Continued)

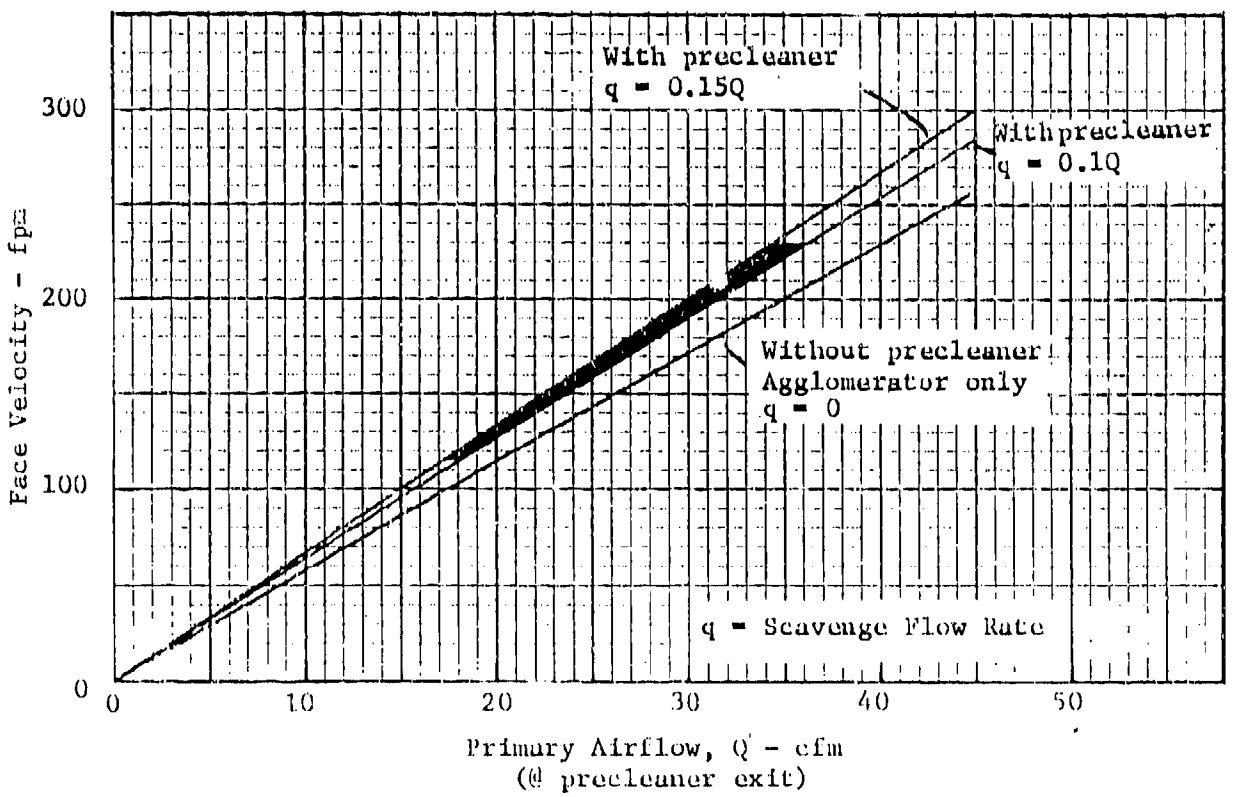

Figure 5-27. Face Velocity Range as a Function of Primary Airflow for Mesh Agglomerator No. 4 During Test Series 6-77

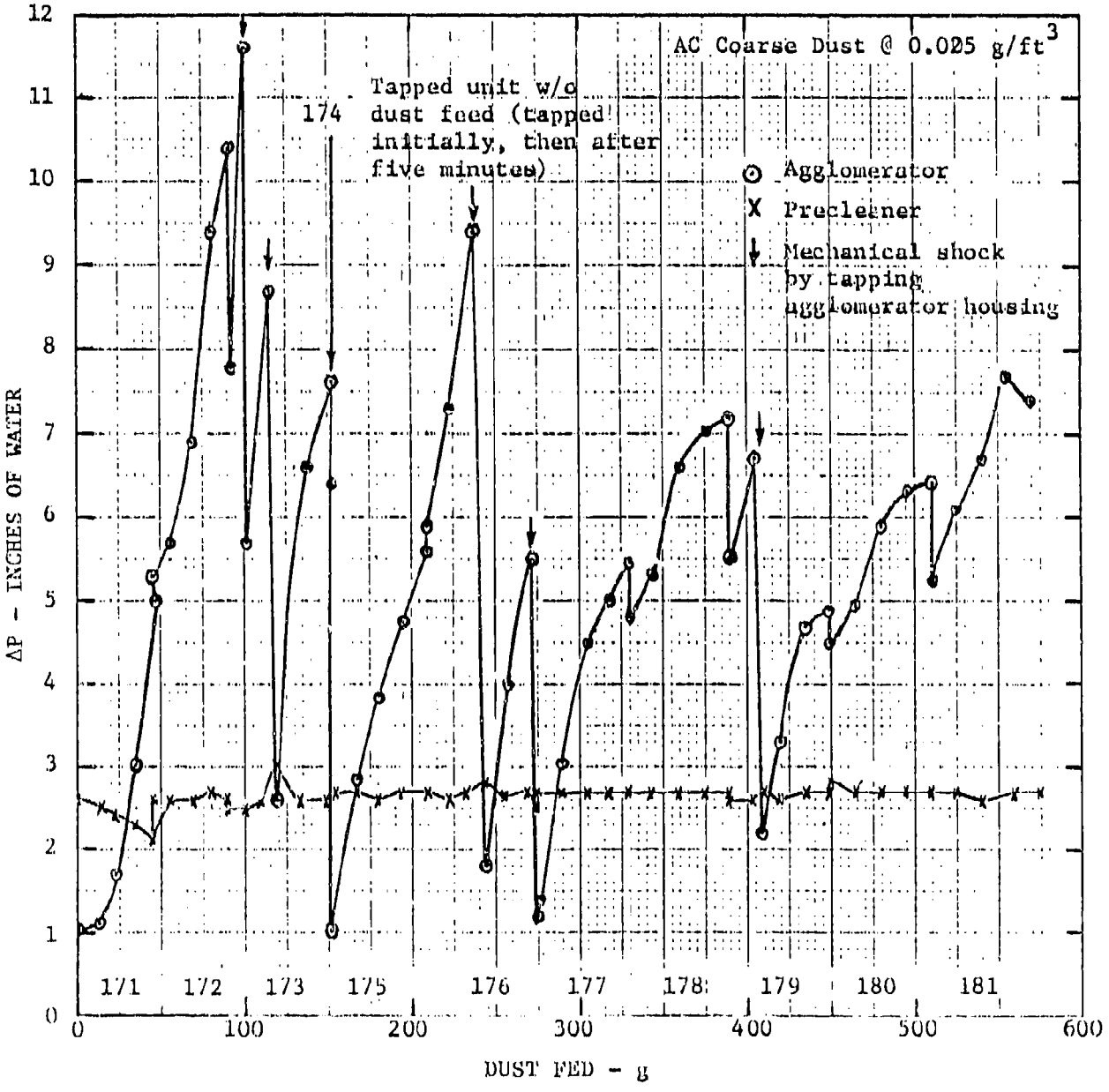

Figure 5-28. Agglomerator and Precleaner Pressure Drop as a Function of Dust Fed, Mesh Agglomerator No. 4, V_f = 380 fpm, AC Coarse Dust, Straight-Through Configuration (Runs 171-181)

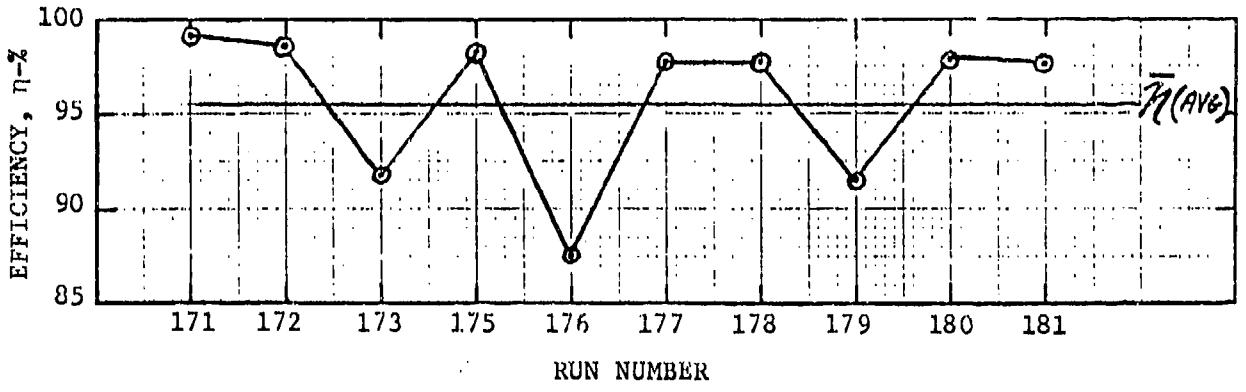

Figure 5-29. System Efficiency (precleaner and agglomerator) per Test Run, Mesh Agglomerator No. 4, V_f = 380 fpm, AC Coarse Dust, Straight-Through Configuration (Runs 171-181)

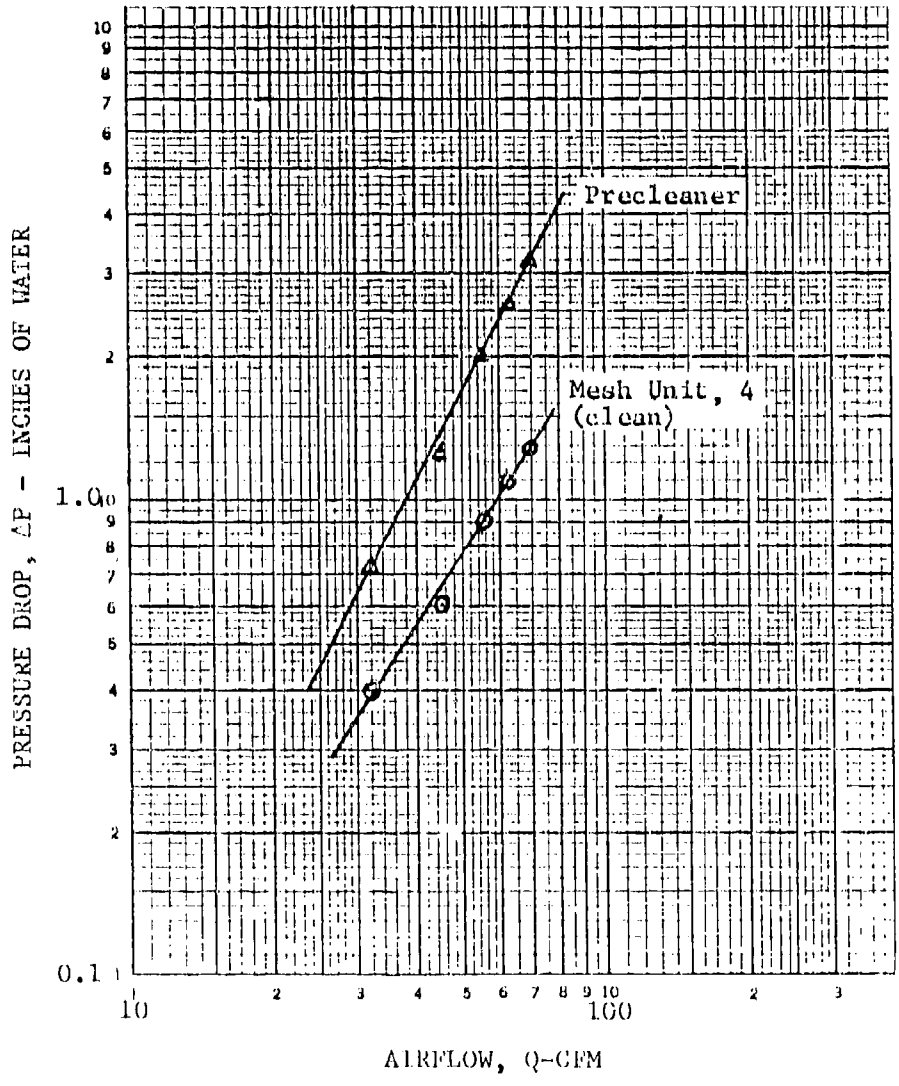

Figure 5-30. Pressure Drop Profile for Precleaner and Agglomerator at the Start of Test Run 171

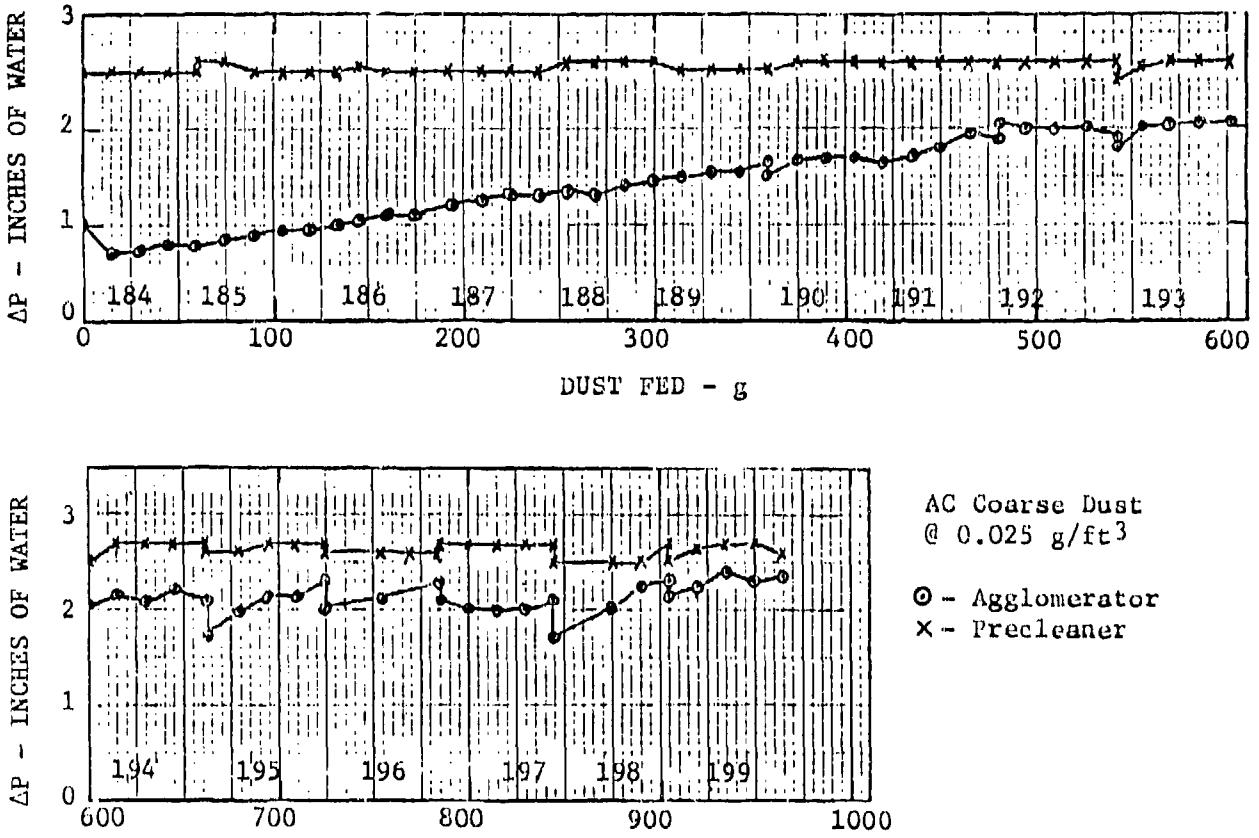

Figure 5-31. Agglomerator and Precleaner Pressure Drop as a Function of Dust Fed, Mesh Agglomerator No. 5, V_f = 380 fpm, AC Coarse Dust, Straight-Through Configuration (Runs 184-199)

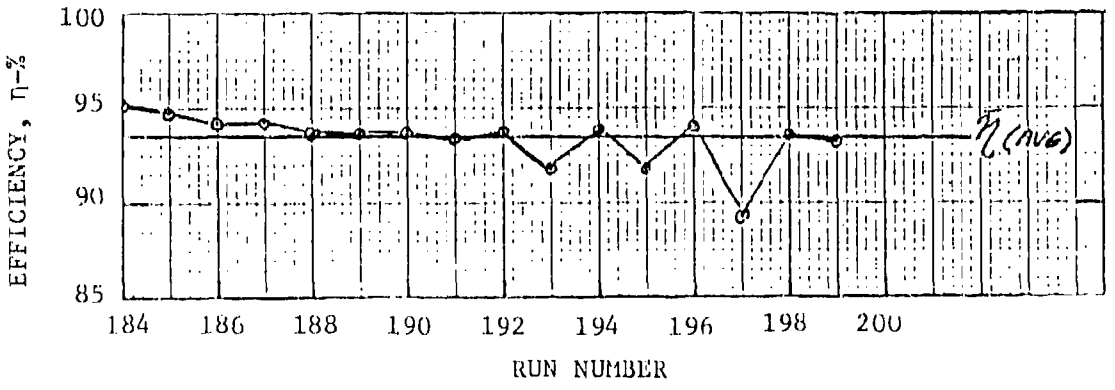

Figure 5-32. System Efficiency (precleaner and agglomerator) per Test Run, Mesh Agglomerator No. 5, V_f = 380 fpm, AC Coarse Dust, Straight-Through Configuration (Runs 184-199)

5.4.2.1.1. Reverse flow regeneration. Tests were also conducted in which unloading was accomplished by reversing the airflow. The face velocity for these tests was 388 fpm, with the flow during loading being directed vertically upward through horizontal layers of the agglomerator. Representative data for three particular mesh configurations are shown in Figures 5-33 and 5-34. As can be seen, cleanability was excellent in each case, although overall efficiencies were lower than desired. This was probably due to the extremely high face velocity, which likely caused some particle breakup during backflushing and which may have been too high to allow efficiency agglomeration during loading. As with the straight-through units, testing was not accomplished to determine the optimum face velocity or to measure performance as a function of face velocity over a wide range of potential operating conditions.

5.4.2.2. Foams. Testing was conducted using an agglomerator consisting of four, ½-inch layers of reticulated flexible polyester urethane foam, graded from 30 to 60 pores-per-linear inch (ppi) (30, 30, 45, 60 ppi). The flow characteristics for this agglomerator (clean) and for the particular precleaner configuration used during testing are shown in Figure 5-35. During testing, face velocity ranged from 150 to 280 fpm. Efficiency and dust loading data are shown in Figures 5-36 and 5-37.

As can be seen, efficiency improved significantly, partly because the foam agglomerator also acted as a prefilter. Typically, improvements of over 10 percentage points were common, at both the higher and lower flows. Cumulative performance was also good, both in terms of efficiency and pressure drop recovery. On-line regeneration by tapping the housing between runs 145 and 146 produced nearly a 100% recovery in pressure drop. In practice, this particular agglomerator would likely be regenerated (on-line) at much lower pressure drop levels, for instance, 4 to 5 inches of water. In this case, the dust exposure level for the agglomerator would be about 30 g/in^2 at a face velocity of 200 fpm. Because some problems were encountered in maintaining the desired test airflow, overall results actually indicate performance over a range of flowrates, generally indicating above average performance. As with the mesh agglomerator, the particle size distribution exiting the precleaner when the agglomerator was on-line was not significantly different from that for the precleaner only (Figure 5-48).

Even better results can be expected after optimization, during which several foam arrangements would be tried so that performance could be characterized over a wider range of airflows and face velocities. System design with respect to agglomerate unloading would also be further investigated. The available data suggest that a foam agglomerator could function both as a partial precleaner and as an agglomerator, and that significant amounts of dust could probably be removed from the system prior to entry into the precleaner if the housing and ductwork for the agglomerator were properly designed. During testing, a large amount of dust was found around the base of the agglomerator, particularly after mechanical regeneration. This dust, which represents the fall-out of heavy agglomerates, should be removable when appropriate ducting is used.

5.4.2.3. Packed beds. Testing was also conducted on a packed-bed, vertically oriented, granular bed agglomerator. Effective bed thickness was one inch; the bed being composed of randomly-packed, non-uniformly sized alumina coated (Al_2O_3) beads having the size distribution given in Figure 5-38. A baffle was included to

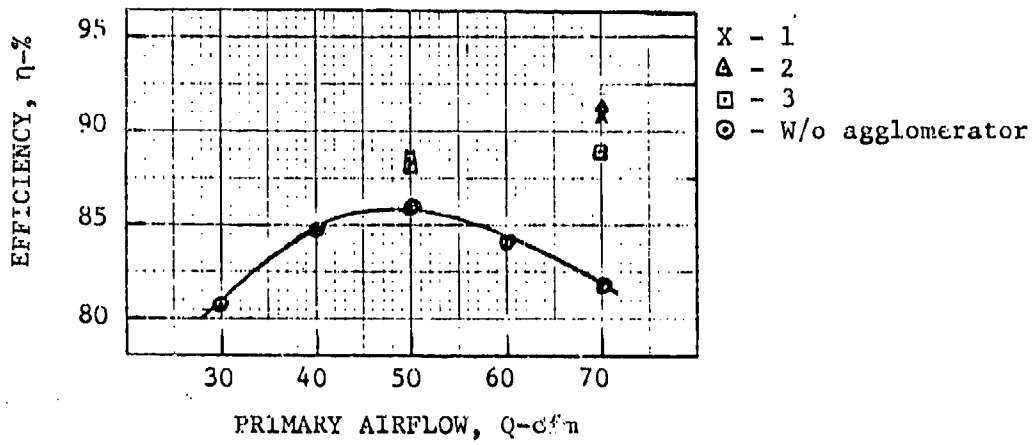

Figure 5-33. Overall Efficiency for a Single Tube Inertial Separator as a Function of Airflow Rate, With and Without Mesh Agglomerator (Configurations 1, 2, and 3), AC Coarse Dust

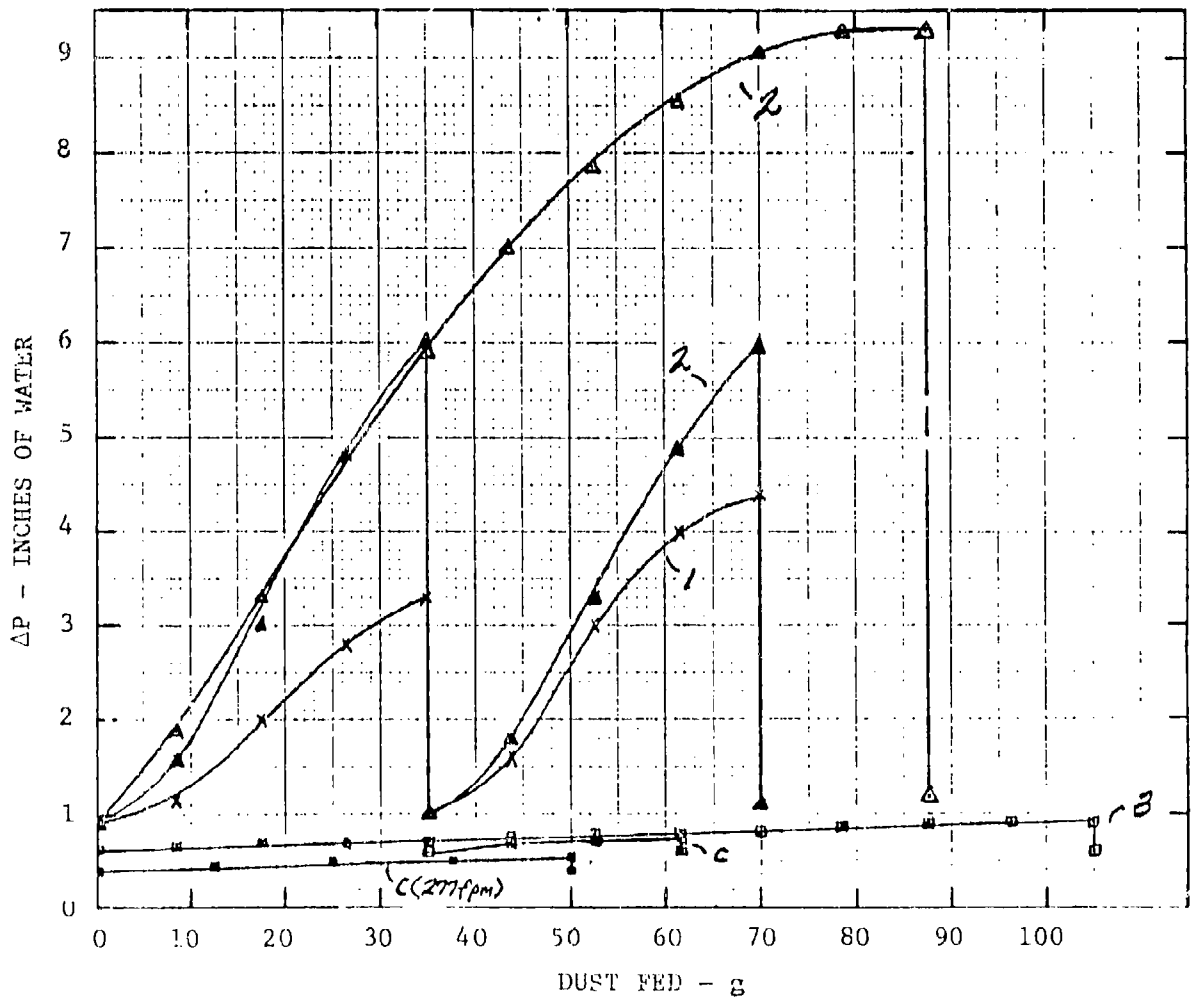

Figure 5-34. Pressure Drop Vs. Dust Fed for Mesh Agglomerators 1, 2, and 3 with Reverse Flow Cleaning, Vf = 388 fpm, AC Coarse Dust

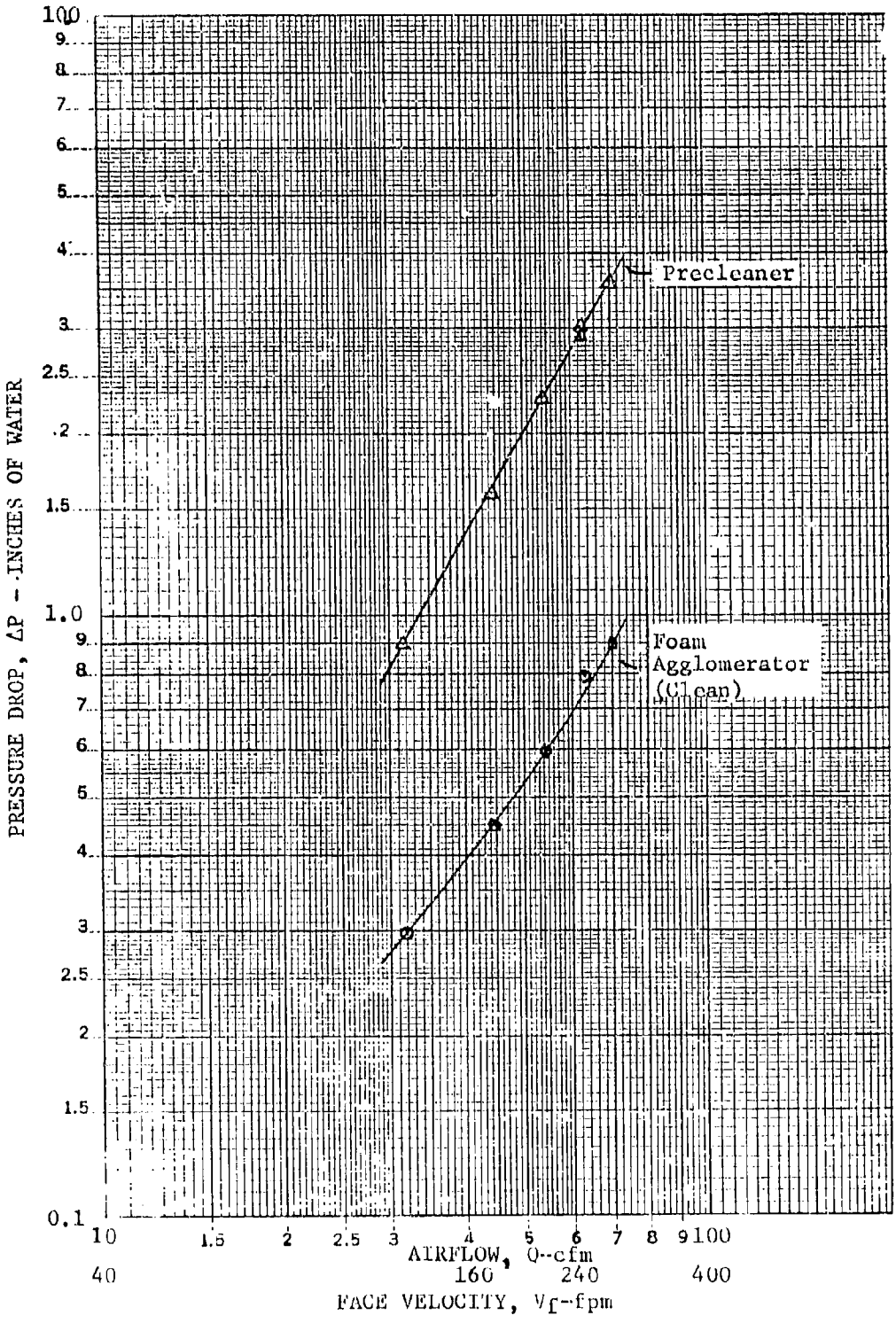

Figure 5-35. Pressure Drop Profile for Foam Agglomerator and for Precleaner Configuration Used During Foam Agglomerator Testing

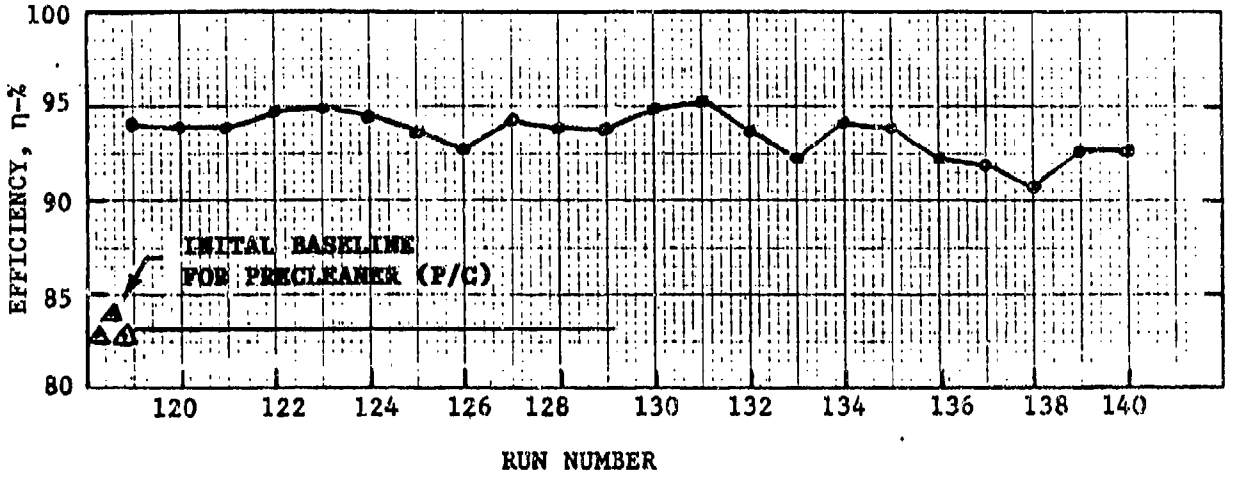

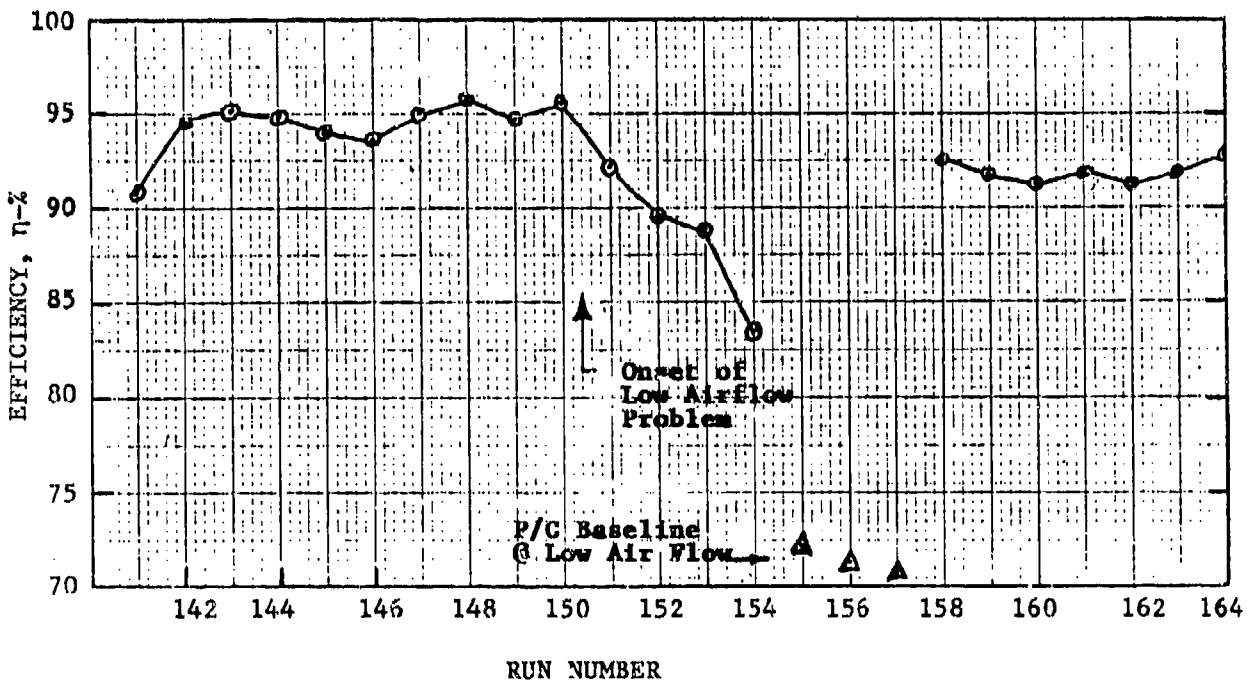

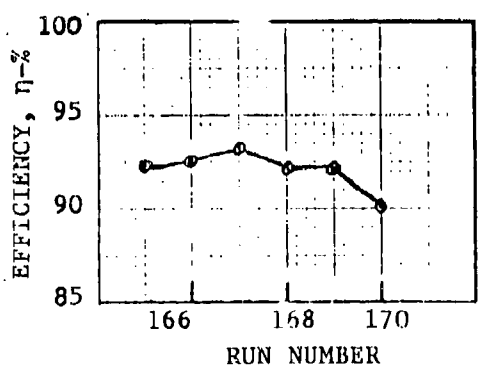

Figure 5-36. System Efficiency (precleaner and agglomerator) per Test Run, Foam Agglomerator, V_f = 150 - 280 fpm, AC Coarse Dust

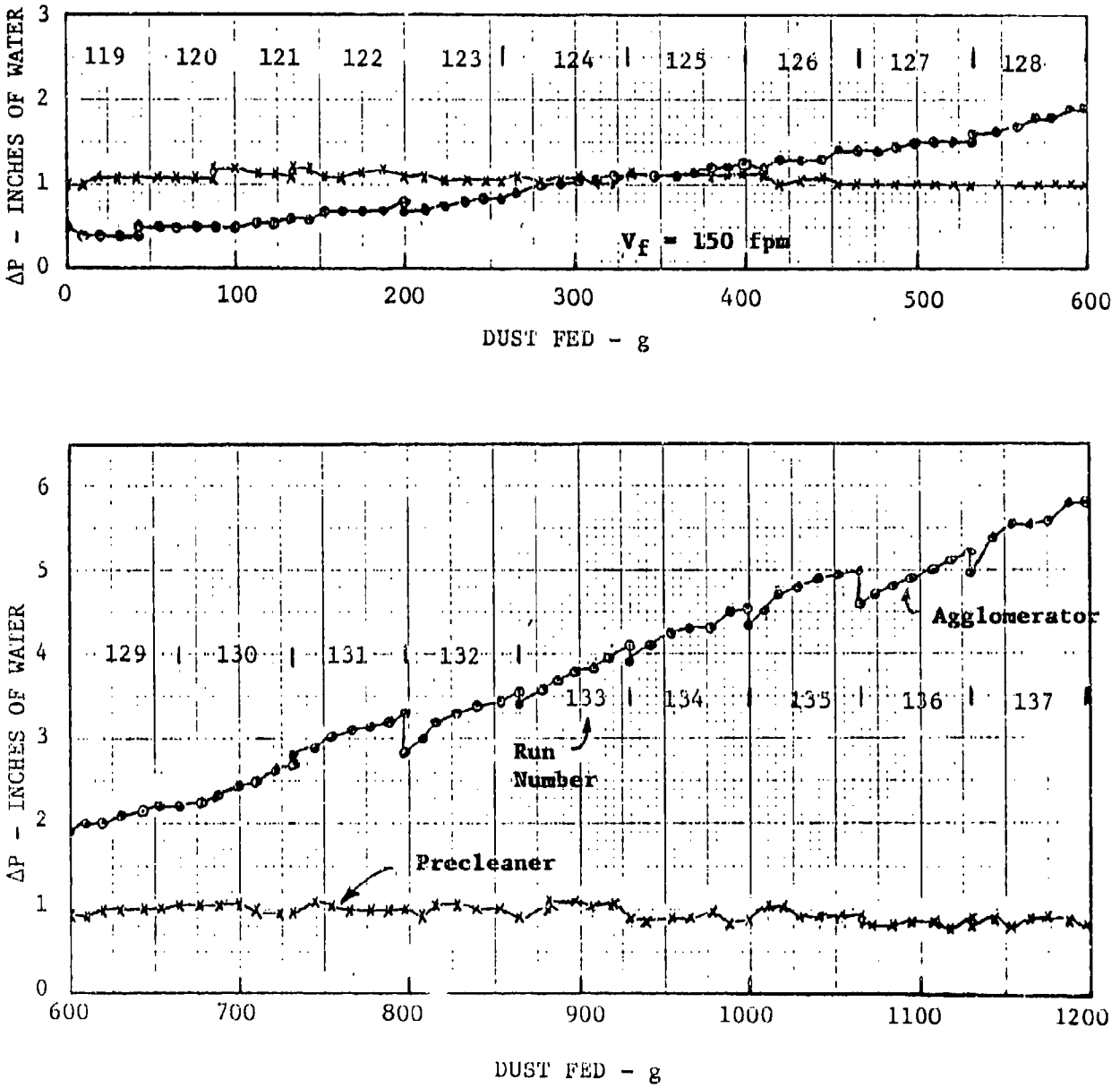

Figure 5-37. Pressure Drop Vs. Dust Fed for Foam Agglomerator, V_f = 150-280 fpm, AC Coarse Dust

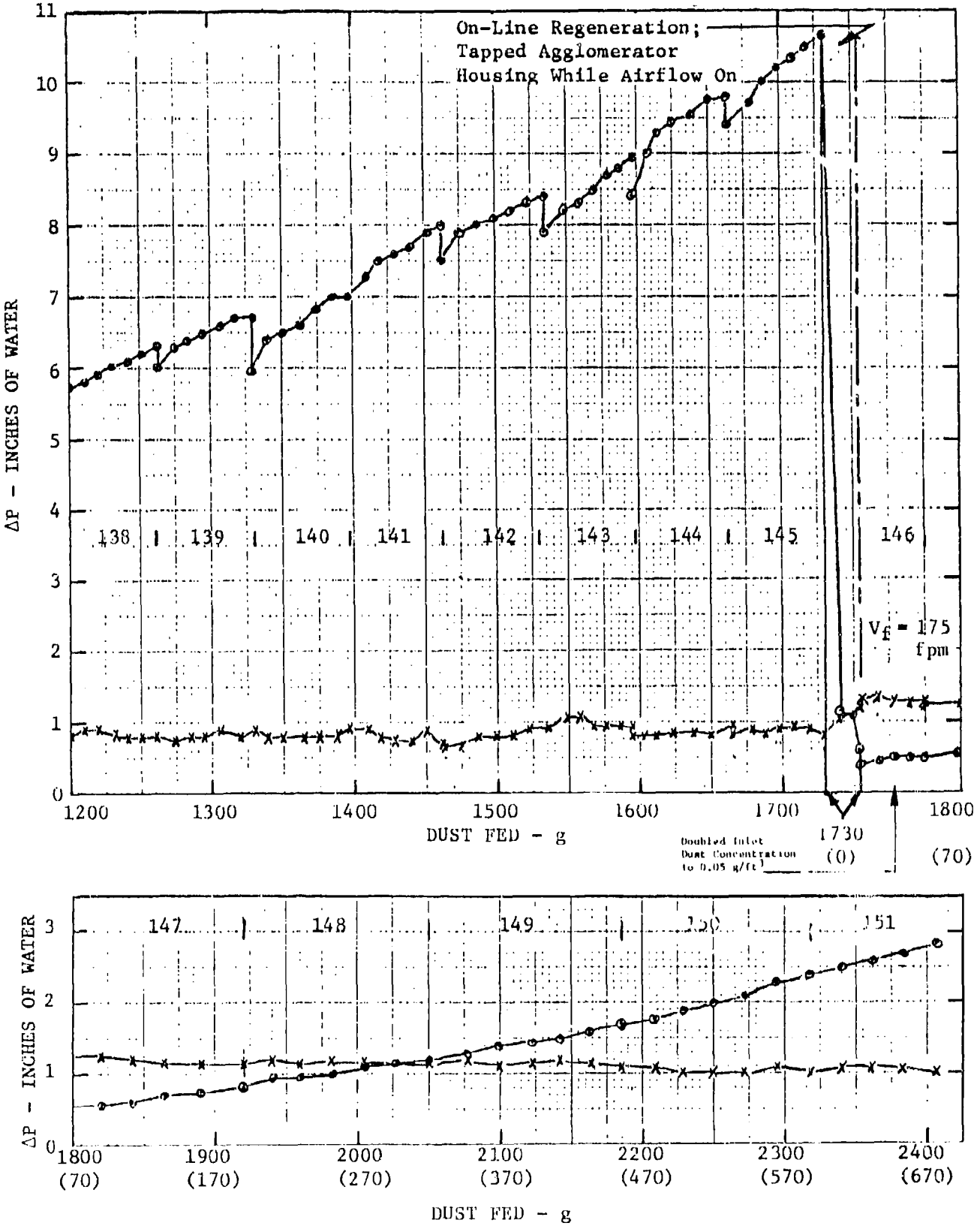

Figure 5-37. Pressure Drop Vs. Dust Fed for Foam Agglomerator, V_f = 150 - 280 fpm, AC Coarse Dust (Continued)

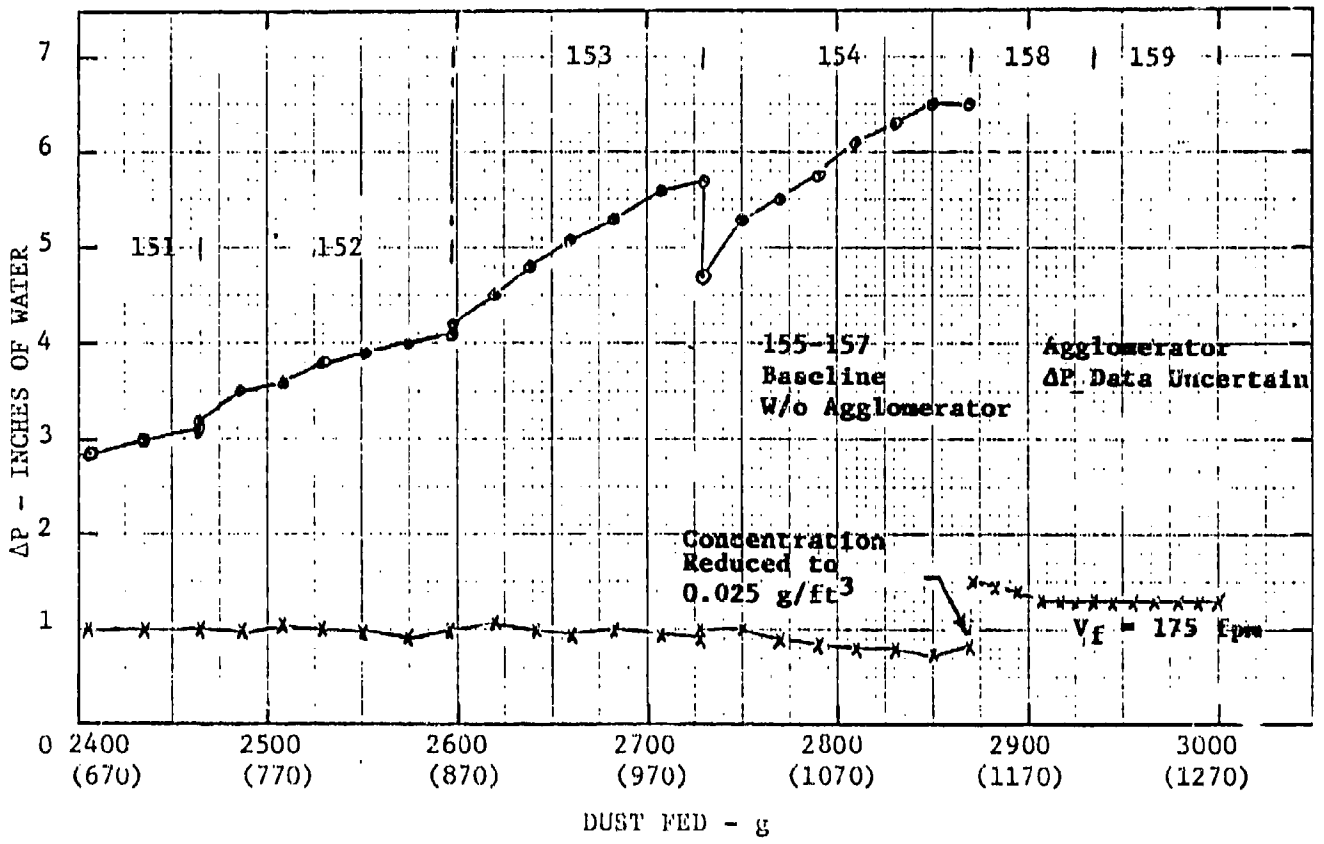

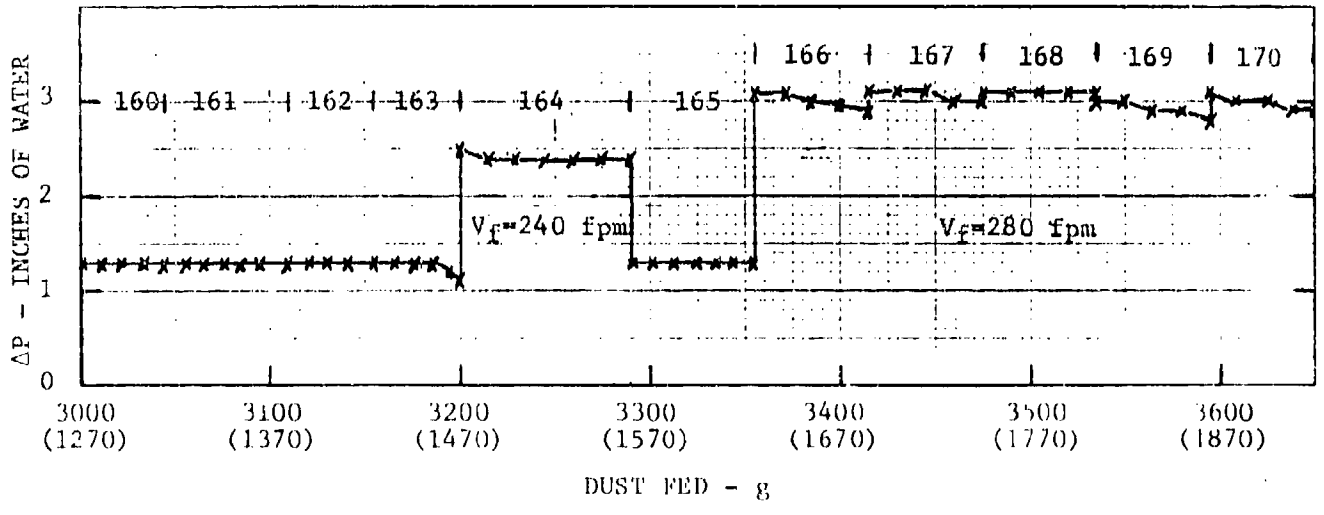

Figure 5-37. Pressure Drop Vs. Dust Fed for Foam Agglomerator, V_f = 150 - 280 fpm, AC Coarse Dust (Continued)

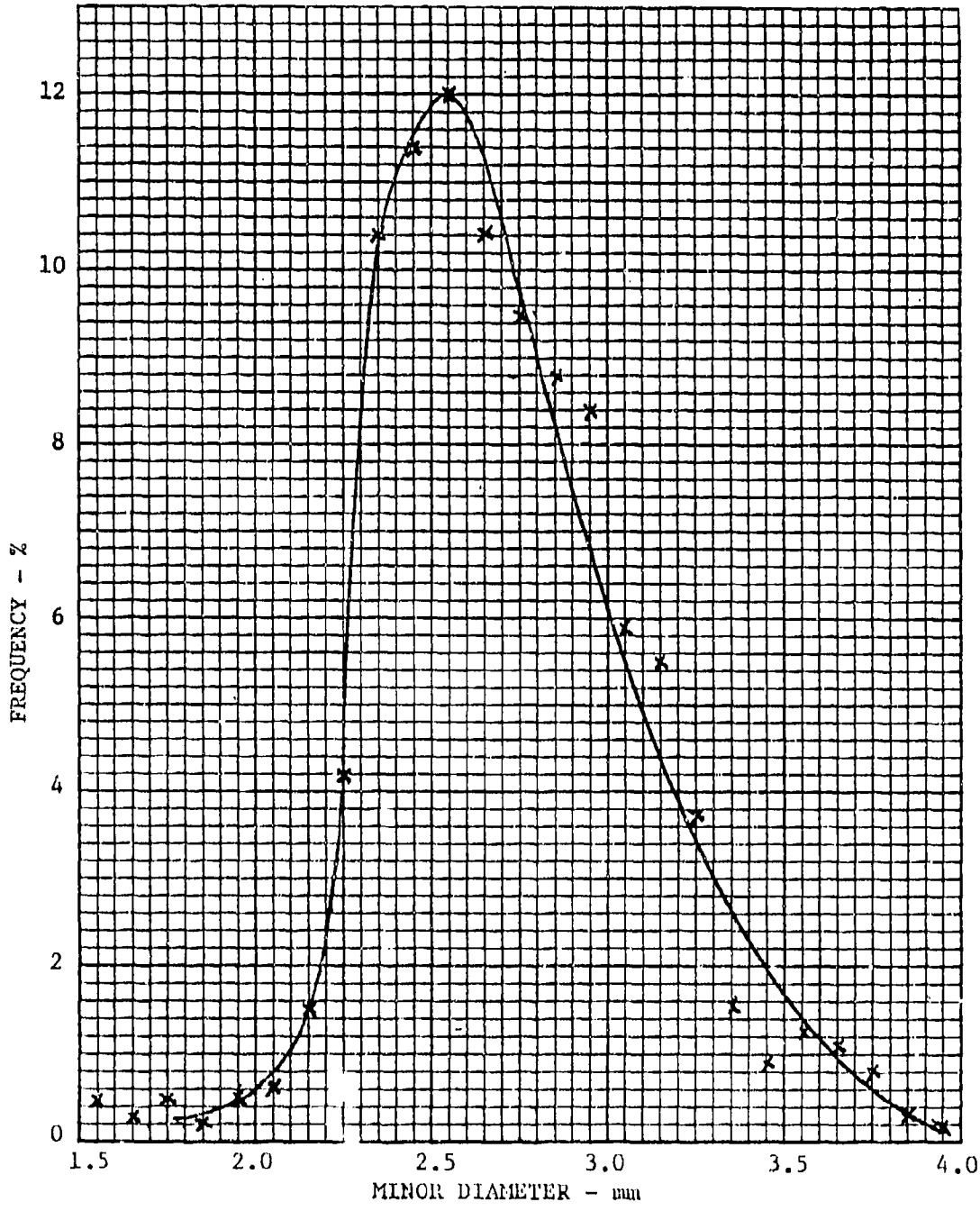

Figure 5-38. Particle Size Distribution of Beads in Packed-Bed Agglomerator

assure that all flow passed through the beads. Since the particles were neither uniformly spherical nor extremely non-spherical, the distribution was biased toward the smaller sizes, but only slightly. This meant that the actual bed was slightly more loosely packed than would be indicated from theoretical considerations, and that cumulative dust collection efficiencies for the bed should be slightly less than those predicted based on bead size alone, bead shape deviations not withstanding. It was felt that the variability in bead size and shape would cumulatively enhance the bed's transition from a filtration unit to an effective agglomerator by introducing irregularities that would affect the dust holding capacity of the bed. In this design, depth filtration was assumed to predominate, with initial dust collection primarily being due to inertial collisions between the dust and the beads. Therefore, increasing the face velocity and/or decreasing the bead size should increase the collision rate which should, in turn, improve overall dust collection efficiency. This would be true, however, only up to some critical velocity, above which reentrainment would eventually come into play, thereby lowering efficiency. If reentrainment could be accomplished without breaking up the dust agglomerates, then effective transition from depth filtration to particle agglomeration could be achieved.

Within a packed bed, dust accumulates internally in a manner that strongly influences subsequent dust collection. Since deposits are continually varying in their amount and state of distribution throughout the bed, dust collection efficiency and pressure drop vary with time, particularly during the early history of the bed. When the bed is relatively clean, the flow through the spaces between the beads corresponds to a high Reynolds number and efficiency is necessarily dependent on inertial impaction. When interstitial deposits are relatively high, the local gas flow through the layer of dust corresponds to a low Reynolds number, since the dust particles have dimensions in the micron range. At low Reynolds number the velocity field around a sphere or cylinder depends primarily on viscous forces, such that combined effects of inertia and interception increase overall efficiency.

Under high specific-deposit conditions, blow-by develops in the dust layer to maintain a flow path. This acts to balance the pressure drop, but also lowers filtration efficiency. However, in the case where the bed is to be used as an agglomerator, it is desirable for blow-bys to occur regularly in the form of agglomerates. As discussed later, results using this particular agglomerator were mixed, but instructive.

Initially, the inlet screen for the bead agglomerator consisted of a piece of 60 x 60 metal mesh media. This produced a rapid pressure drop increase, as shown in Figure 5-39, because the metal mesh media loaded heavily. Following the initial test, the metal mesh media was replaced with a more opened screen and new beads were installed. The clean pressure drop as a function of flow for both units (A and B) is shown in Figure 5-40. Overall unit efficiency per test run is given in Figure 5-41, while pressure drop versus the amount of dust fed to the unit is shown in Figures 5-42 and 5-43. As in previous tests, efficiency is based on the amount of dust penetrating the precleaner relative to the amount introduced to the system. The baseline efficiency of the precleaner, without agglomeration, was about 83 percent in this configuration. Efficiency values for configuration C (runs 94 to 106) started at 94 percent, then slowly declined to 89 percent, with an average value of 91 percent, showing some degree of agglomeration. Pressure drop was relatively level

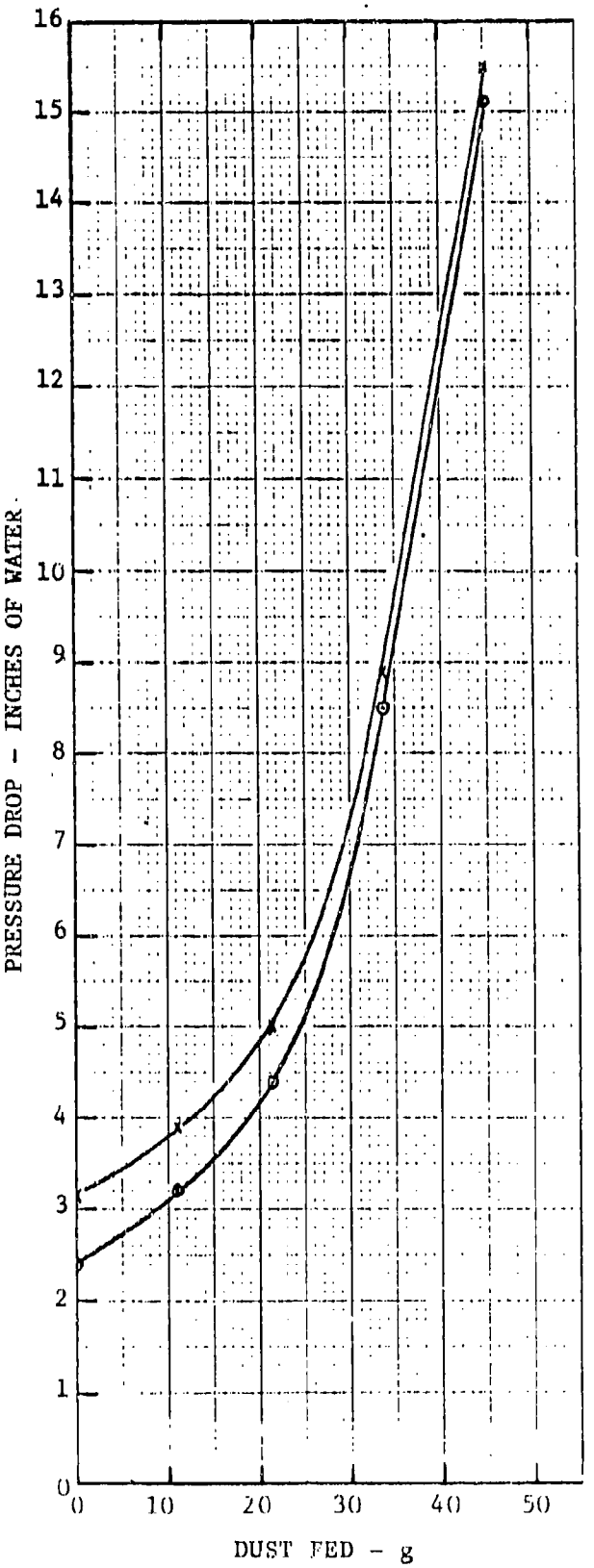

Figure 5-39. Pressure Drop Vs. Dust Fed for Granular Bed Agglomerator with Metal Mesh Screen, Unit A, V_f = 250 fpm, AC Coarse Dust

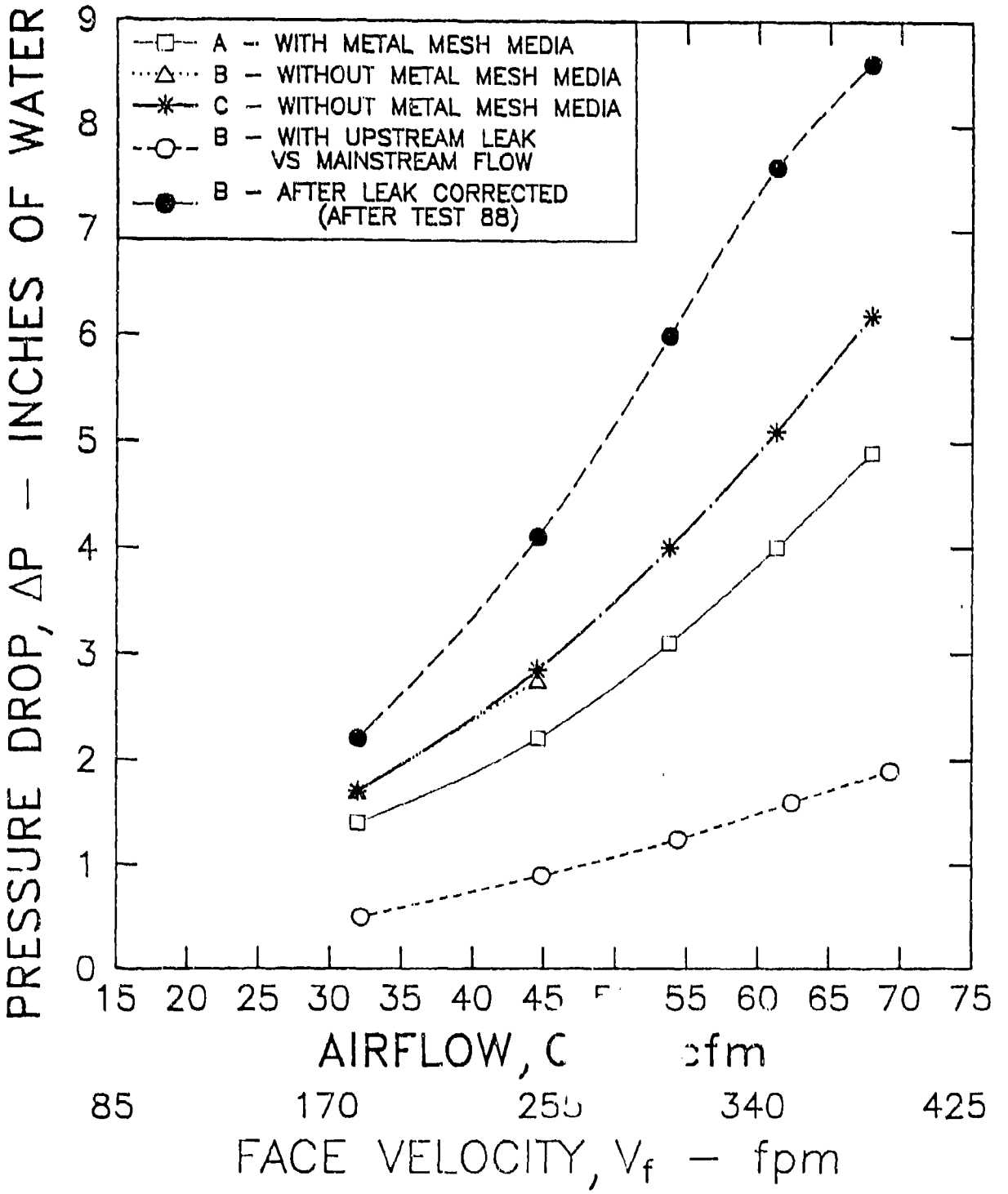

Figure 5-40. Pressure Drop Characteristics of Granular Bed Agglomeration

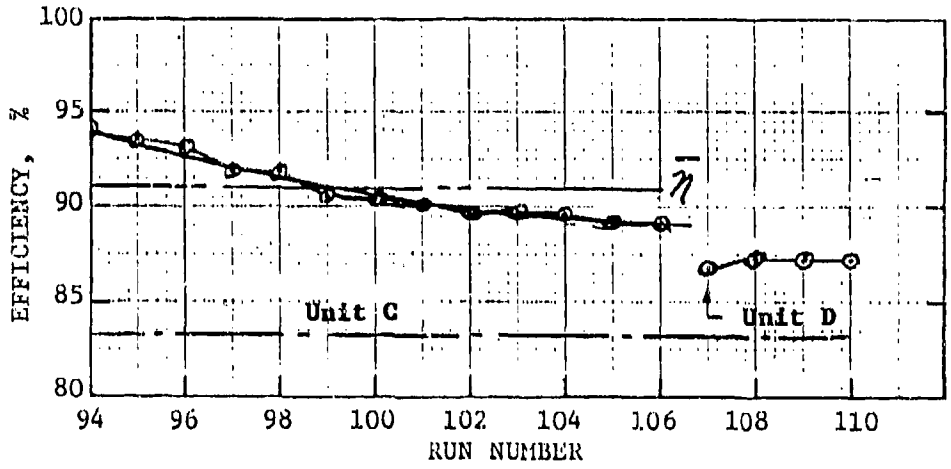

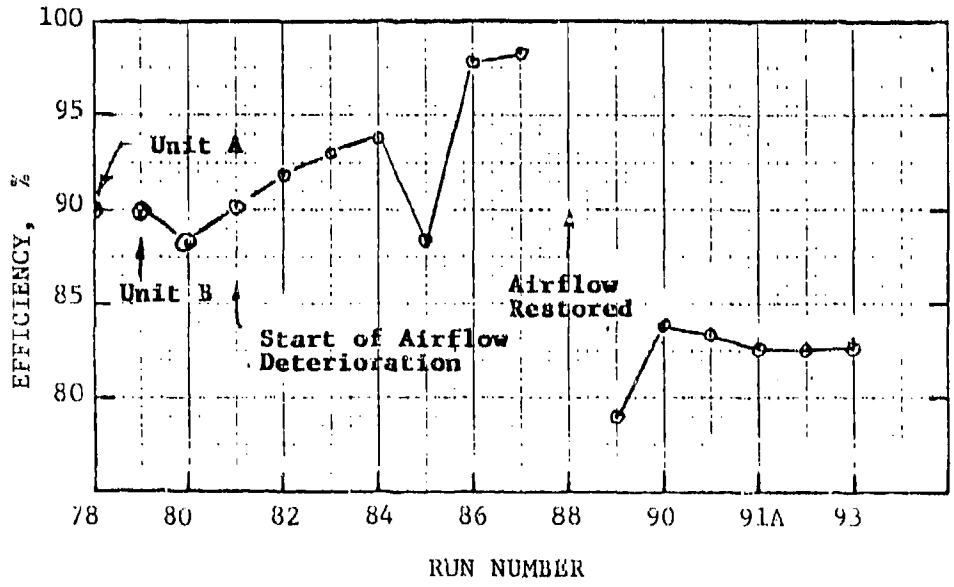

Figure 5-41. Overall System Efficiency With Respect to Test Run for Granular Bed Agglomerator, Units A, B, C and D, V_f = 125-250 fpm, AC Coarse Dust

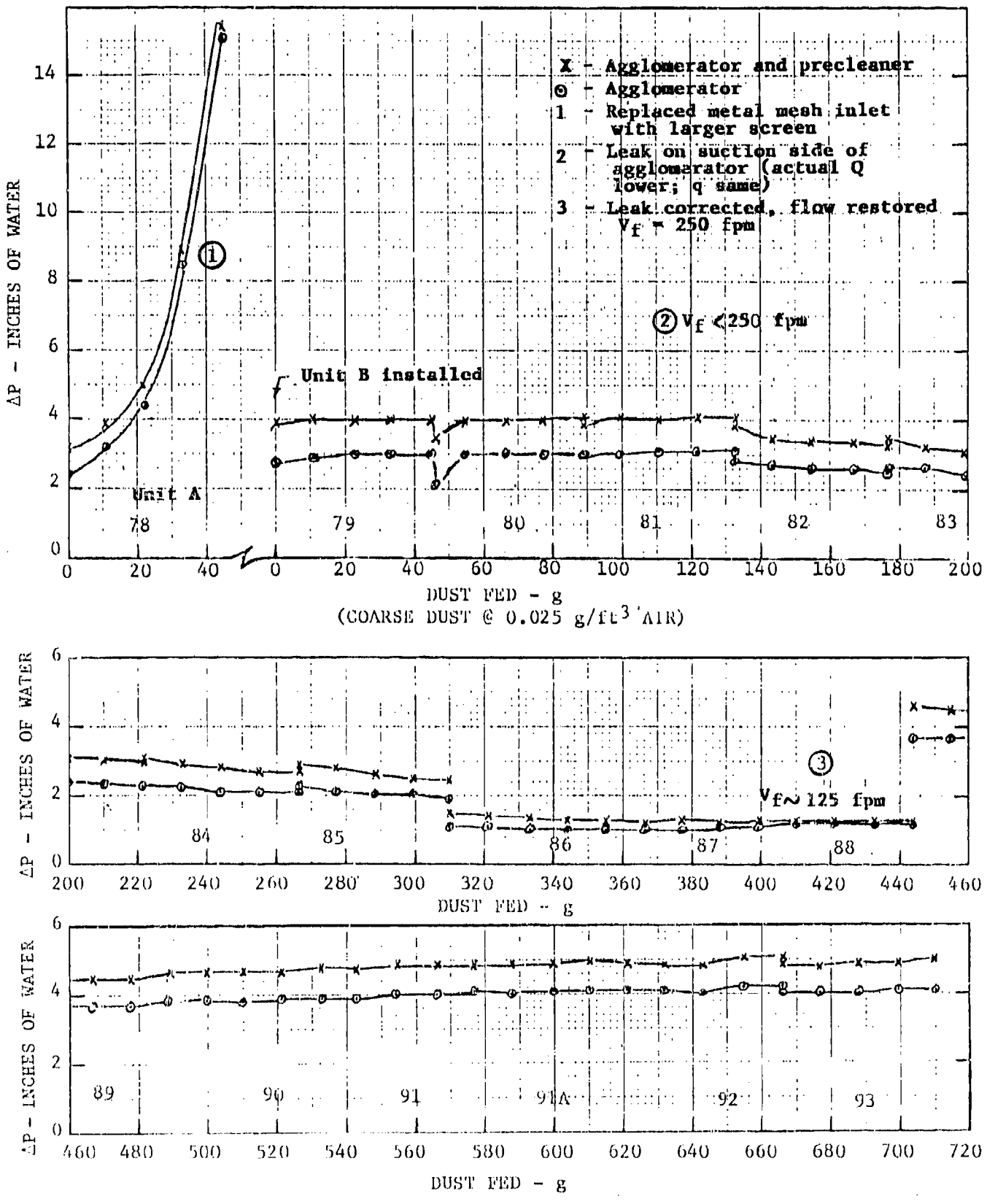

Figure 5-42. Pressure Drop Vs. Dust Fed for Granular Bed Agglomerator, V_f = 250 fpm (except as noted), AC Coarse Dust, Test 1, Units A and B

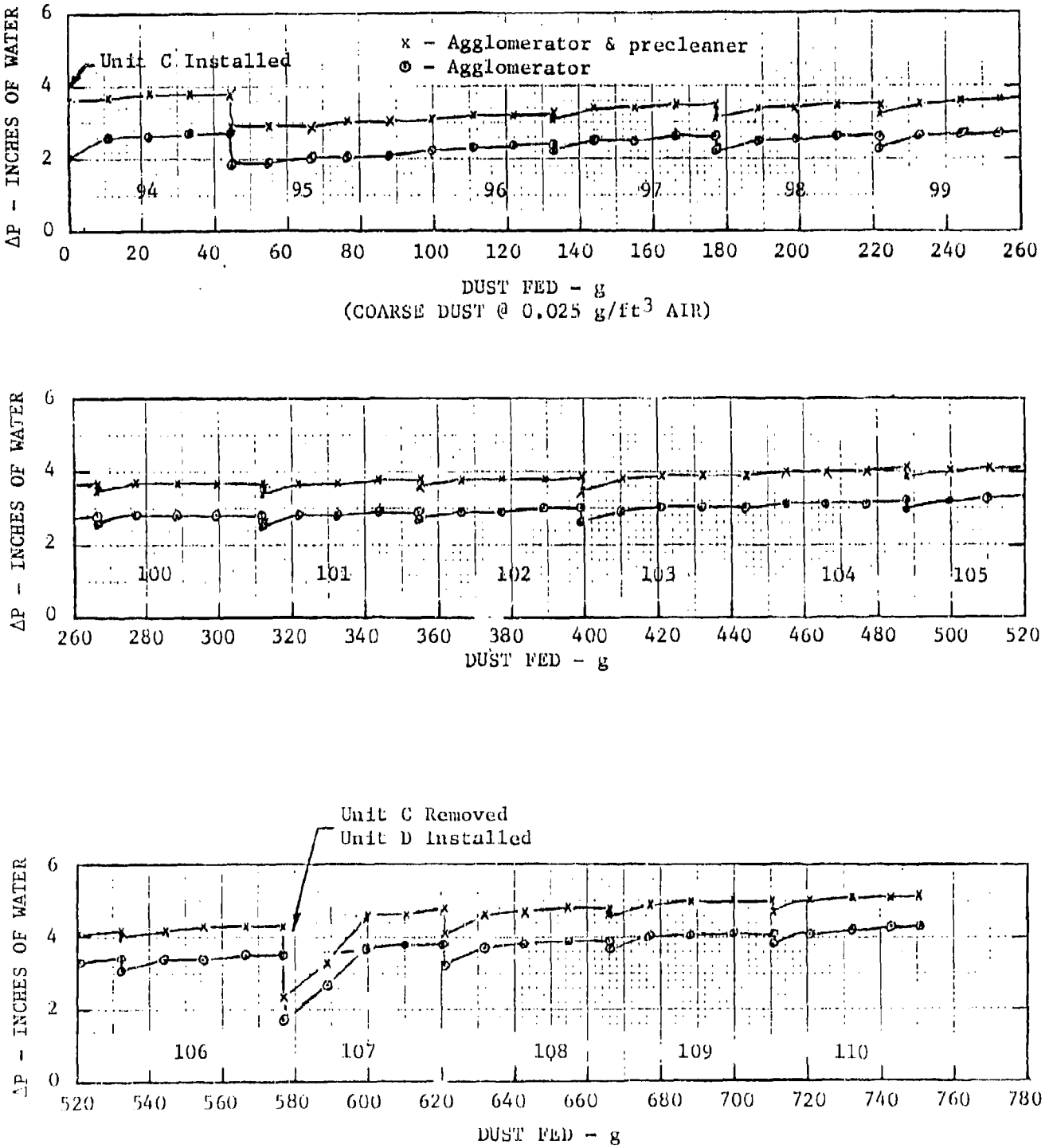

Figure 5-43. Pressure Drop Vs. Dust Fed for Granular Bed Agglomerator, V_f = 250 fpm, AC Coarse Dust, Test 2, Units C and D

reaching a steady state value of about 3½ inches of water across the agglomerator, or about 4½ inches for the combined precleaner/agglomerator unit. Values for unit B were inconsistent because of leakage between the agglomerator and the precleaner during part of the test. This caused the airflow rate through the agglomerator to steadily fall off, leading to significant dust fall-out in and around the bed. As a result, unrealistic incremental efficiency values were obtained since efficiency is based on dust penetration relative to the amount of dust fed, which assumes a constant fed rate with a fairly constant inlet dust concentration. Average efficiency over this test series was 88.3 percent.

These data, however, are not particularly relevant, although they do point out that further work would be needed to define the performance characteristics of this agglomerator, especially as a function of face velocity. The reasons for this and the reasons why more rigorous testing wasn't done are that the mesh and foam agglomerators tended to provide better performance and would be easier to design and integrate into a vehicle. Furthermore, with the mesh and foam agglomerators, unlike with the bead agglomerators, there is much less concern about settling or about the possible loss of abraded material.

As was the mesh and foam agglomerators, the particle size distribution for dust exiting the precleaner was relatively constant (Figure 5-48) regardless of whether the upstream distribution was agglomerated or not.

5.4.3. Particle size investigation. Measurements were made of the particle size distribution leaving the precleaner for the agglomerated and unagglomerated cases. The purpose of these measurements was to determine the effect of agglomeration on dust size and concentration for the dust reaching the final filter, since these parameters usually have a direct effect on final filter service life (dust holding capacity) and design. Theoretically, there should be no significant shift in the cut point for the precleaner due to a change in the upstream particle size distribution. In fact, the purpose of the agglomerator is not to change the cut point, but merely to shift particles from the region below the cut point to the region above the cut point (by virtue of increasing their mass) so they will be removed from the flow stream. The net result will be an increase in precleaner removal efficiency with respect to the original dust, since downstream (out of the precleaner) concentration values for particle sizes above the cut point should be minimal.

Impactor size data were taken on numerous tests to measure downstream distributions for a particular test configuration. In general, these data indicate that the mass median aerodynamic diameter for dust penetrating the precleaner, on unagglomerated coarse dust for the given test conditions, is on the order of 2-3.5 μm, as shown in Figure 5-44. With on line agglomeration, this value approaches 2-2.5 μm, as shown in Figures 5-45 to 5-49.

Figure 5-50 shows the downstream particle size distribution for four test runs immediately following agglomerator removal (mesh, unit No. 4). Figure 5-51 shows this distribution for the agglomerator only, while Figure 5-52 shows the distribution just prior to agglomerator removal and just after agglomerator reinsertion. The essential results are the effects of the agglomerator on particle size and the influence of particle size on overall system efficiency. As is apparent in Figure 5-51, the particle size distribution exiting the agglomerator, and therefore presented

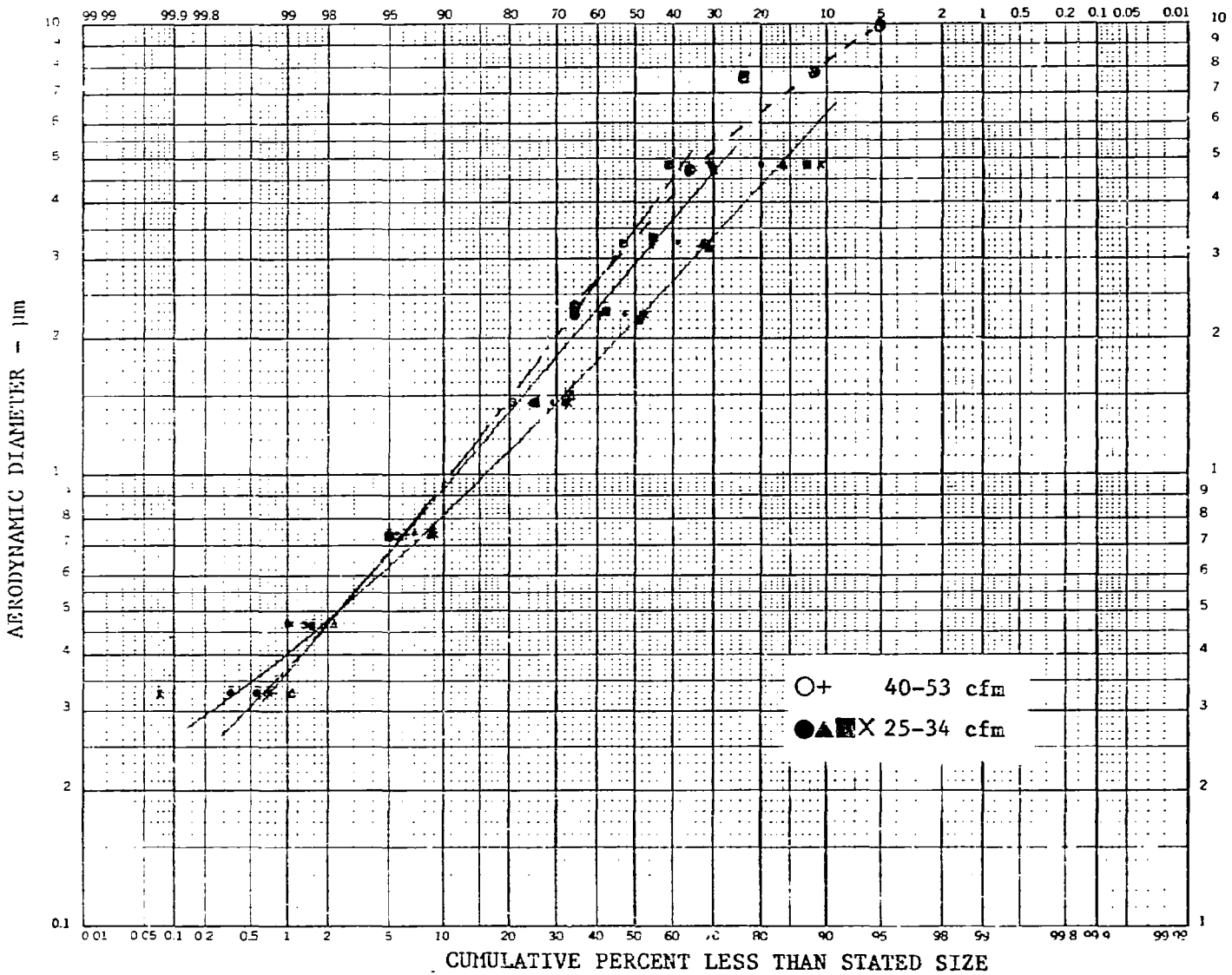

Figure 5-44. Typical Downstream Particle Size Distributions for Unagglomerated AC Coarse Dust for Precleaner and Test Conditions Used for Agglomerator Evaluation

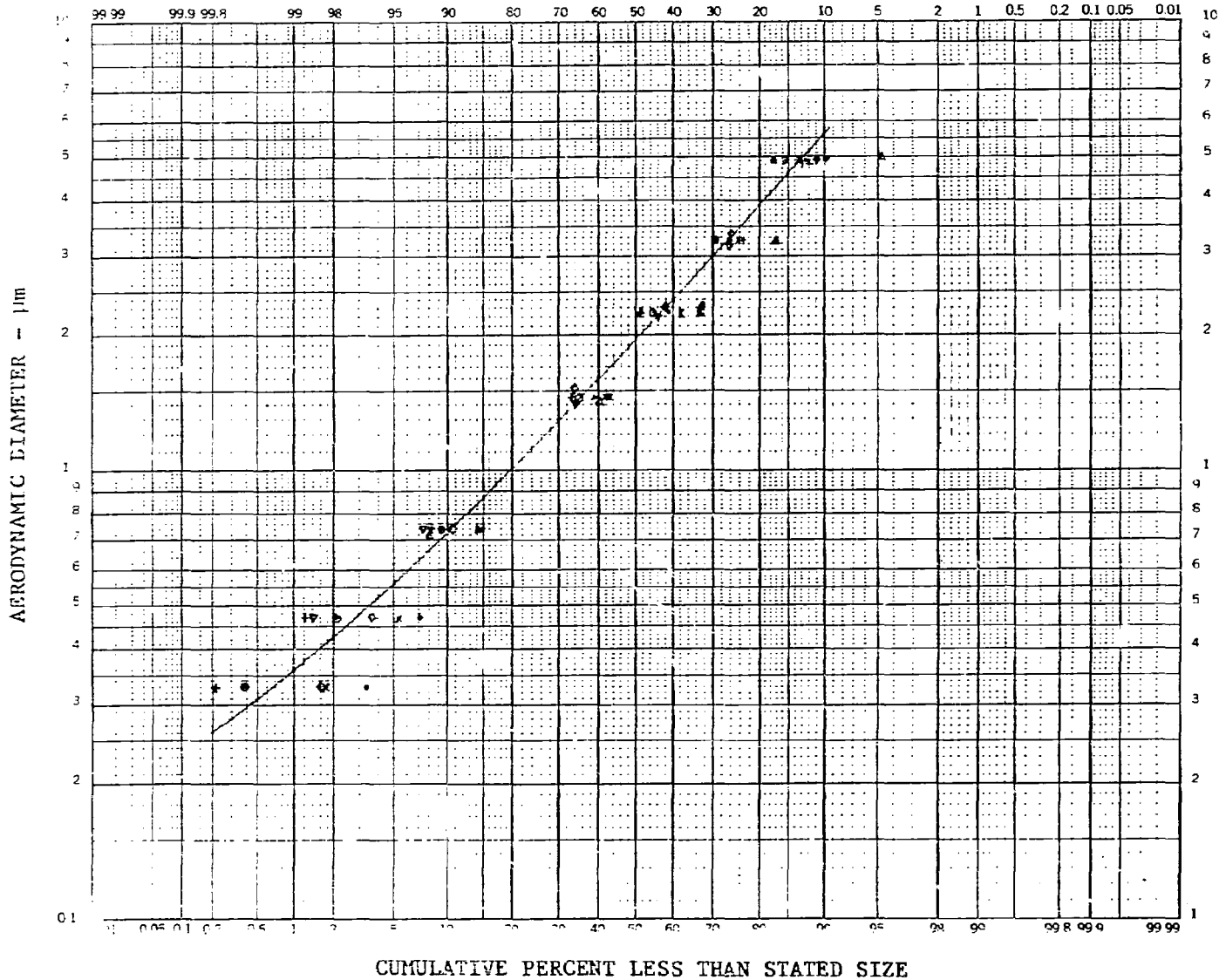

Figure 5-45. Particle Size Distribution Exiting Precleaner with Upstream Mesh Agglomerator, 10-12½ Percent Scavenge, AC Coarse Dust, Agglomerator Vertical

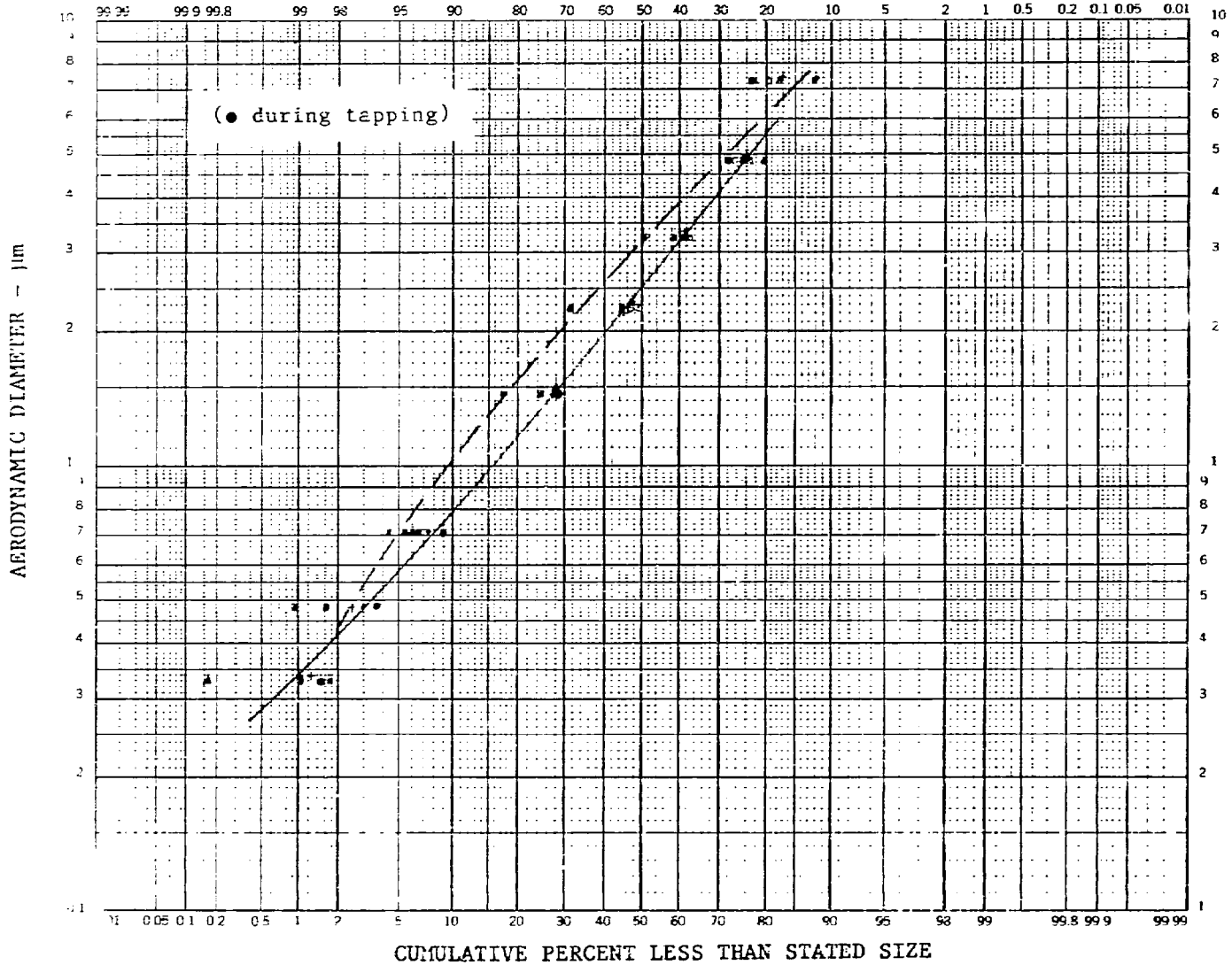

Figure 5-46. Particle Size Distribution Exiting Precleaner with Upstream Mesh Agglomerator, 10-11½ Percent Scavenge, AC Coarse Dust, Agglomerator Vertical

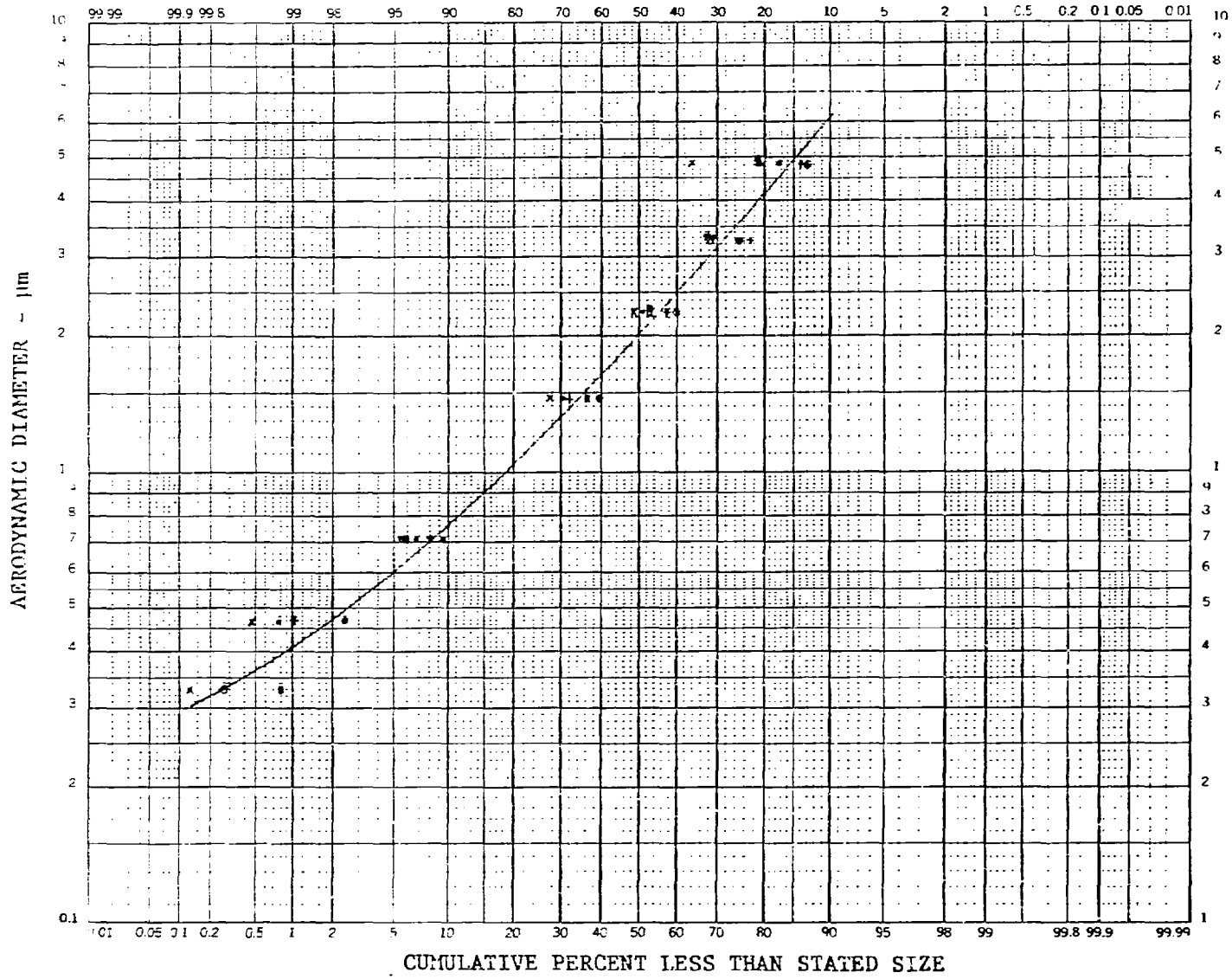

Figure 5-47. Particle Size Distribution Exiting Precleaner with Upstream Mesh Agglomerator, 10 Percent Scavenge, Agglomerator Horizontal

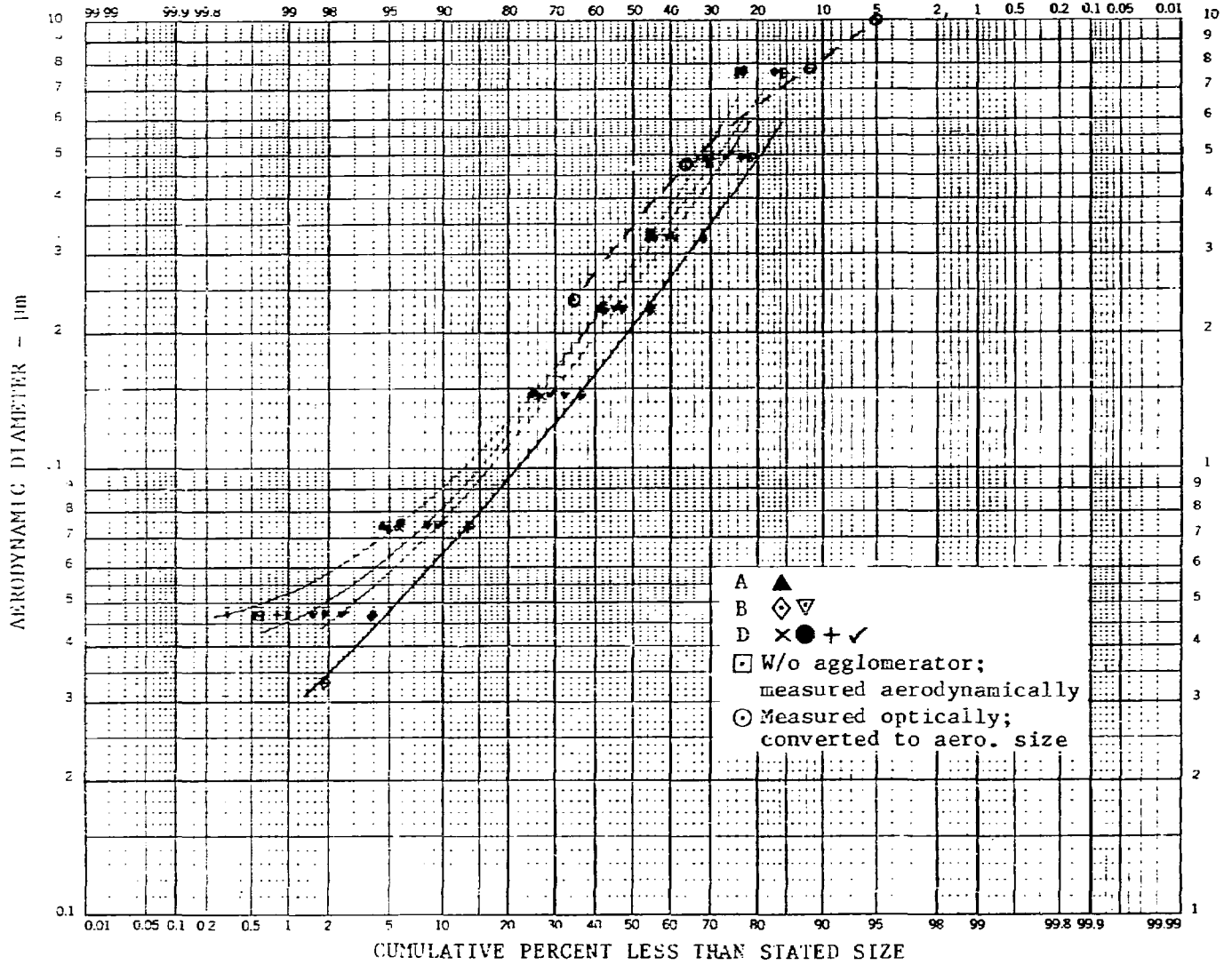

Figure 5-48. Particle Size Distribution Exiting Precleaner with Upstream Granular Bed Agglomerator, Units A, B, and D

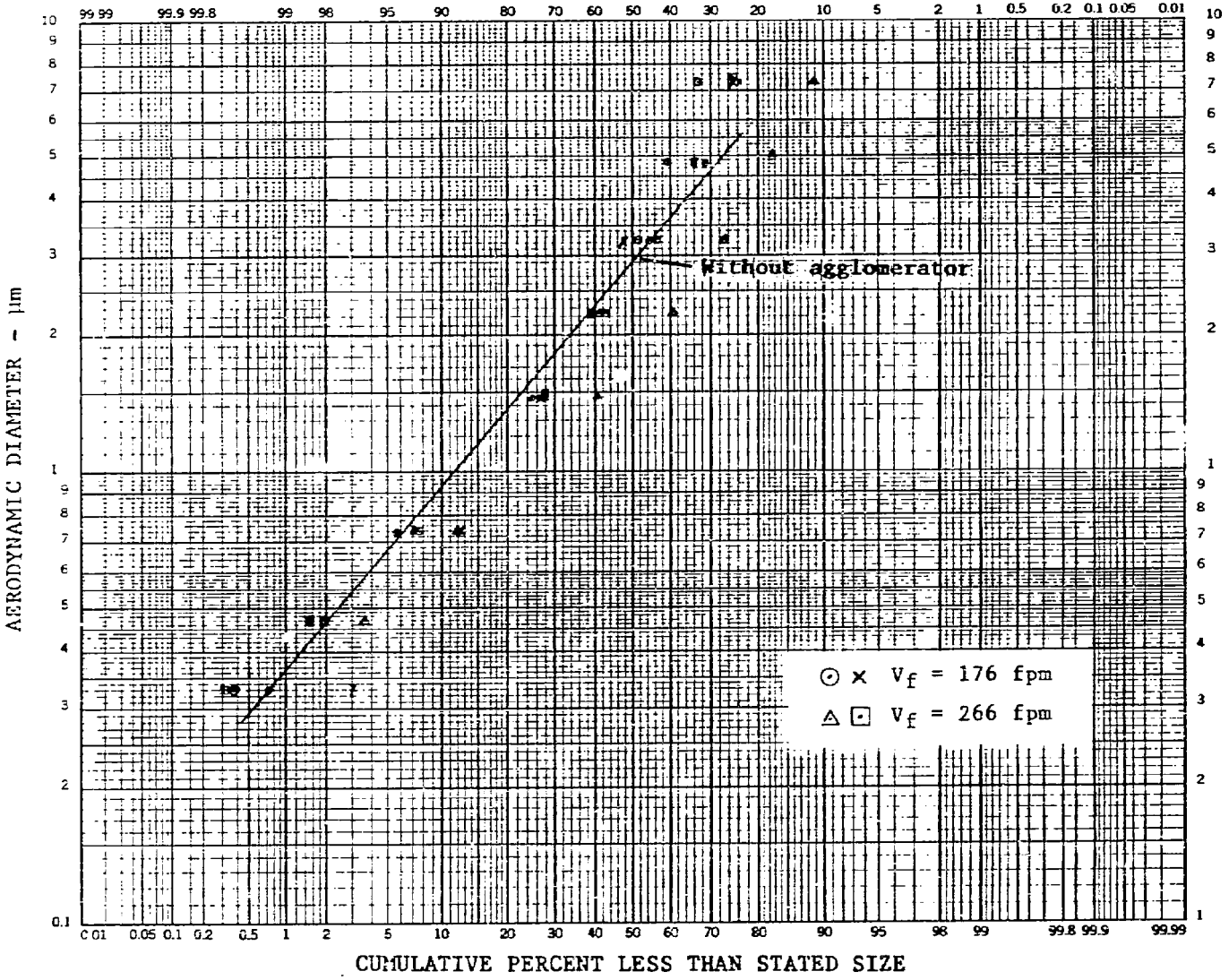

Figure 5-49. Particle Size Distribution Exiting Precleaner with Upstream Foam Agglomerator

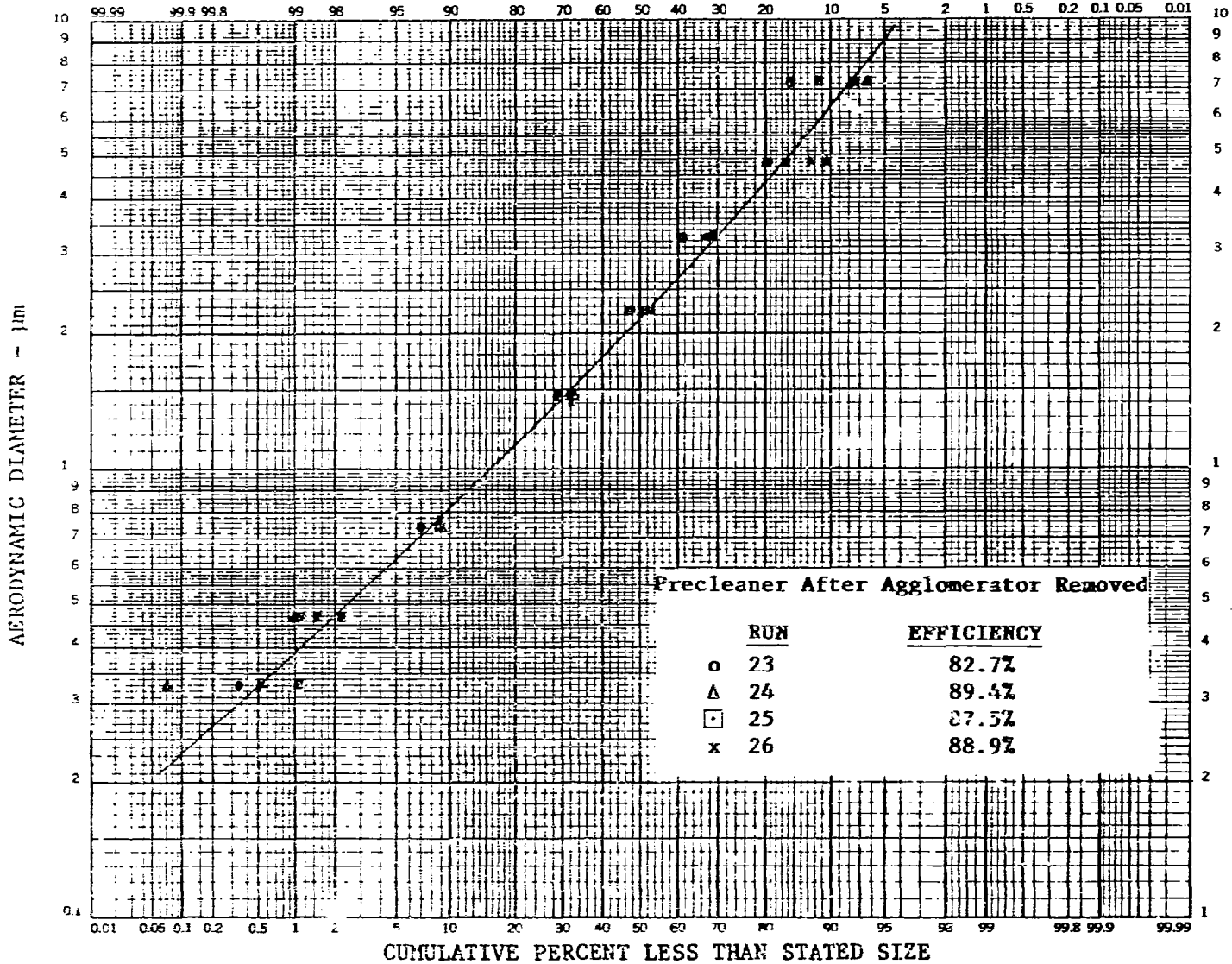

Figure 5-50. Particle Size Distribution Exiting Precleaner Immediately Following Removal of Mesh Agglomerator No. 4, AC Coarse Dust, Runs 23-26

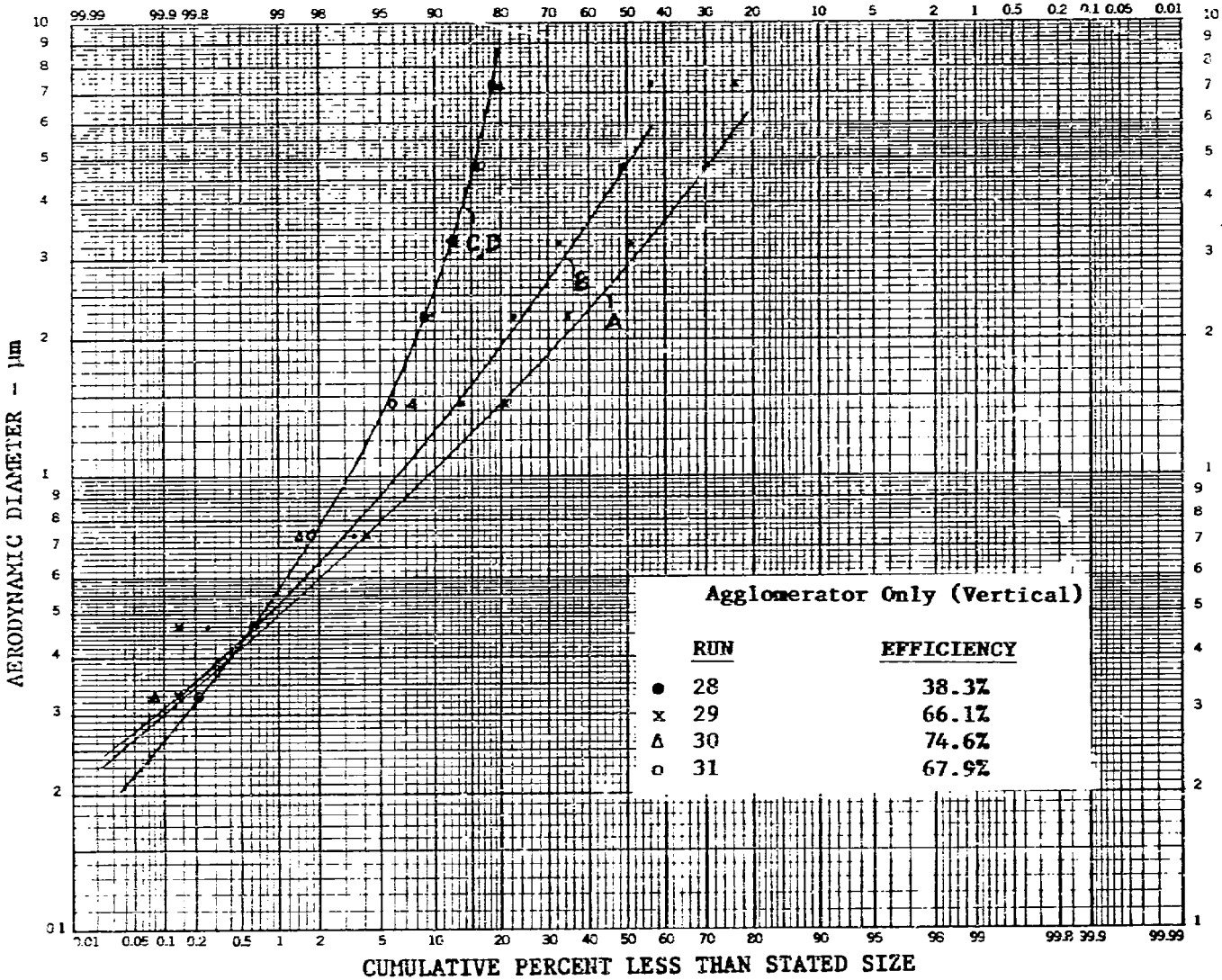

Figure 5-51. Downstream Particle Size Distribution for Mesh Agglomerator No. 4 for Runs 28-31, AC Coarse Dust

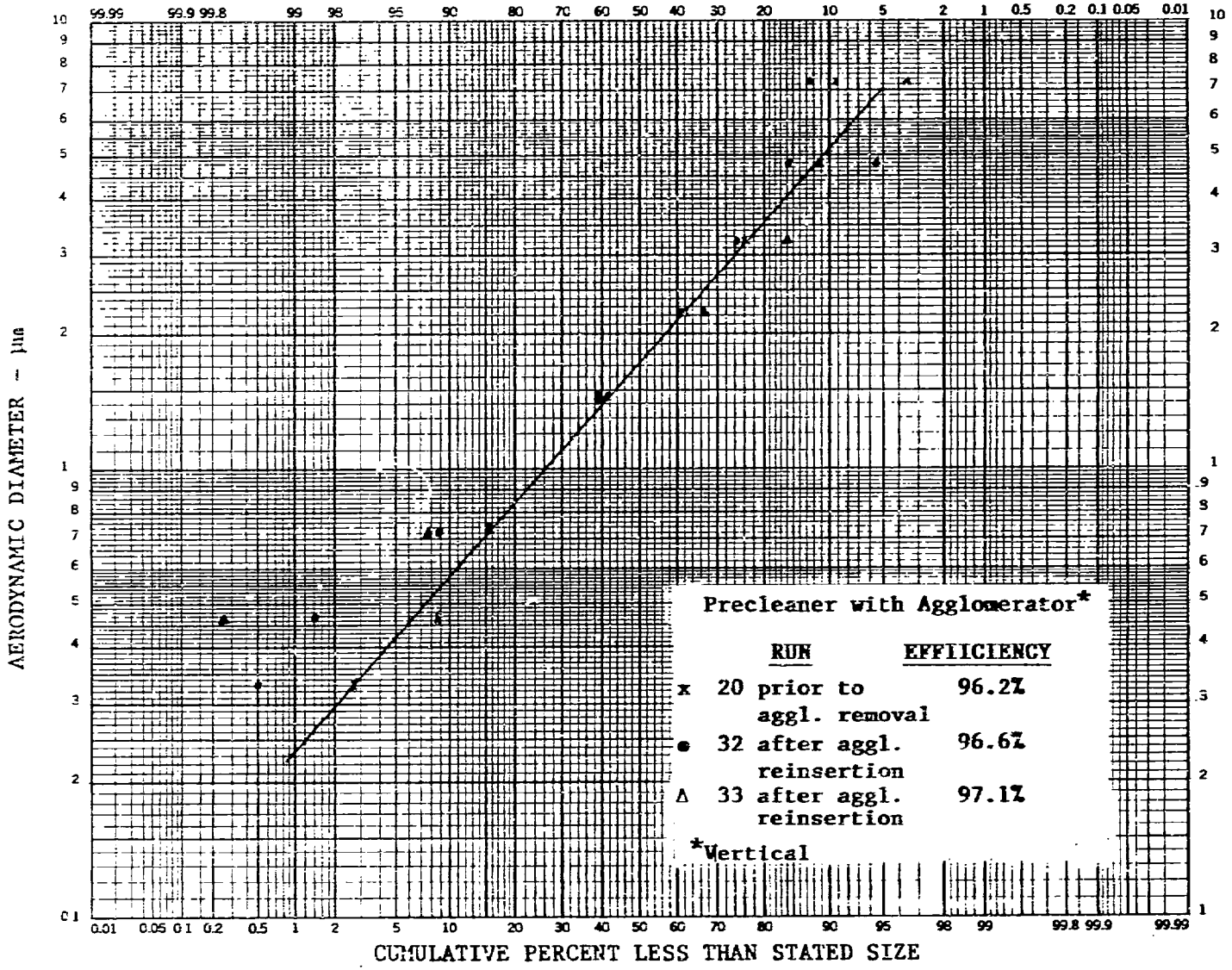

Figure 5-52. Particle Size Distribution Exiting Precleaner Just Prior to Agglomerator Removal and After Reinsertion, Unit No. 4, AC Coarse Dust

to the precleaner, is well within a range that should enhance precleaner separation efficiency, which in fact it did. Furthermore, the progression of curves A to D indicates agglomerate build up and release. These results, and the fact that agglomerator restriction tends to stabilize within acceptable limits, are encouraging. This is of particular interest because the depth-type unit will lend itself to a more convenient and flexible design and packaging arrangement than would a surface-type unit.

Downstream concentration as a function of aerodynamic particle size is given in Figure 5-53 for several test runs conducted during experimentation with the mesh agglomerator (unit No. 4). Data for the foam and packed bed agglomerators are given in Figure 5-54. These data clearly show that the downstream concentration is significantly reduced when the agglomerator is on line. For particles greater than 5 μm, downstream concentrations are improved by nearly an order of magnitude. Naturally, the reduction in downstream concentration accounts for the increase in system efficiency.

5.4.4. Summary of straight-through agglomerator performance. In general, four important observations can be made from the data. First, the increase in precleaner efficiency with the agglomerator in place is significant. System efficiencies typically moved up 10 percentage points. Second, the particle size distributions exiting the precleaner, with the agglomerator in place did not differ significantly from those exiting without upstream agglomeration. This is important because it shows that the particle size distribution of the dust presented to the final filter will be nearly the same as that which would reach the filter under ordinary (unagglomerated) conditions, for which the filter is designed. Had the particle size distribution been significantly smaller as a result of upstream agglomeration, then there might be concern that the standard filter would load faster than normal, negating some benefits of the agglomerator concept. However, since the particle size distribution remains favorable while the dust concentration is greatly reduced, filter life should be significantly increased. Third, acceptable agglomerator face velocities for this type of agglomerator are quite high, current configurations typically operating in the 200-380 fpm range. Even if these values turn out to be higher than those which finally result for an optimized system, it is clear that operating face velocities for the depth-type agglomerators will greatly exceed those expected for surface-type units, and will be well over an order of magnitude larger than those experienced by typical filters. This will facilitate packaging and systems integration, and should enhance incorporation by retrofit. Finally, agglomerator restriction, operating in the straight-through mode, tends to stabilize within generally acceptable limits. Since this will allow long-term operation without a need for onboard backflushing, it further enhances systems integration and ease of operation. Even if periodic cleaning is necessary, it would be quite infrequent and easy to accomplish.

5.5. Design Component and Component Integration Study

The primary reason for employing the agglomerator concept is to improve the service life of a two stage air cleaner system by improving precleaner separation efficiency relative to the initial dust environment. This, in turn, reduces the dust burden on the final filter element, extending its life for a given input concentration. The improvement in precleaner separation efficiency results from shifting the inlet particle size distribution (increase) relative to the distribution of the pre-

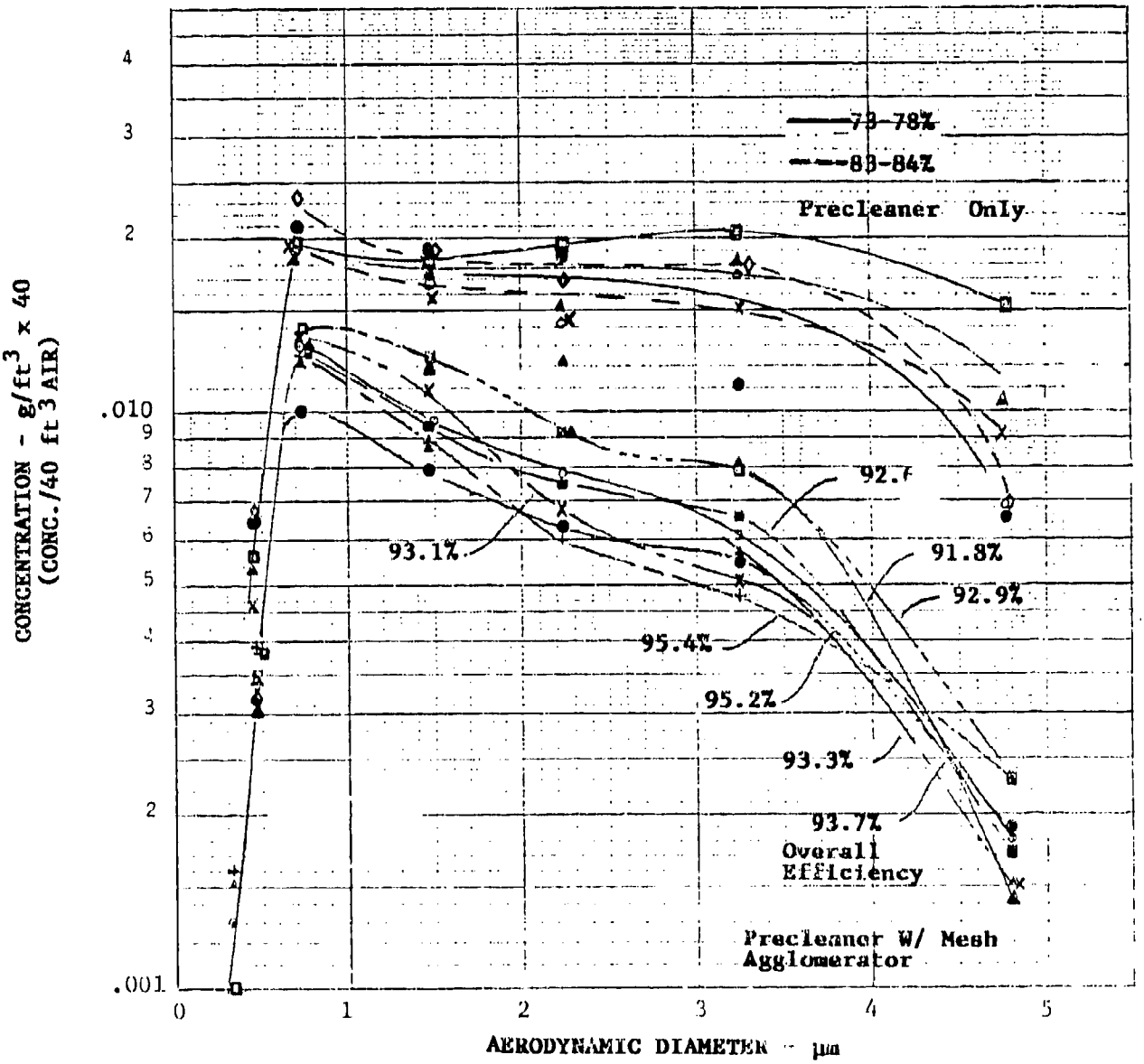

Figure 5-53. Downstream Concentration as a Function of Aerodynamic Particle Size for Precleaner with Upstream Mesh Agglomerator (Unit No. 4), AC Coarse Dust

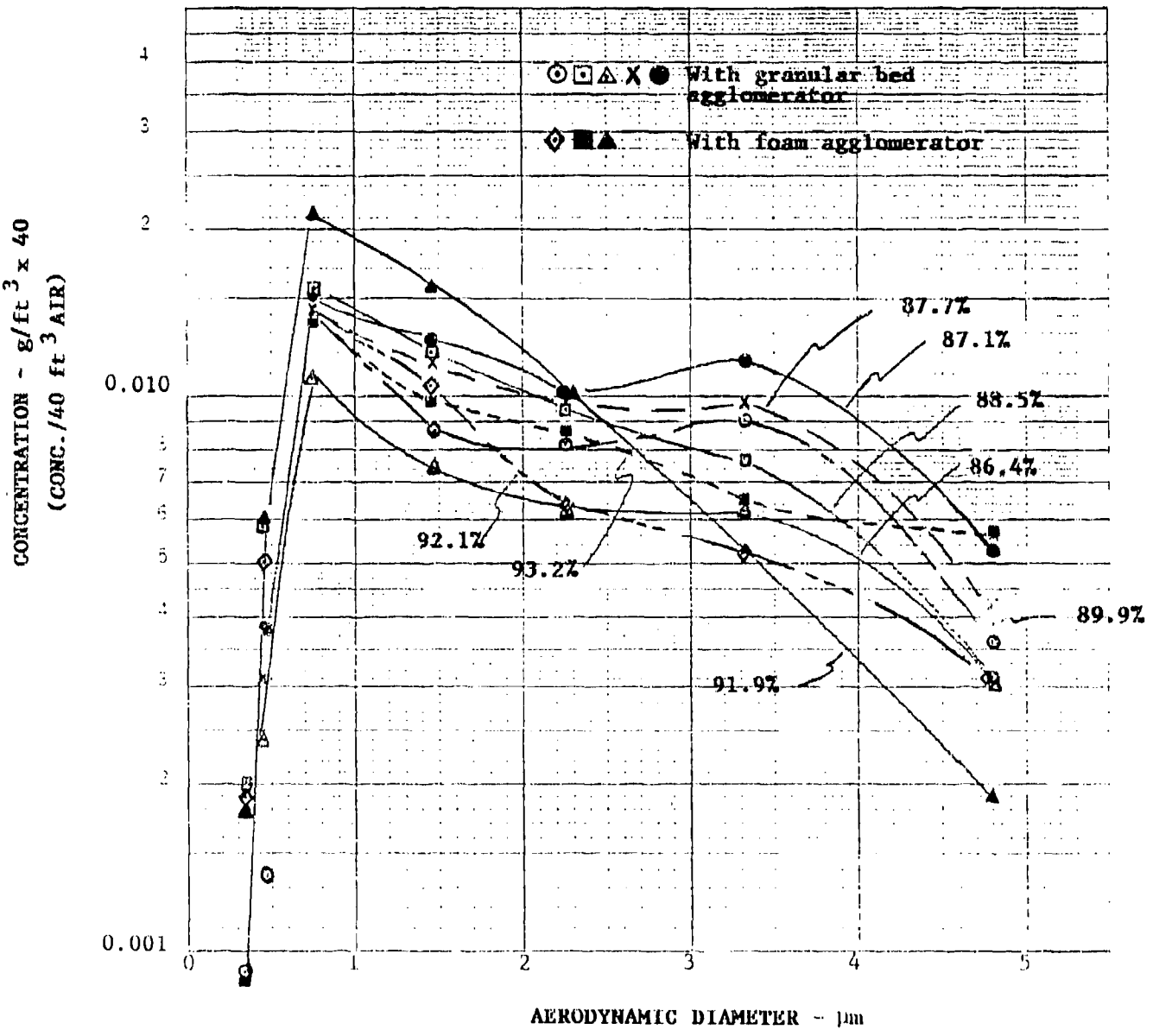

Figure 5-54. Downstream Concentration as a Function of Aerodynamic Particle Size for Precleaner with Upstream Foam and Granular Bed Agglomerator

agglomerated dust. The impact on service life can be substantial, even for apparently small changes in separator efficiency. For instance, an improvement in precleaner efficiency from 90 to 95 percent would reduce the dust burden on the final filter by 50 percent compared to the unagglomerated case, theoretically doubling service life.

Usually a precleaner can be added to a single-stage air cleaner system to remove a large amount of the dust that would otherwise have to be handled by the filter. Since the pressure loss across the precleaner does not increase with time, the overall affect is to slow the pressure drop increase across the filter by lessening its dust burden over time. The improvement in service life, however, is not directly proportional to the performance of the precleaner. In fact, there are cases where service life is barely increased, even though precleaner efficiency is high. The reasons for this are associated with the increase in initial restriction caused by adding the precleaner and the relationship between the new initial restriction, the dust loading rate, and the final allowable restriction. The interaction of these parameters can be studied by developing a model to predict service life as a function of the dust concentration reaching the final filter. Two systems can be used, one consisting of a filter, the other consisting of a filter preceded by a precleaner. Service life for these systems is inversely proportional to the dust concentration X_f reaching the filter, and in the second case, also to a factor ($1/\beta$) related to the incremental change in initial restriction caused by adding the precleaner:

$$(L_1) \propto \left(1/X_{f_1}\right) \tag{10}$$

$$(L_2) \propto \left(1/X_{f_2}(1/\beta)\right) \tag{11}$$

In terms of the amount of dust being introduced to the system X_o, the dust reaching the filter equals:

$$X_{f_1} = X_0 \tag{12}$$

$$X_{f_2} = X_0(1-\eta) \tag{13}$$

where η is the efficiency of the precleaner. The relative change in service life caused by adding the precleaner can then be written as:

$$\Delta L = \frac{L_2 - L_1}{L_1} = \frac{1 + \eta\beta - \beta}{(1-\eta)\beta} \tag{14}$$

so that L_2 becomes:

$$L_2 = \frac{L_1}{(1-\eta)\beta} \tag{15}$$

The impact of β and η on service life is shown in Figures 5-55 and 5-56. As can be seen, in the typical range of interest, service life is very sensitive to changes in

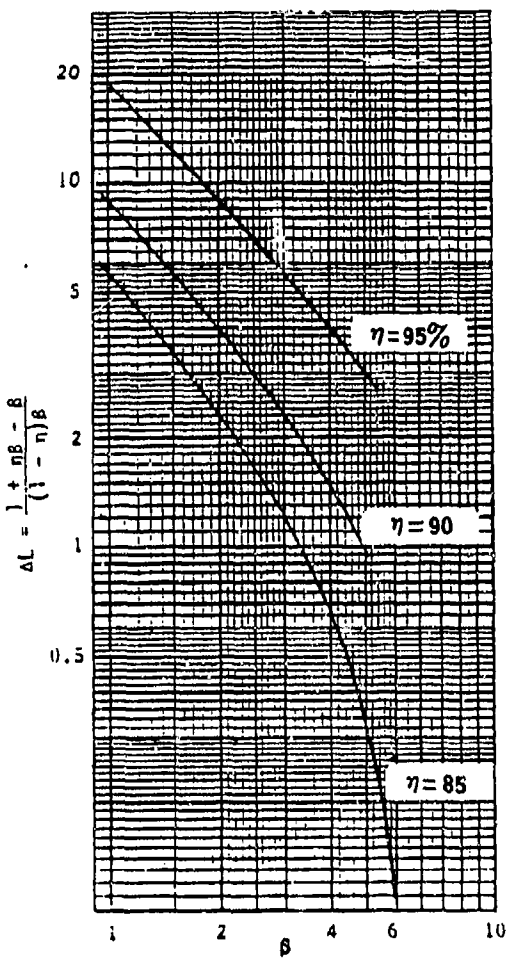

Figure 5-55. Relative Change in Service Life $(L_2 - L_1)/L_1$ as a Function of β and η

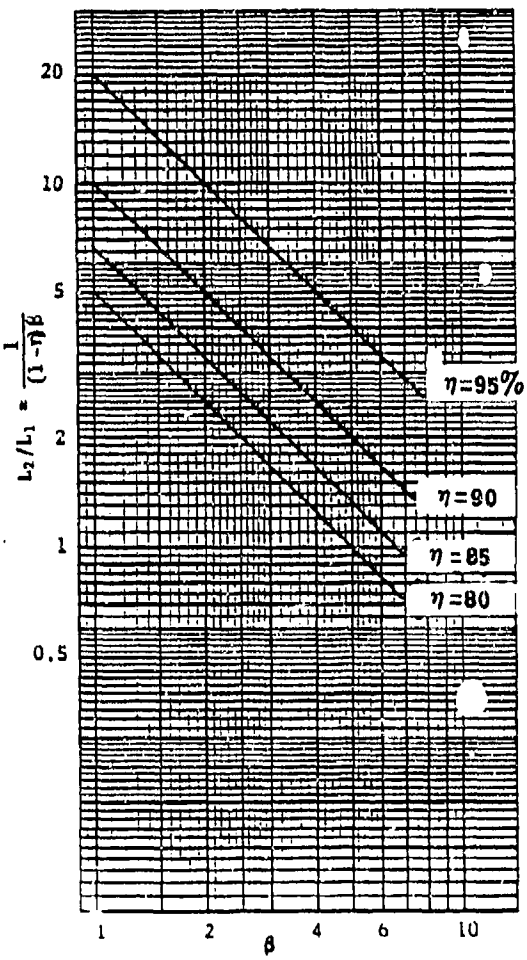

Figure 5-56. Ratio L_2/L_1 as a Function of β and η

efficiency for a given value of β. Conversely, minor improvements in efficiency will have little, if any, effect on service life if β must be increased significantly to increase efficiency.

It has been noted that β is related to the increase in initial pressure drop caused by adding the precleaner to the system. This is because increasing ΔP_i decreases the allowable pressure drop remaining for dust loading, since:

$$\Delta P_\ell + \Delta P_i = \Delta P_f = \text{a constant} \tag{16}$$

where: ΔP = ΔP available for dust loading
ΔP_f = maximum allowable ΔP
ΔP_i = initial (clean) ΔP

Quantitatively, the relationship among these variables and service life is illustrated in Figure 5-57. As can be seen, if adding the precleaner does not appreciably change the slope of the loading curve (for instance, by significantly reducing the dust concentration to the filter), life will decrease (L'_2, L'_3) because loading starts at a higher ΔP_i. However, if the loading slope is sufficiently reduced, then service life is improved because the decrease in dust concentration over time more than compensates for the increase in initial restriction.

It is convenient to assume that for equal particle size distributions, the slope will be proportional to the amount of dust reaching the filter, and therefore inversely proportional to the efficiency of the precleaner. In practice, if a precleaner is added to the system, the particle size distribution of the dust reaching the filter and the concentration as a function of particle size will change. This will affect life in two ways. First, since less dust reaches the filter, life will tend to increase. Second, if the filter is not redesigned, it will (probably) clog faster than normal when exposed to the smaller particle size distribution. This would tend to reduce service life. The net result, in general terms, is that overall service life will be increased by adding the precleaner, but not to the extent possible if the filter were also redesigned to accommodate the smaller particle size distribution. The model developed here assumes no loss in life due to the shift in the particle size distribution. This is reasonable since a filter that is matched to the new distribution will restore the balance, as far as particle size is concerned. β then is related primarily to the change in initial pressure drop, and as a first approximation can be written as:

$$\frac{1}{\beta} = \frac{\Delta P_f - \Delta P_x}{\Delta P_f - \Delta P_i} \tag{17}$$

where ΔP_x is the new initial pressure drop caused by adding the precleaner, as shown in Figure 5-57. This shows that when:

$$\Delta P_x \to \Delta P_f \; ; \; \frac{1}{\beta} \to 0 \text{ and } L \to 0 \tag{18}$$

$$\Delta P_x \to \Delta P_i \; ; \; \frac{1}{\beta} \to 1 \text{ and } L \to L_0 \tag{19}$$

For the case where adding the precleaner doubles the initial pressure drop, $\Delta P_x = 2\Delta P_i$. If $\Delta P_f = 4\Delta P_i$, which is quite reasonable, $1/\beta$ becomes 0.67, which means that service life would decrease 33 percent if there is no change in the

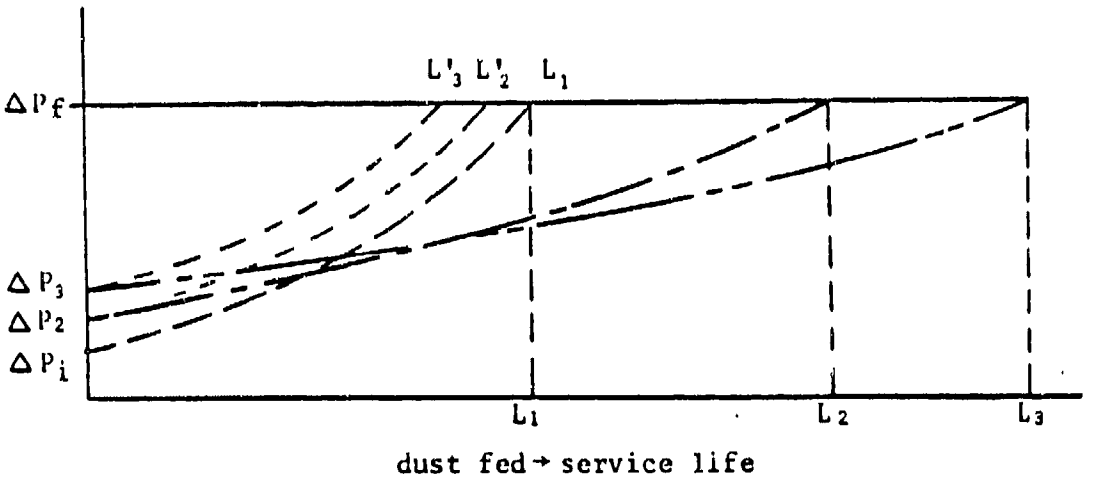

Figure 5-57. Relationship Between the Pressure Drop Variables and the Slope of the Dust Loading Curve and Service Life

loading slope. If loading is proportional to dust concentration, precleaner efficiency would have to exceed 33 percent to produce any gain in overall system life.

If precleaner efficiency is 85 percent, the dust reaching the filter is decreased by 85 percent, hence life should (intuitively) increase by a factor of 100/15 = 6.67, not taking into account the effect of initial pressure drop increase. When this factor is considered, it is found that life would only increase by a factor of 6.67 x .67 = 4.47. From equation 15, the new service life L_2 in this example becomes:

$$L_2 = \frac{L_1}{(1 - .85)} (.67) = 4.47\ L_1 \tag{20}$$

If precleaner efficiency is increased from 85 to 95 percent, but at a cost of some increase in the initial pressure drop, the amount of dust reaching the filter is only 5 percent of the input dust, instead of 15 percent, hence:

$$L_3 \sim \frac{100}{5}\left(\frac{1}{\beta'}\right) L_1 \tag{21}$$

If $\Delta P'_x = 1.1\ \Delta P_x$ (a 10 percent penalty in initial pressure drop in going from 85 to 95 percent efficiency), $1/\beta$ in the previous example becomes 0.6. This indicates that the life of the new system should be approximately 12 times the life before adding the precleaner, and about 2.7 times that when the 85 percent efficient precleaner was used. If $\Delta P'_x = 1.2\ \Delta P_x$ (a 20 percent pressure drop penalty), these factors drop to 10.7 and 2.4 respectively. At $\Delta P'_x = 1.5 \Delta P_x$, these factors are 6.7 and 1.5. Figure 5-58 shows L_2/L_1 and β as a function of $\Delta P_x/\Delta P_i$ for the hypothetical situation where $\Delta P_f = 4\Delta P_i$. For this case, $1/\beta$ equals:

$$\frac{1}{\beta} = \frac{4 - \Delta P_x/\Delta P_i}{3} \tag{22}$$

Again, these curves show that L_2 is very sensitive to efficiency provided the pressure drop penalty is small. For example, for $\Delta P_x/\Delta P_i = 2$ and η = 85 percent, L_2/L_1 equals 4.4. If η can be increased to 90 percent while P_x is only increased 10 percent from its current level, L_2/L_1 can be increased 35 percent to 6. Conversely, if a ΔP increase of 30 percent is required, then life remains constant even though efficiency was increased from 85 to 90 percent. However, if the 30 percent increase in ΔP were to produce a 95 percent efficiency, the theoretical L_2/L_1 factor would approach 9, twice the value at 85 percent efficiency. If β were not significant, one would expect L_2/L_1 with a 95 percent precleaner system to be three times that for a 85 percent precleaner system.

As a way of illustration, the theoretical model can be applied to the air cleaner system used on the 2½-ton truck for which laboratory data were developed in another program (DAAE07-84-C-R045).[2] Currently, this system consists of as final filter for which $\Delta P_i \sim 5$ inches of water, while ΔP_f is 20 inches of water. For this system, $1/\beta$ becomes:

$$\frac{1}{\beta} = \frac{20 - \Delta P_x}{15} \tag{23}$$

which for $9 \leq P_x \leq 11$ gives $1.36 \leq \beta \leq 1.67$. L_2/L_1 over this range of β is given in Table 5-3 for η = 85, 90 and 95 percent.

Table 5-3. Theoretical Values for L_2/L_1 as a Function of β and Precleaner Efficiency η for 2-1/2-ton Truck System

η \ β	1.36	1.50	1.67
85	4.9	4.4	4.0
90	7.4	6.7	6.0
95	14.7	13.3	12.0

Since ΔP_x increases as η increases, it may be reasonable to look along the diagonal to estimate the potential for improving service life. These data are shown in Figure 5-59. Values of L_2/L_1 achieved during laboratory testing, using two different precleaners operating at 10 percent scavenge flow, were on the order of 2 to 2½ with β on the order of 1.3 to 1.4. These values compare fairly well with the theoretical values in Figure 5-58 for these βs, suggesting precleaner operation in the lower efficiency range. It is important to note that the precleaner was not matched to the 2½-ton unit nor was the filter element adjusted for the change in particle size distribution. By optimizing design parameters, greater improvements in service life should be possible and by incorporating an effective agglomerator, overall efficiency for the combined precleaner/agglomerator systems should easily approach 95 to 97 percent on coarse dust. This will produce L_2/L_1 values in excess of 12 (ref. Figure 5-59) provided the pressure drop penalty for adding the agglomerator is small.

In general, the above model which shows the impact on service life caused by adding a precleaner, also applies to the precleaner/agglomerator system. In this case, the increase in initial restriction is the sum of the increases caused by both the precleaner and the agglomerator. If the system already contains a precleaner, the increase in initial restriction will only pertain to the added initial restriction of the agglomerator. Unlike the precleaner, however, which has a constant pressure drop for a given airflow rate, the agglomerator, depending on type and design, could have a variable restriction over its lifetime. In the case where a surface loading media is used in the agglomerator section, a periodic, saw-tooth loading curve can be expected for the agglomerator's pressure drop contribution. As illustrated in Figure 5-60, this contribution can be added to the precleaner plus final filter pressure drop level to give a band showing maximum pressure drop as a function of operating time. For the depth media agglomerator, system restriction is eventually increased by the steady-state agglomerator component (Figure 5-60b). In this case, the above equations are appropriate if ΔP_x is taken as the combined pressure drop for the precleaner and (steady-state) agglomerator.

In the case of a surface loading agglomerator, overall life will be influenced by the manner in which the media reacts under exposure to high and low pressure drop. For most media there is a pressure drop threshold above which effective cleaning and efficient pressure drop recovery are reduced because the higher pressure drop between cleaning cycles drives some particles into the media. In this case, the trend line for service life remaining after cleaning will be slightly downward because the loading time interval will eventually become quite short. The net tradeoff, however, between remaining service life and increased allowable restriction should remain favorable as illustrated in Figure 5-61.

If a media possesses good high and low pressure drop properties with respect to loading and cleanability, system life can probably be maximized by allowing high restriction operation when final filter pressure drop is low without sacrificing cleanability later when the final filter pressure drop has significantly increased. This would flatten the trendline for remaining service life (Figure 5-61) for the higher restriction system. For this unit, cleaning would be initiated when total restriction reached the design limit, ΔP_f. For the low resistance system, cleaning would be initiated based on agglomerator restriction rather than overall system restriction.

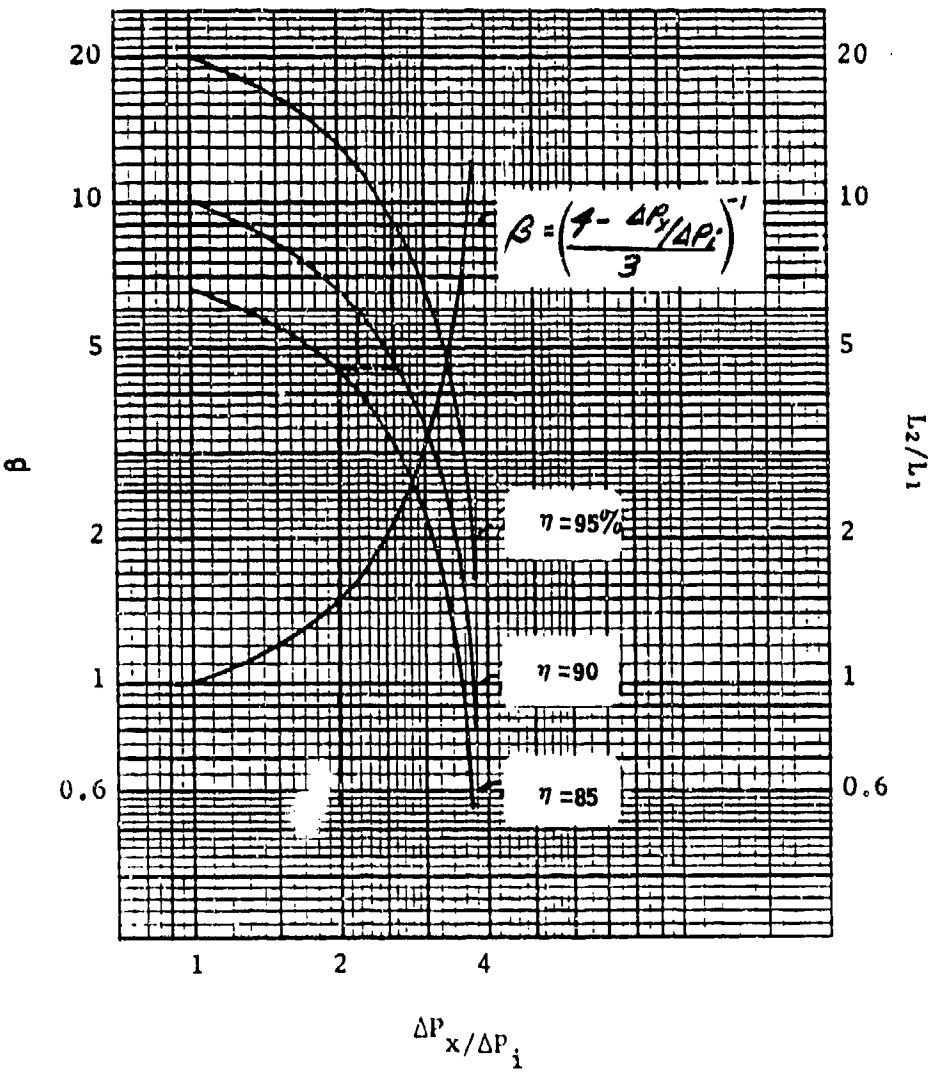

Figure 5-58. β and L_2/L_1 as a Function of $\Delta P_x/\Delta P_i$ and η

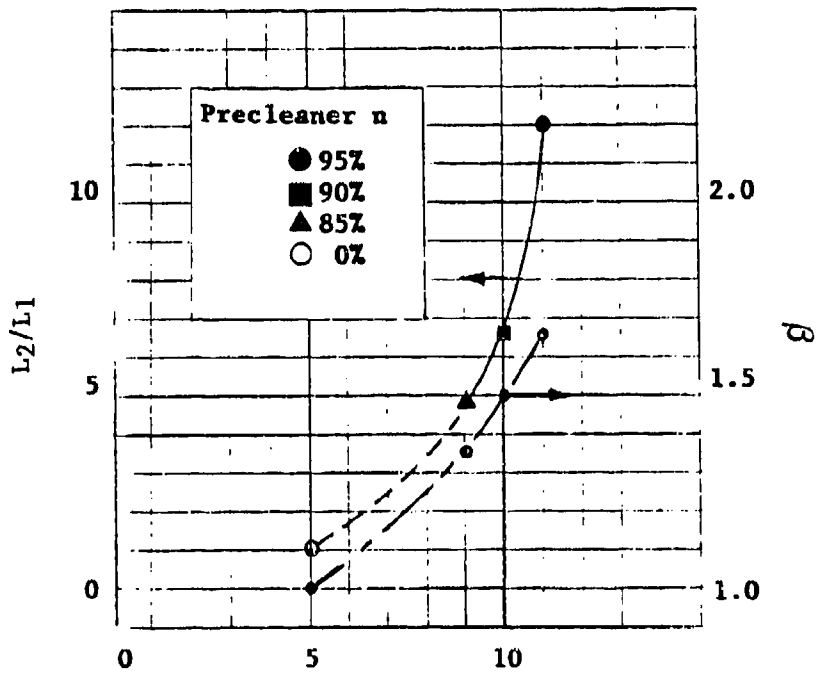

Figure 5-59 L_2/L_1 and β as a Function of ΔP_x Based on Data in Table 5-6

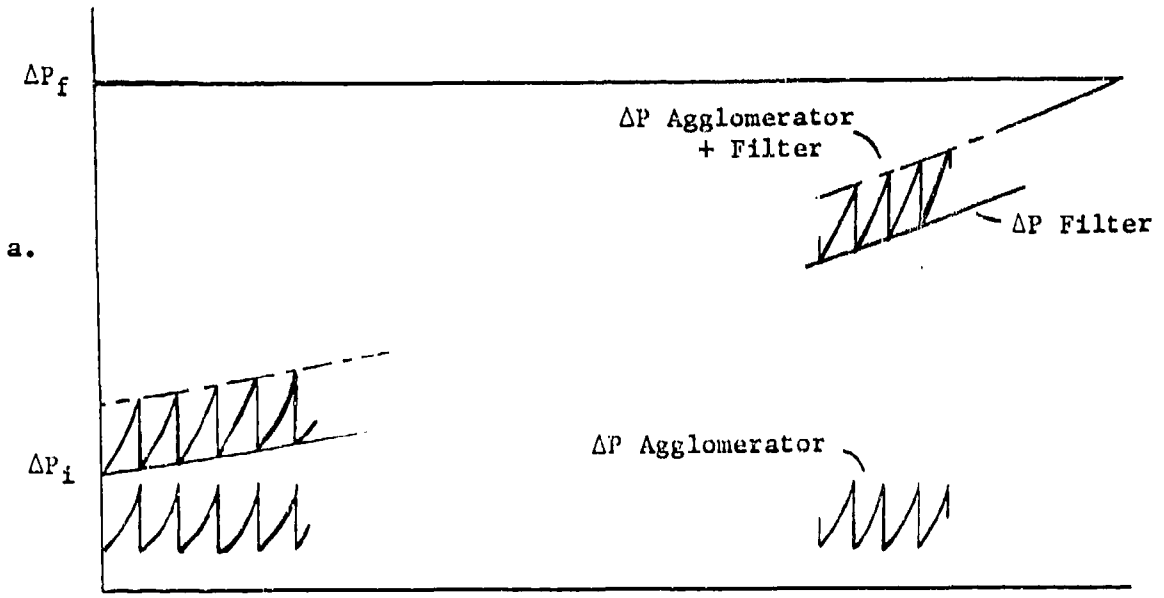

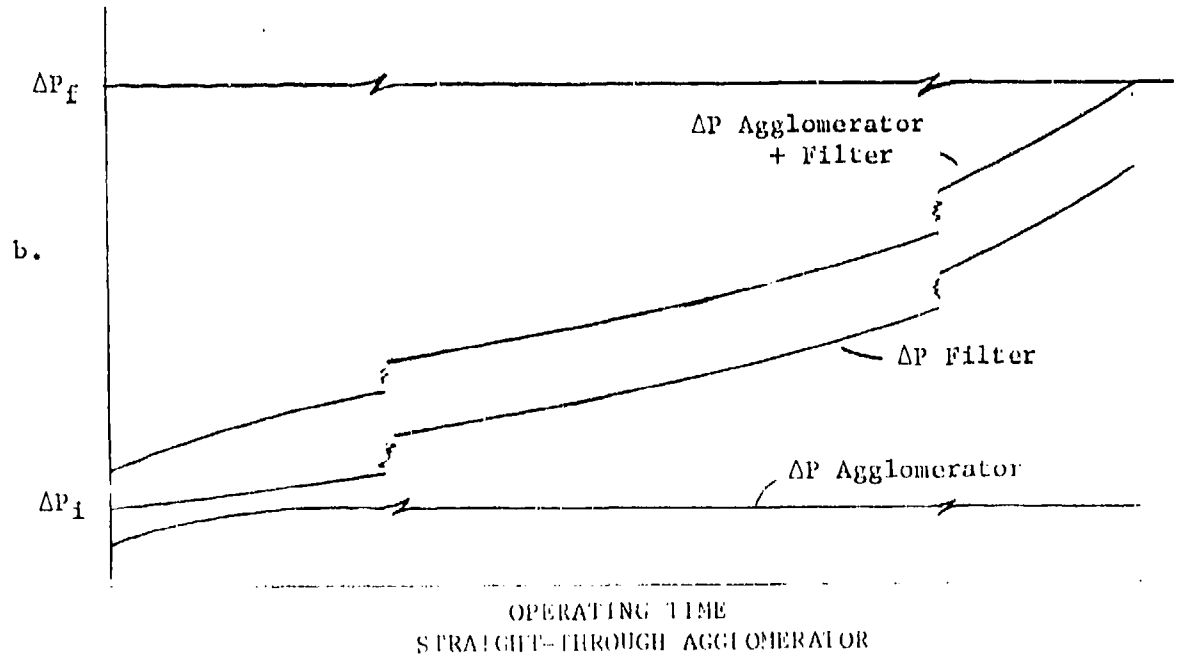

Figure 5-60. Illustration of Precleaner, Agglomerator and Filter Contributions to Pressure Drop as a Function of Time

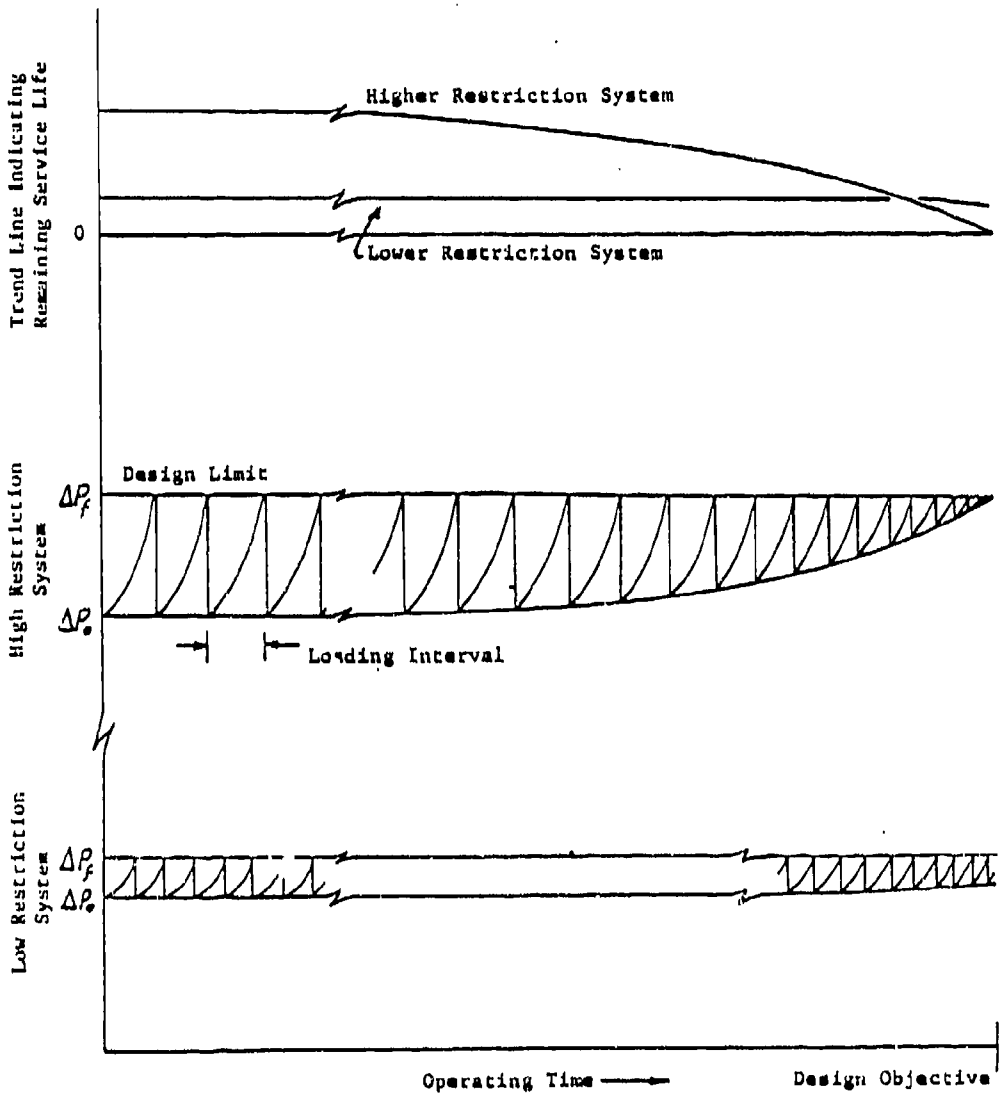

Figure 5-61. Illustration of High Restriction and Low Restriction Surface Agglomerators as a Function of Time

LIST OF REFERENCES

[1] Treuhaft, Martin B. and Wood, Charles D., "Air Cleaner Development," Southwest Research Institute, February 1971, Final Report on Contract DAAE07-70-C-3345

[2] Treuhaft, Martin B., "Study of Fan-Airpump Applicability to Two-Stage Air Cleaner Systems," Southwest Research Institute, June 1985, Final Report on Contract DAAE07-84-C-R045.

[3] Magill, Paul L., "Air Pollution Handbook," McGraw-Hill Book Company, Inc., New York, 1956.

THIS PAGE LEFT BLANK INTENTIONALLY

APPENDIX A

INITIAL RESISTANCE DATA FOR SELECTED CANDIDATE MEDIA

THIS PAGE LEFT BLANK INTENTIONALLY

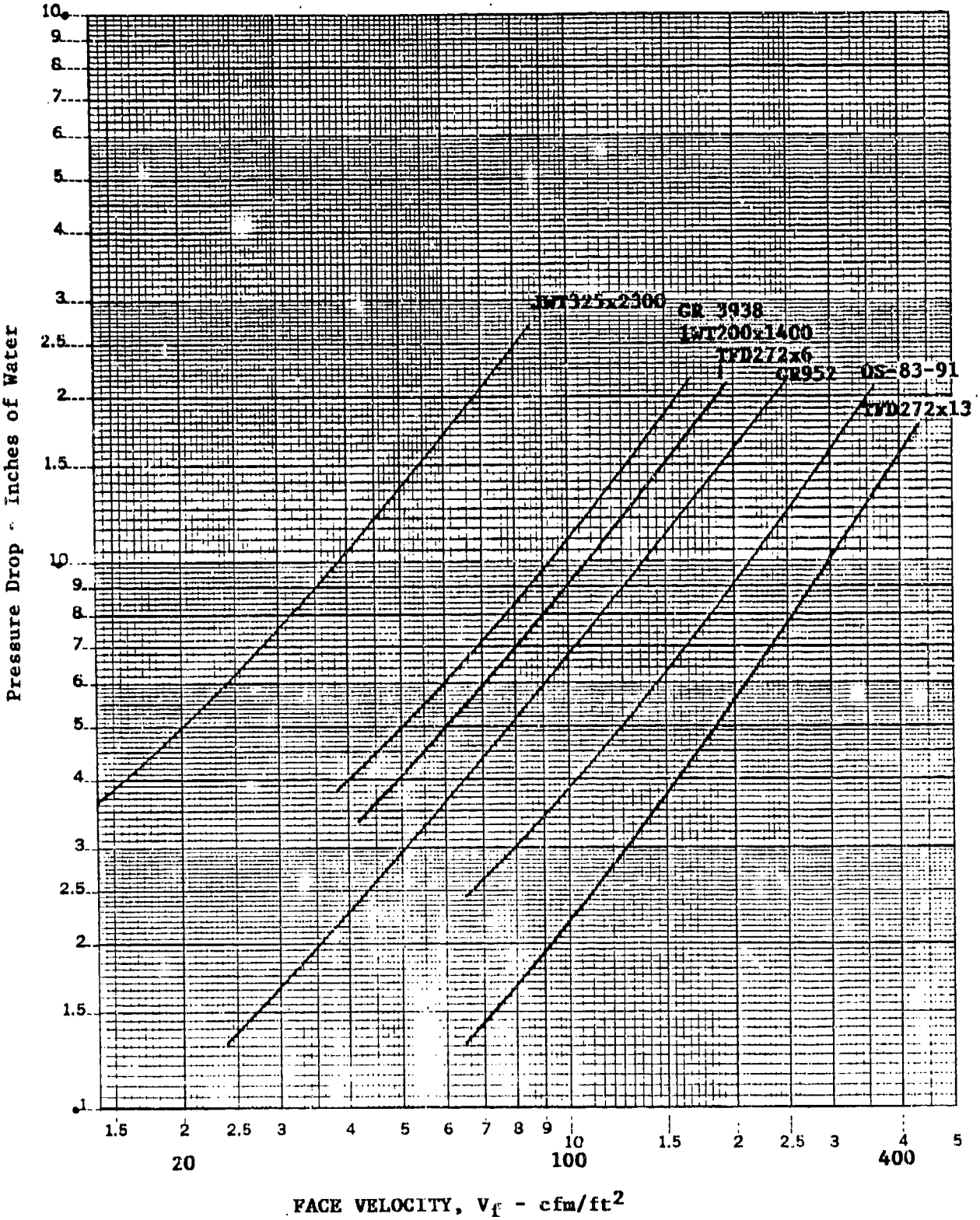

Figure A-1. Pressure Drop vs. Face Velocity for Media in Test Fixture

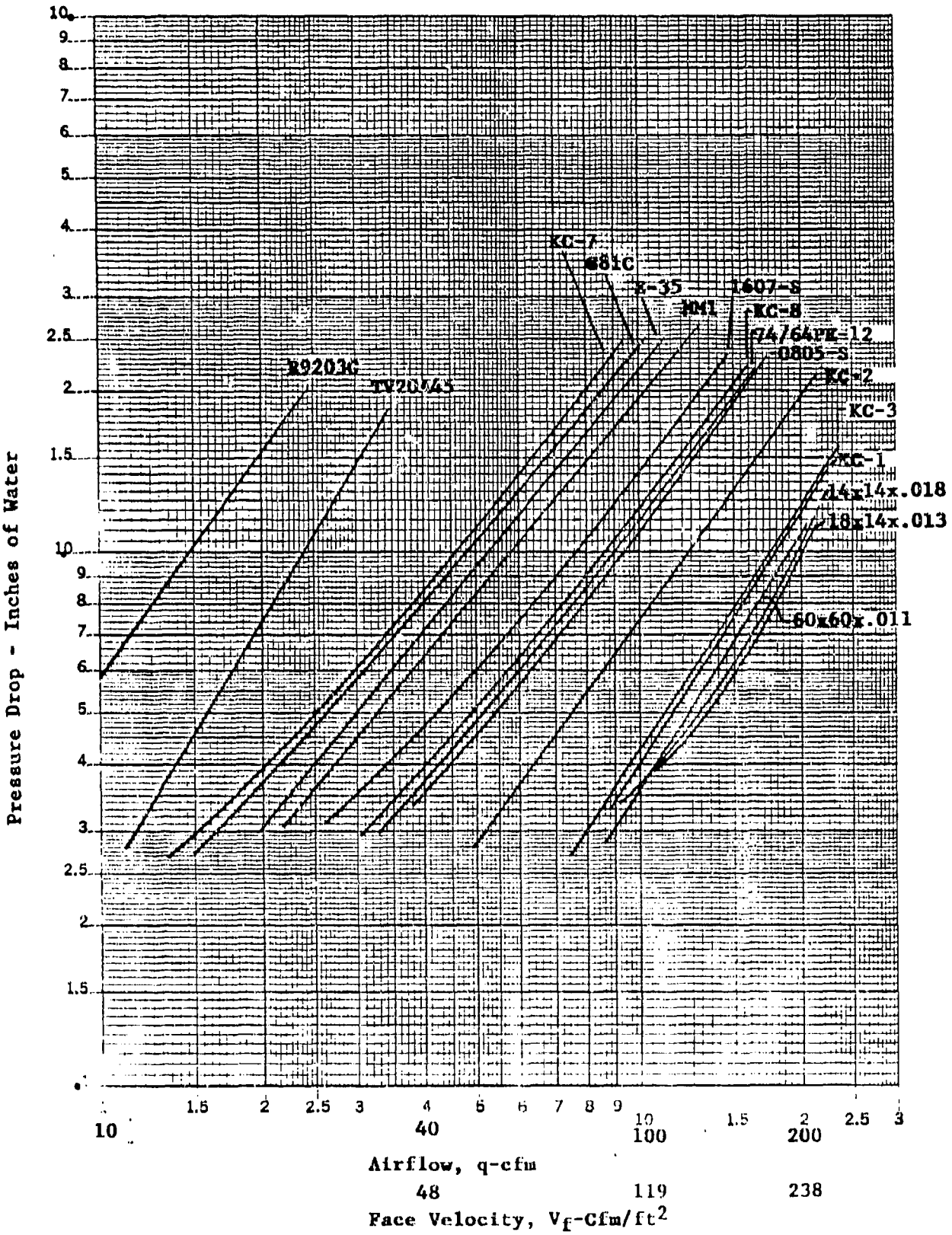

Figure A-2. Pressure Drop vs. Airflow and Face Velocity For Media in Test Fixture

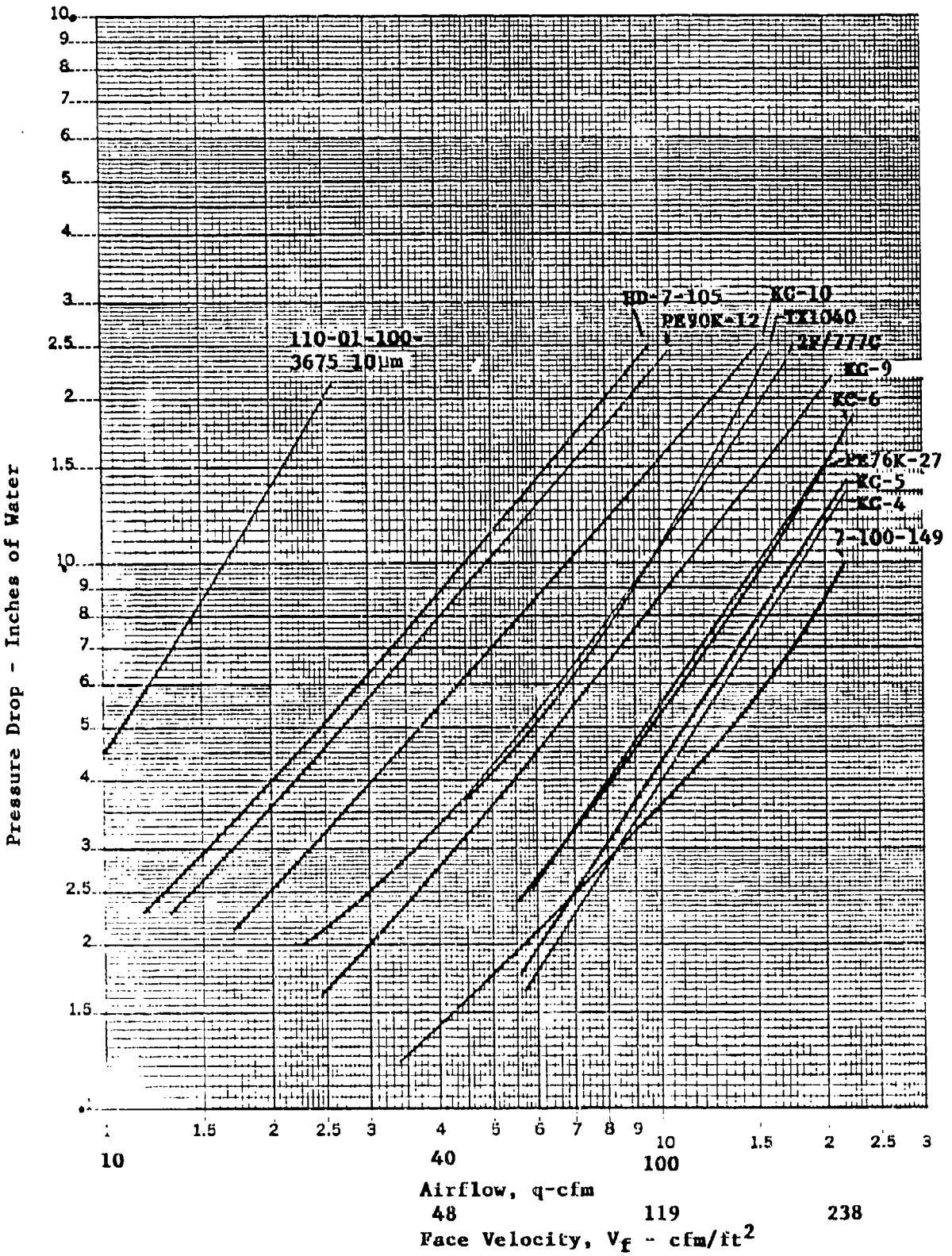

Figure A-3. Pressure Drop vs. Airflow and Face Velocity For Media in Test Fixture

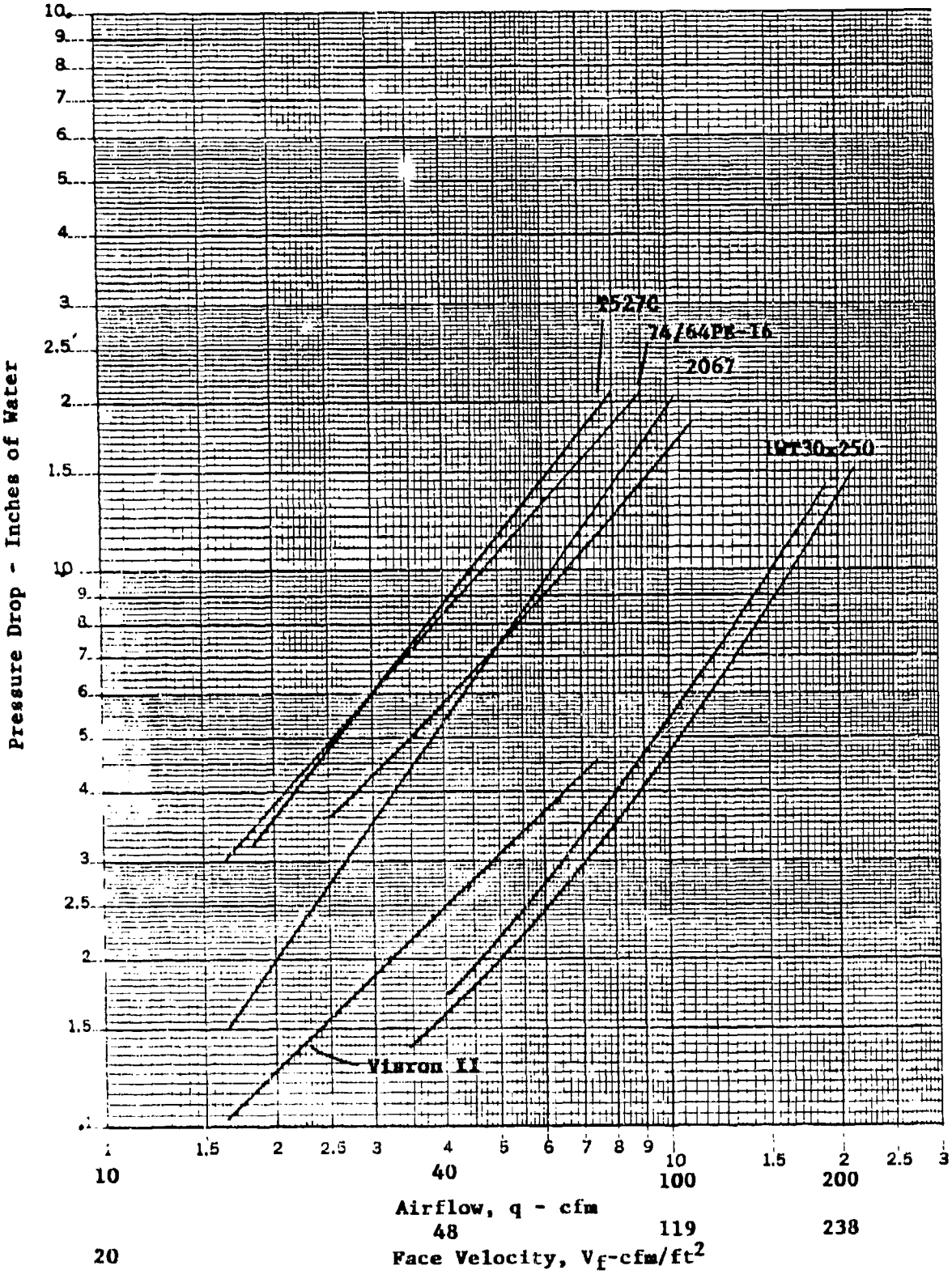

Figure A-4. Pressure Drop vs. Airflow and Face Velocity For Media in Test Fixture

APPENDIX B

REPRESENTATIVE DATA FOR SELECTED CANDIDATE MEDIA

THIS PAGE LEFT BLANK INTENTIONALLY

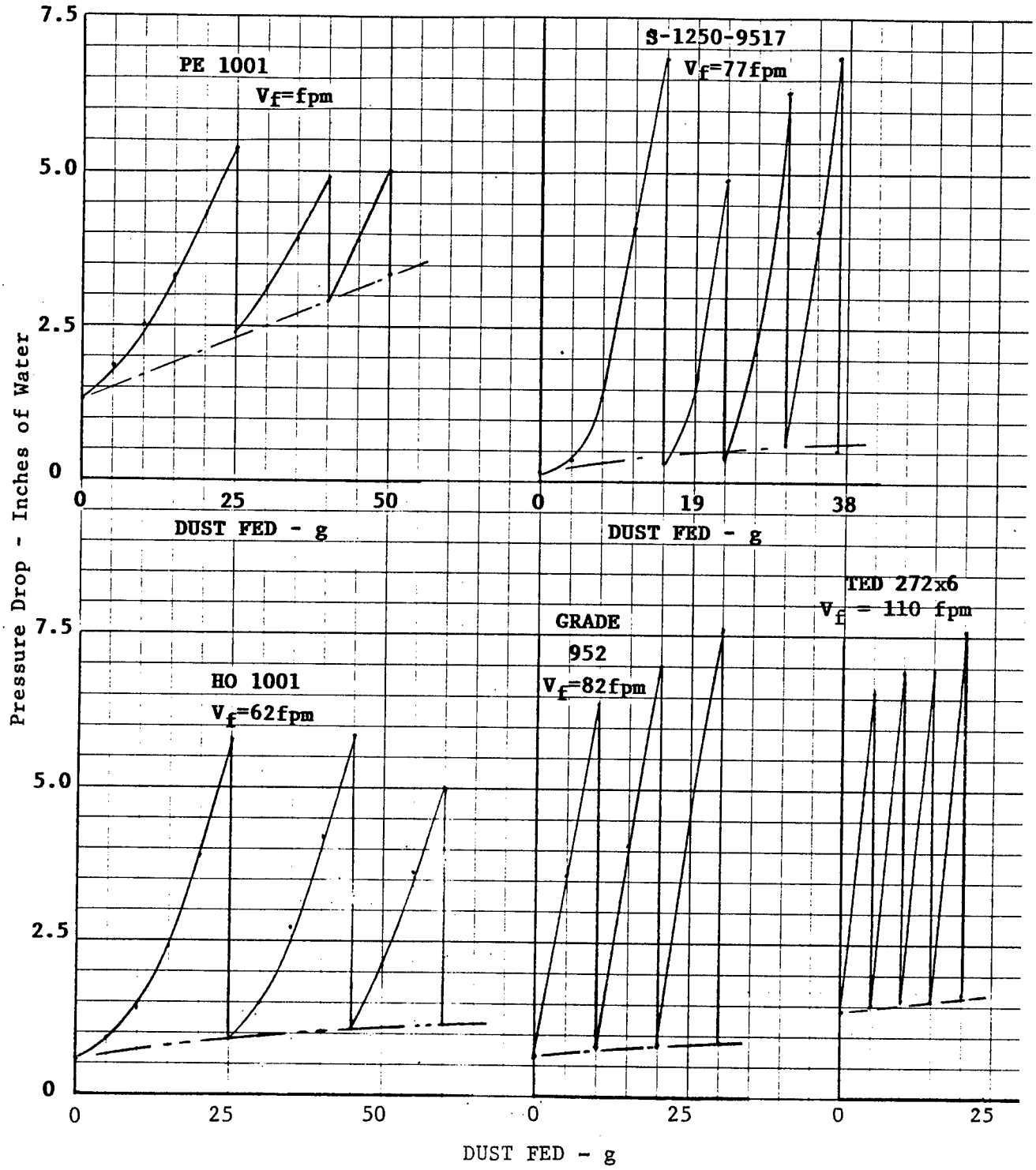

Figure B-1. Agglomerator Pressure Drop Vs. Dust Fed, PE 1001; S-1250-9517; HD1001; G952; and TFD272x6 Media, AC Coarse Dust

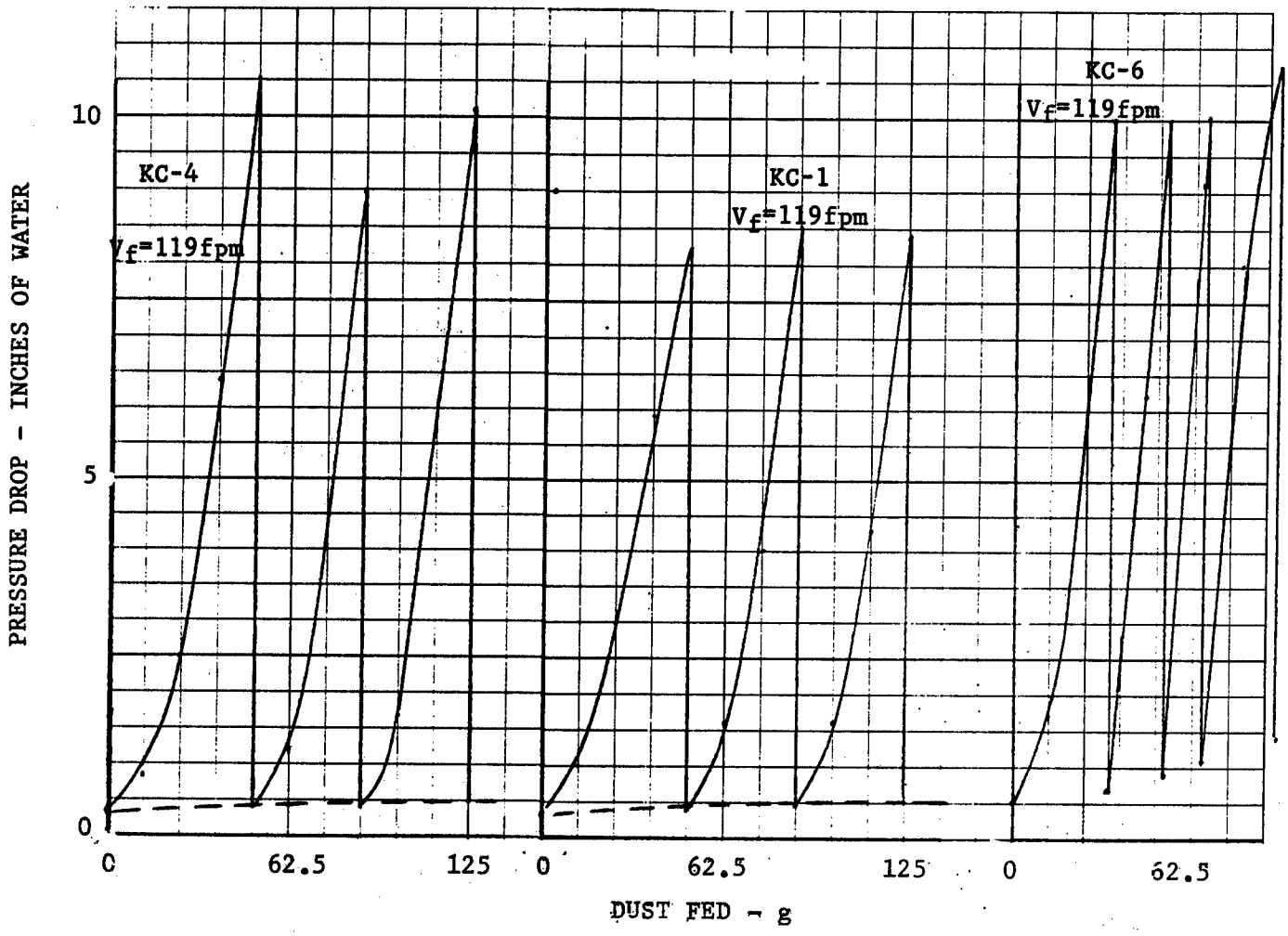

Figure B-2. Agglomerator Pressure vs Dust Fed, KC-1, V_f = 119 fpm, KC-4, V_f = 119 fpm, KC-6, V_f = 119 fpm, AC Coarse dust.

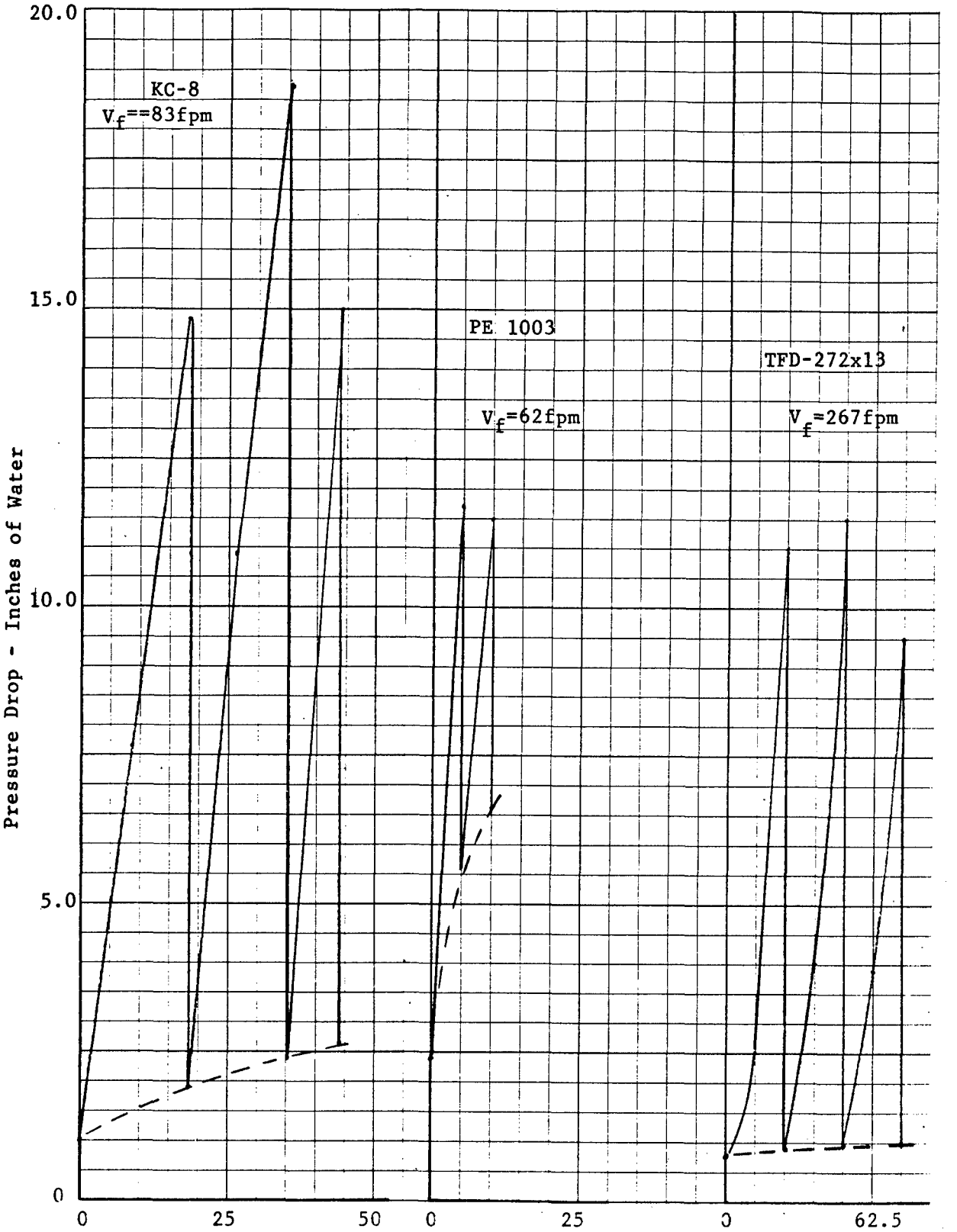

Figure B-3. Agglomerator Pressure vs Dust Fed; KC-8, V_f = 83 fpm; PE1003, V_f = 62 fpm; TFD-272x13, V_f = 267 fpm; AC Coarse dust.

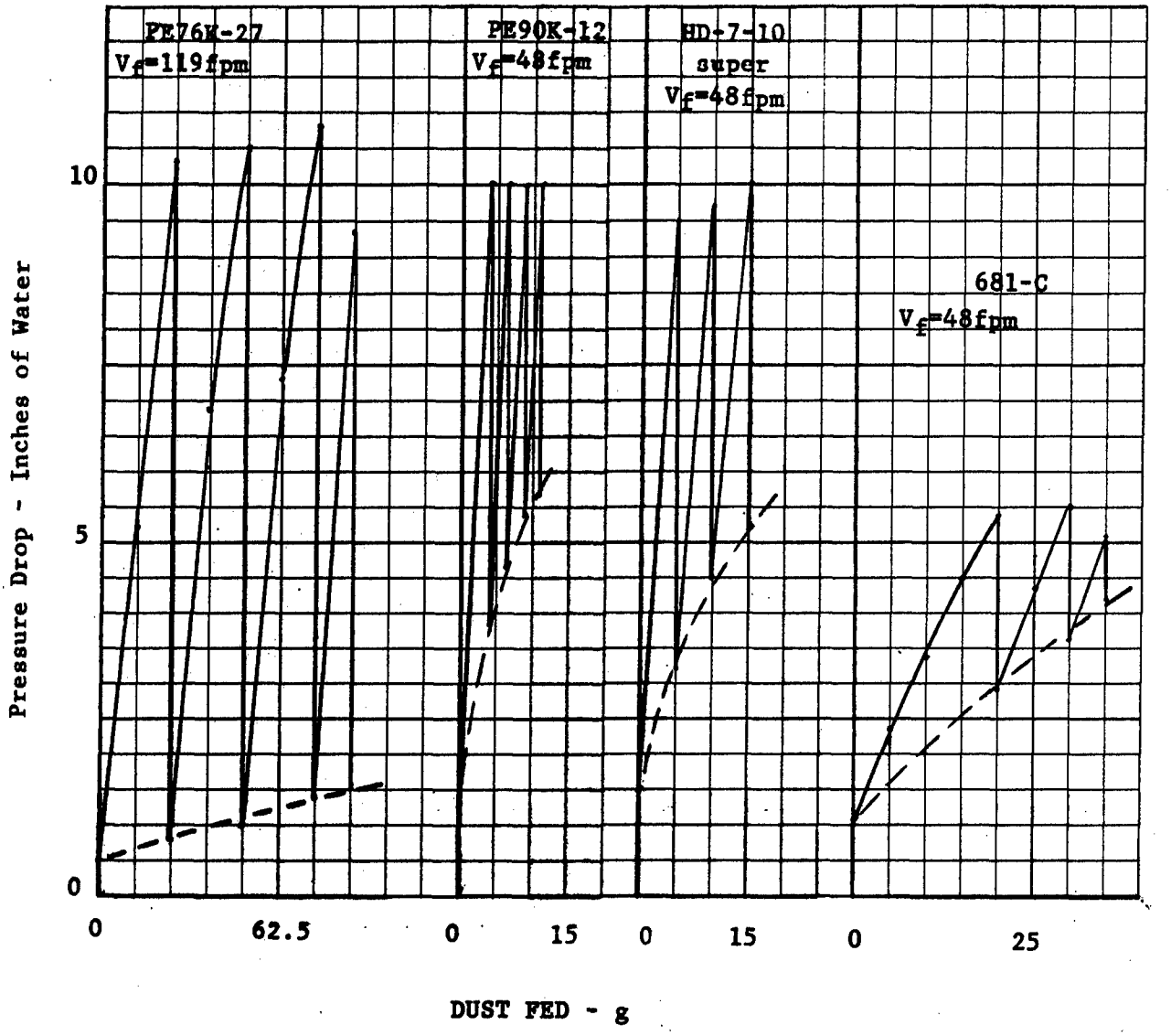

Figure B-4. Agglomerator Pressure vs. Dust Fed, PE76K-27, V_f = 119 fpm; PE90K-12, V_f = 48 fpm; HD-7-10 super, V_f = 48 fpm; 681-C, V_f = 48 fpm, AC Coarse dust.

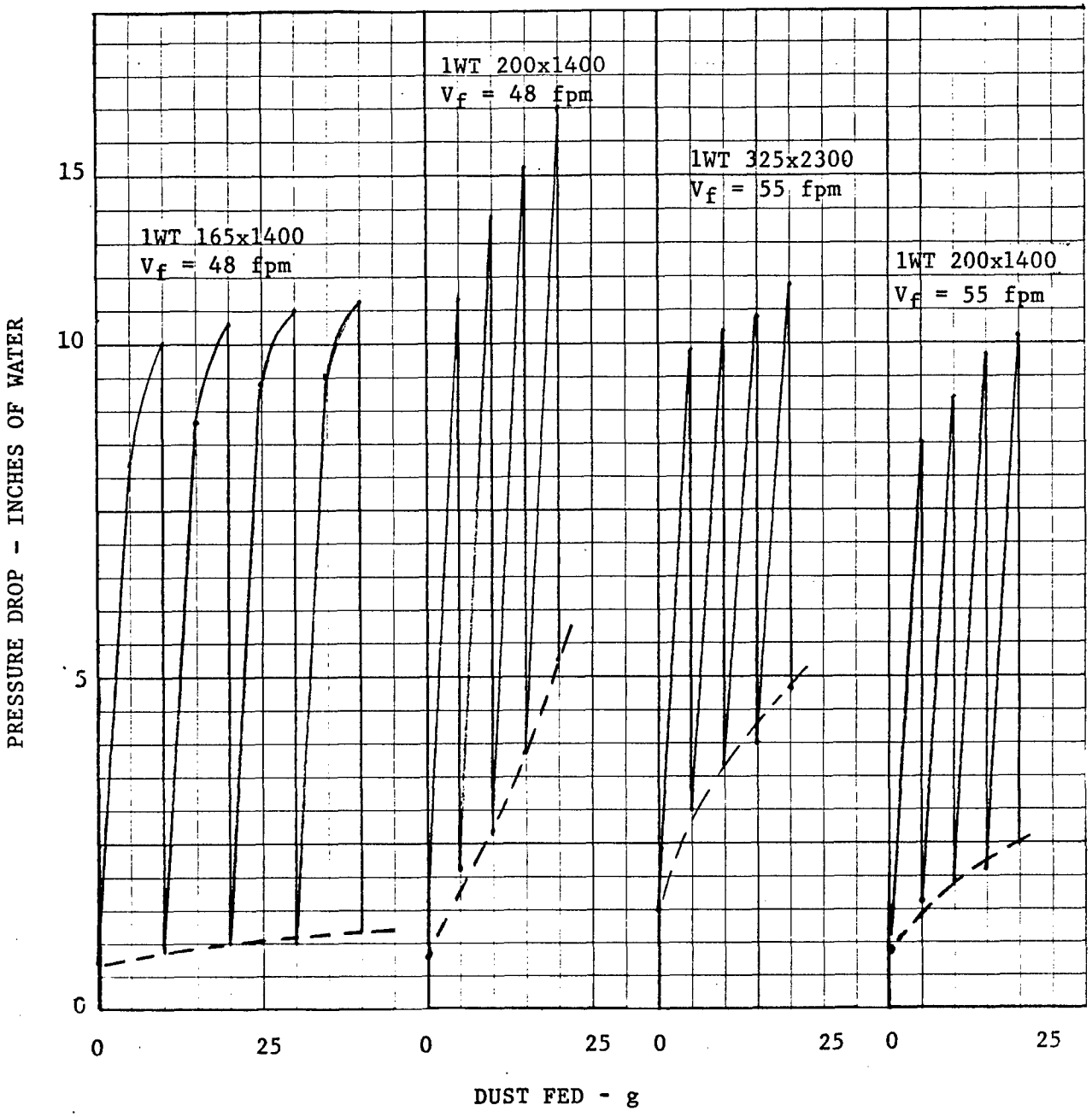

Figure B-5. Agglomerator Pressure Vs. Dust Fed, 1WT 165x1400, V_f = 48 fpm; 1WT 200x1400, V_f = 48 fpm; 1WT 325x2300, V_f = 55 fpm; 1WT 200x1400, V_f = 55 fpm; AC Coarse Dust

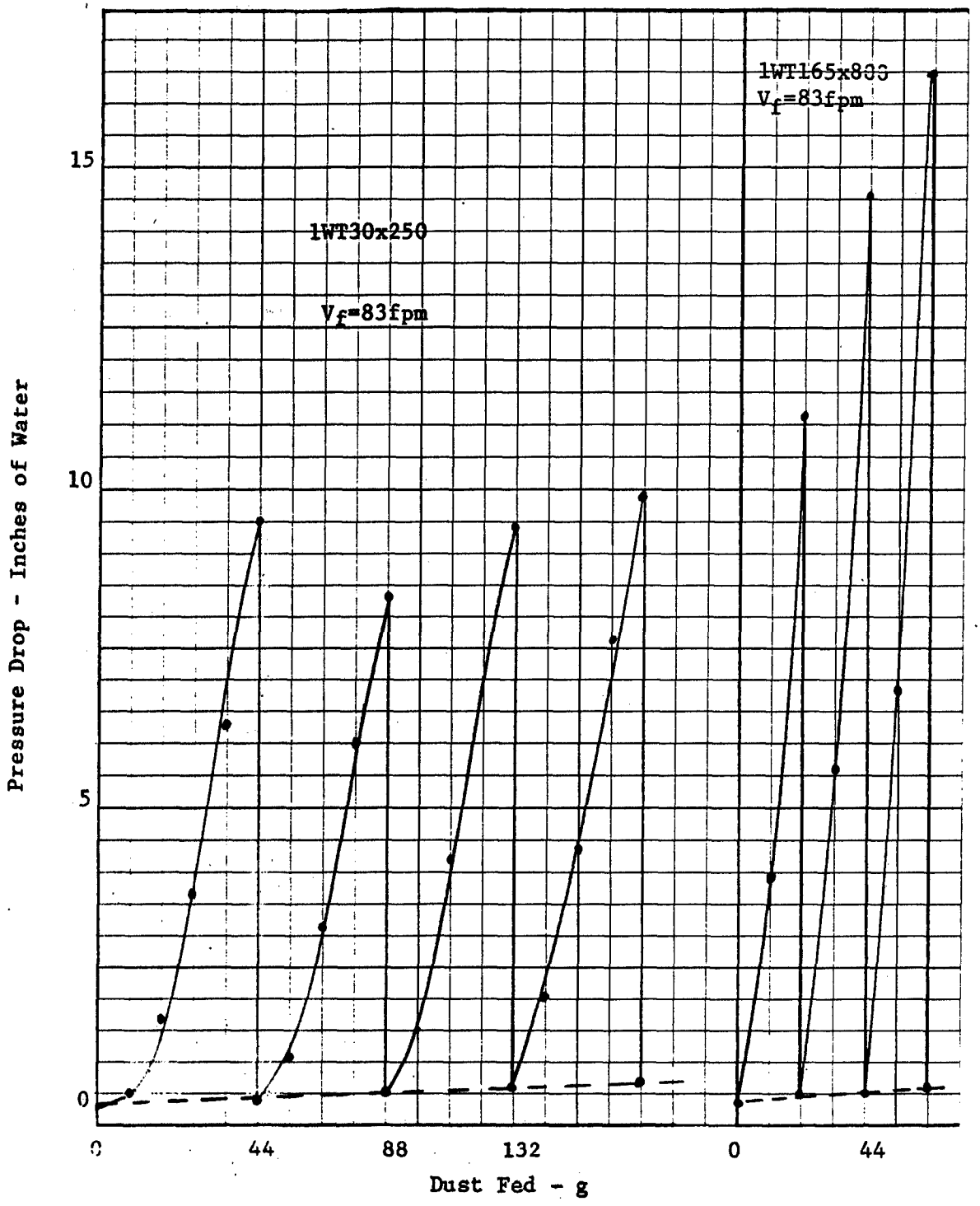

Figure B-6. Agglomerator Pressure vs. Dust Fed, 1WT30x250, V_f = 83 fpm, 1WT165x800, V_f = 83 fpm, AC Coarse dust.

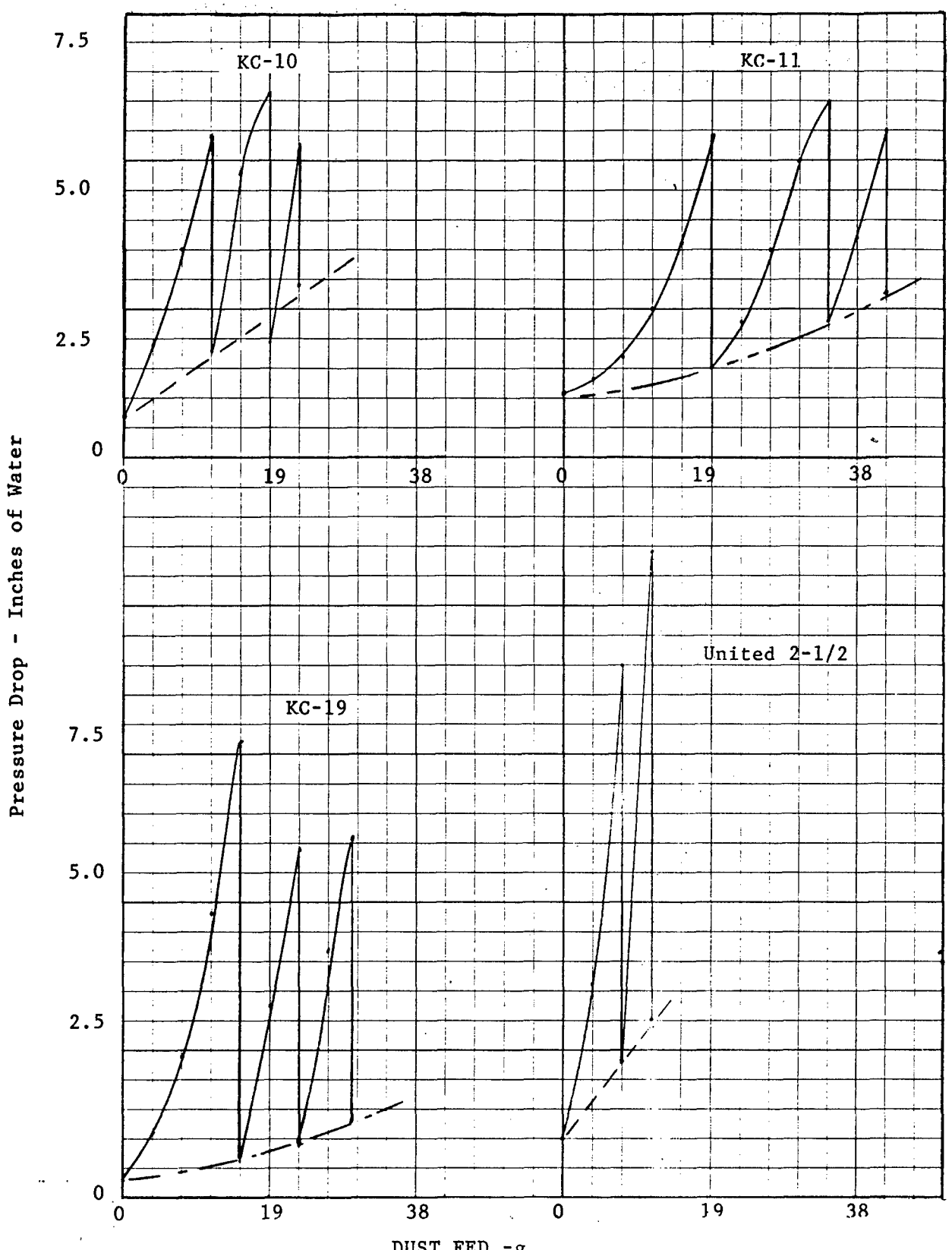

Figure B-7. Agglomerator Pressure vs Dust fed, KC-9, KC-10, KC-11 and United 2-1/2 media, V_f = 36 fpm, AC Coarse dust.

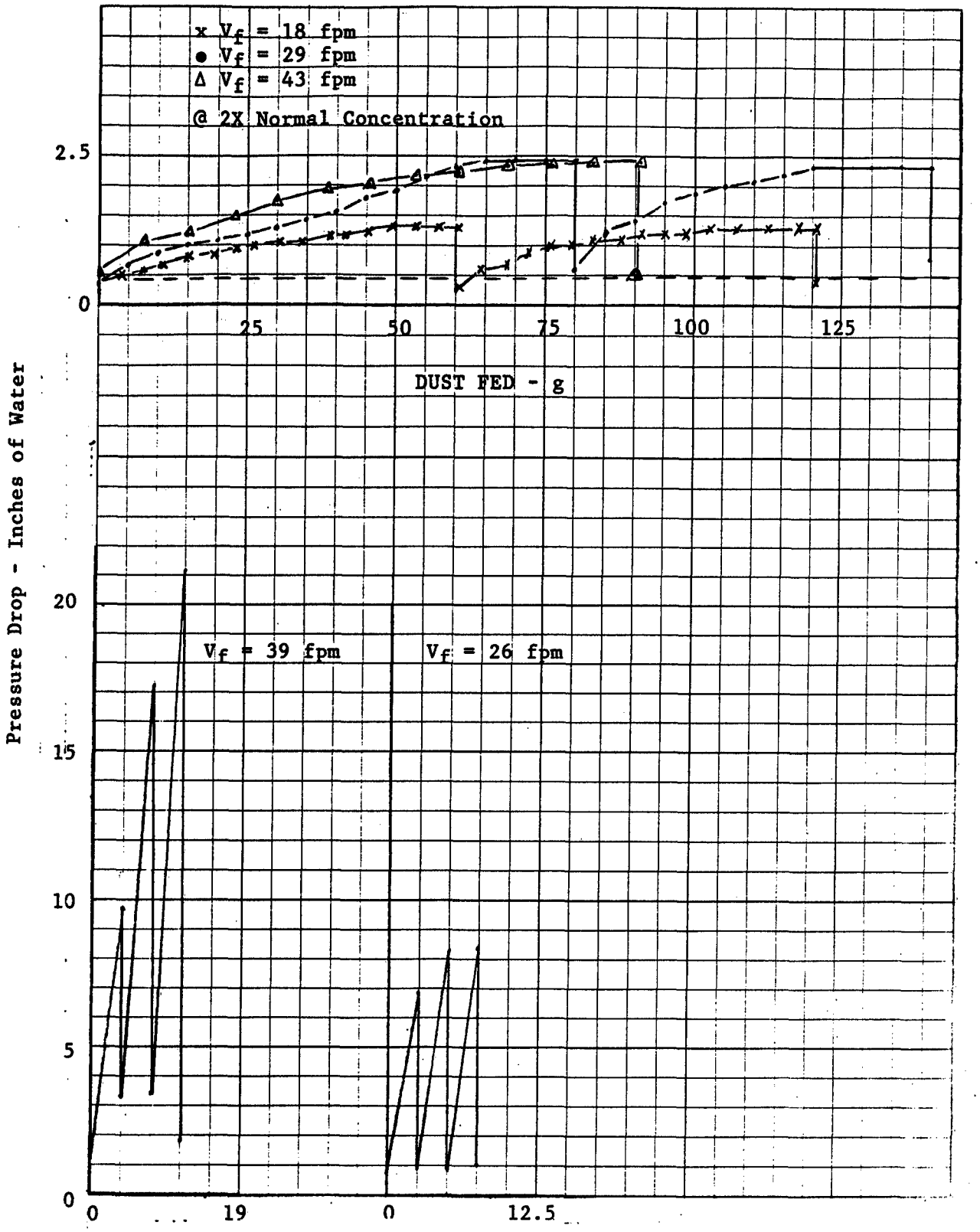

Figure B-8. Agglomerator Pressure Drop Vs. Dust Fed, BP 312 Media, AC Coarse Dust

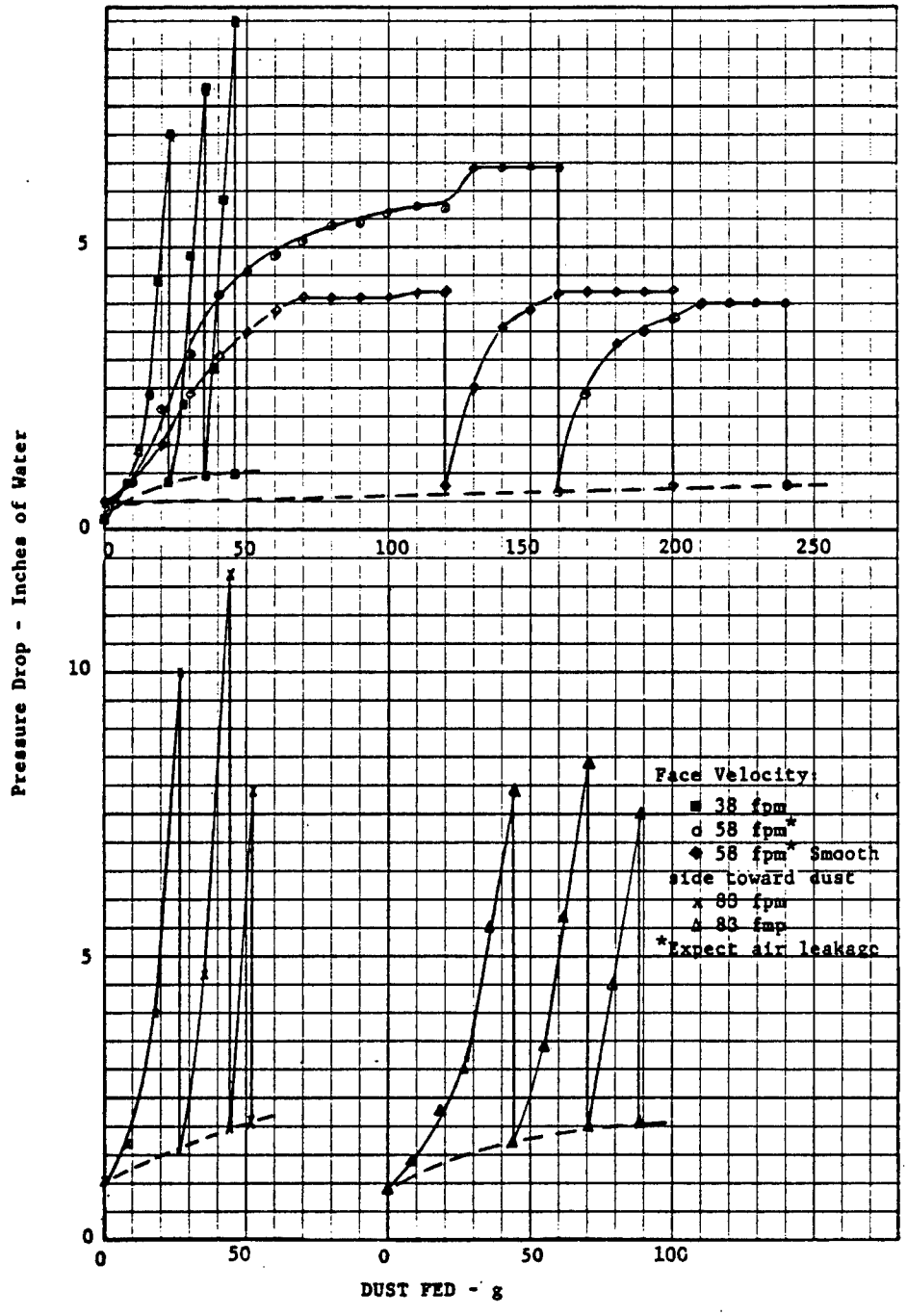

Figure B-9. Agglomerator Pressure Drop Vs. Dust Fed, 805-9 Media, AC Coarse Dust

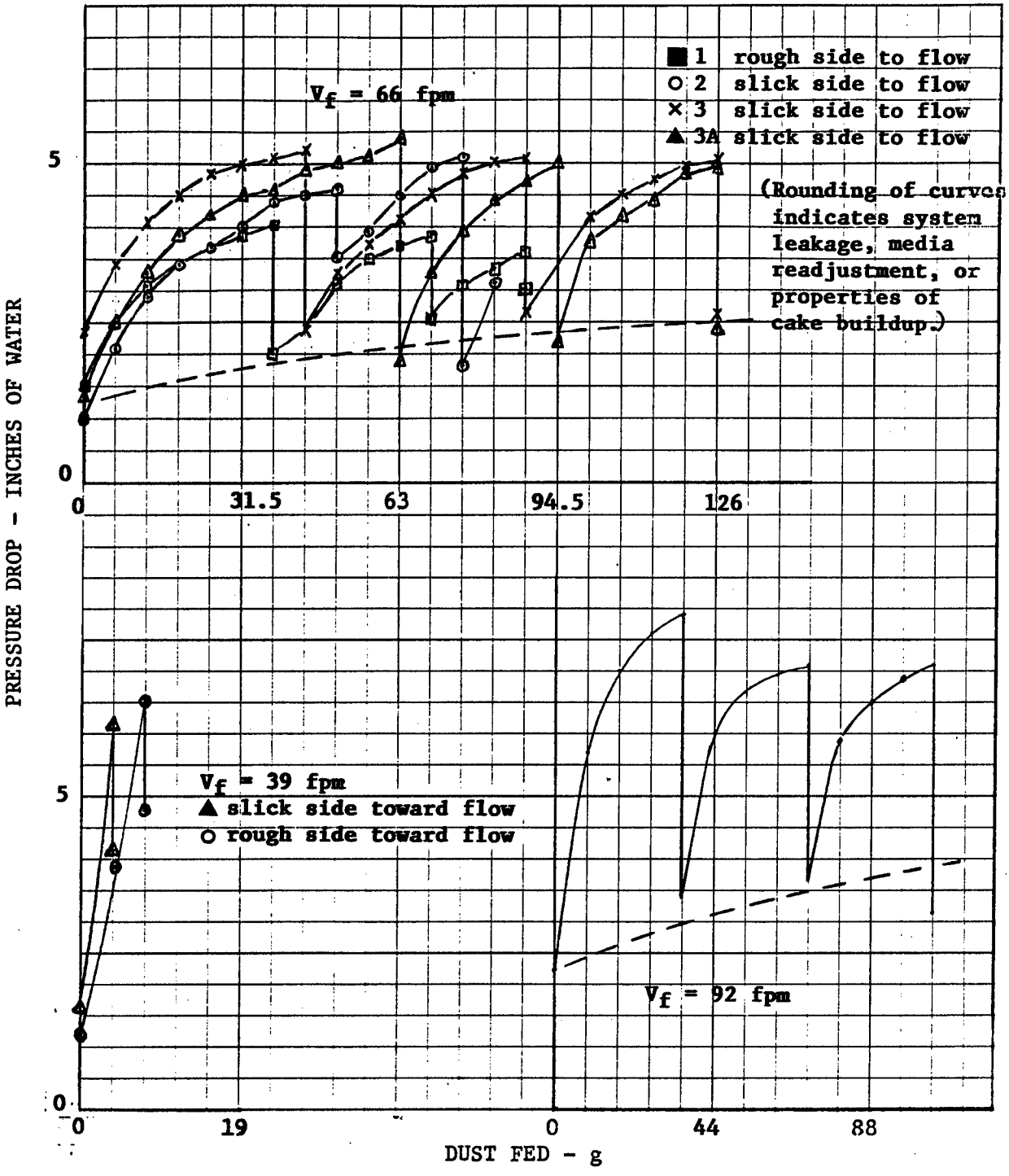

Figure B-10. Agglomerator Pressure Drop Vs. Dust Fed, V_f = 39 to 92 fpm, Gore Tex 3 oz., AC Coarse Dust

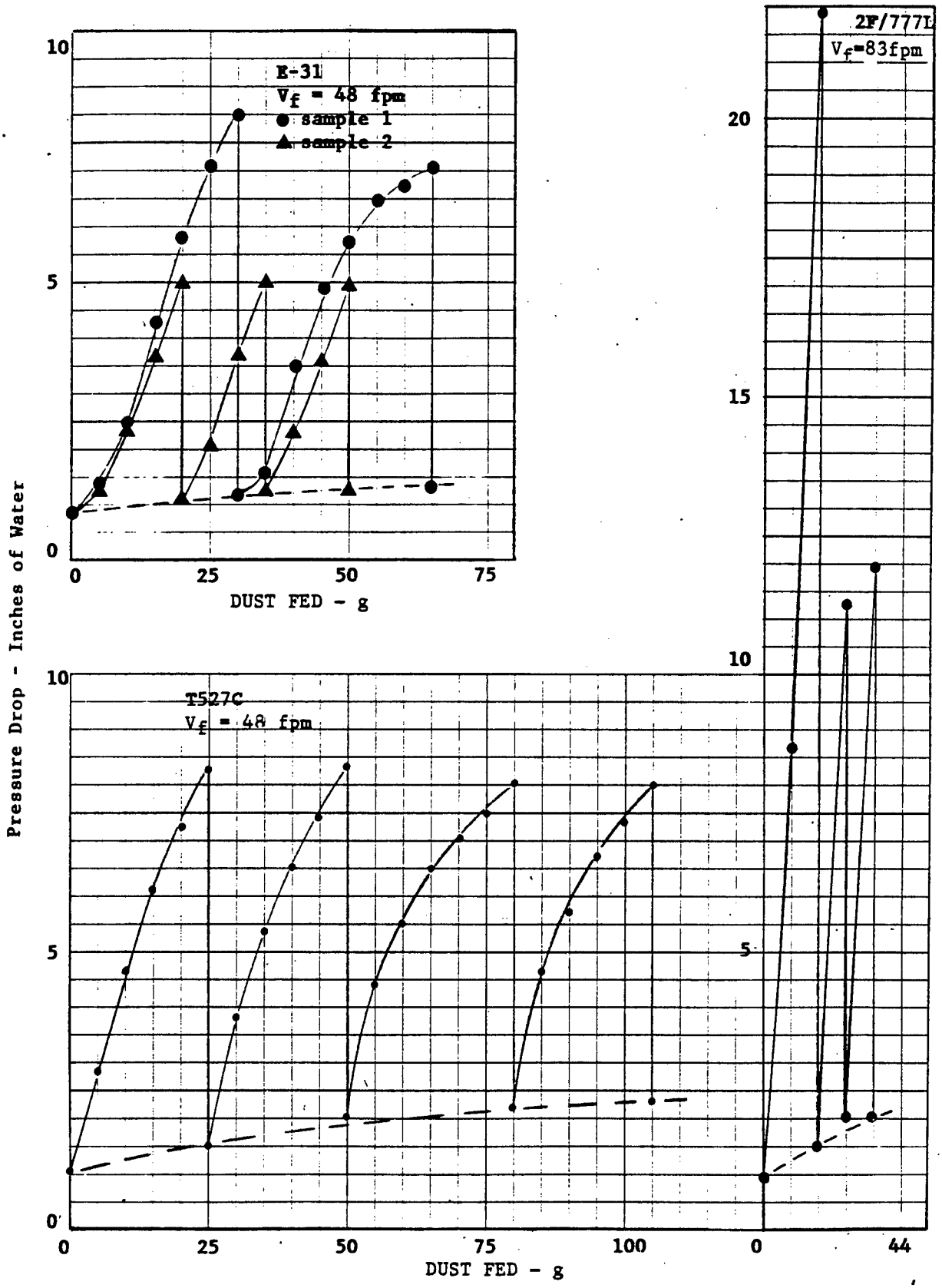

Figure B-11. Agglomerator Pressure Drop Vs. Dust Fed, E-31, 2F/777L, and T527C Media, AC Coarse Dust

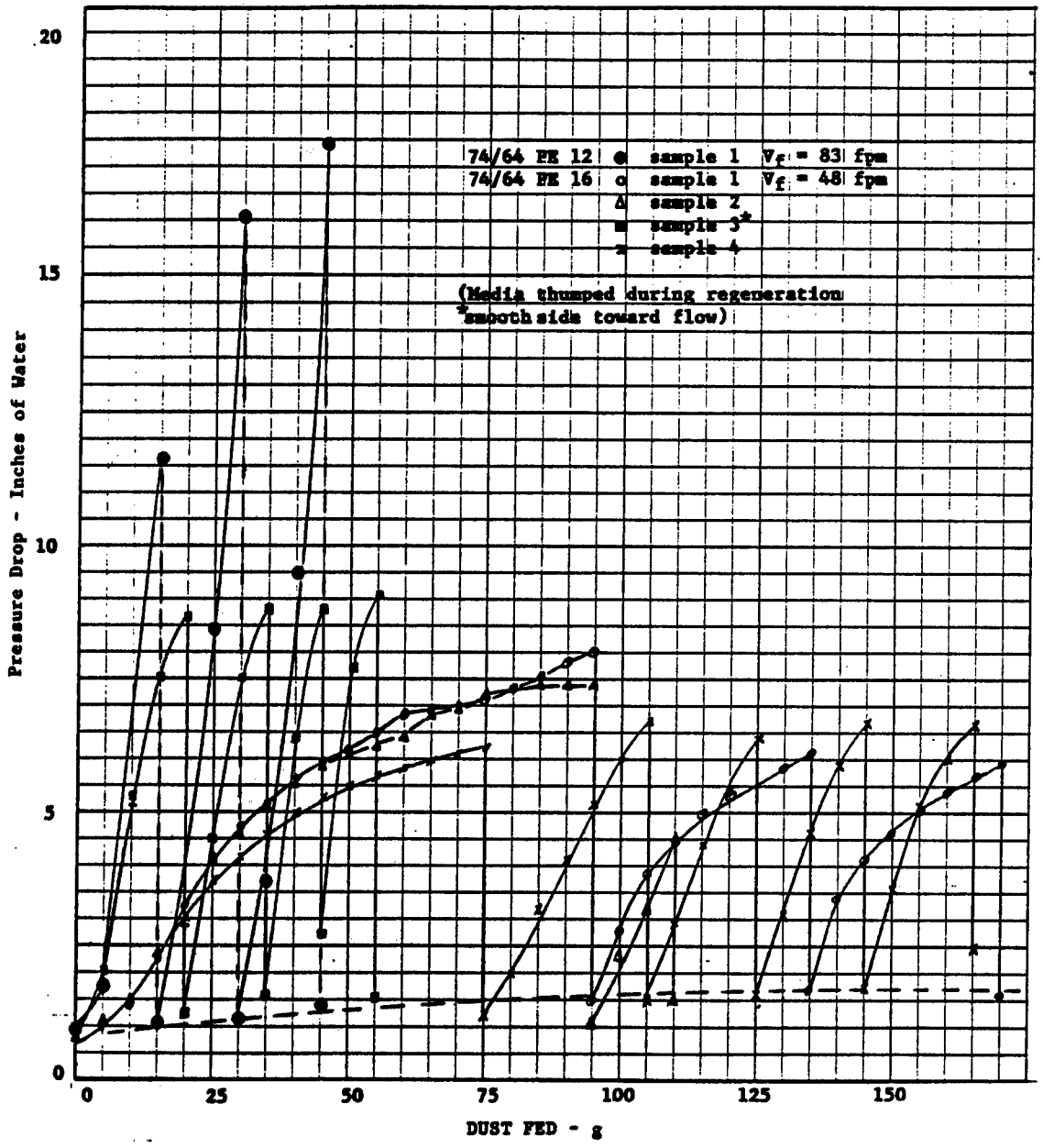

Figure B-12. Agglomerator Pressure Drop Vs. Dust Fed, 74/64PE12 and 74/64PE16 Media, AC Coarse Dust

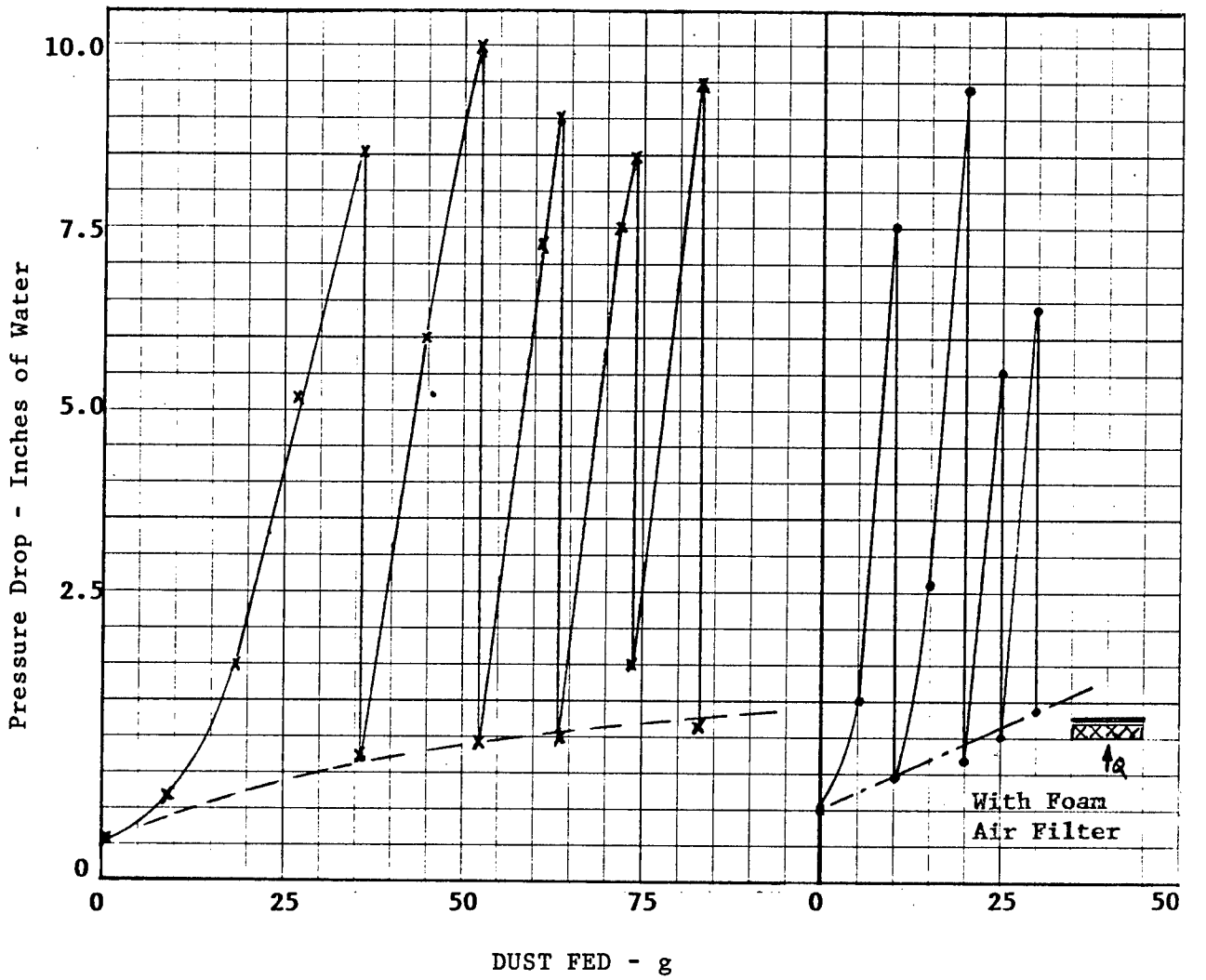

Figure B-13. Agglomerator Pressure Drop vs Dust Fed, JR347, AC Coarse dust.

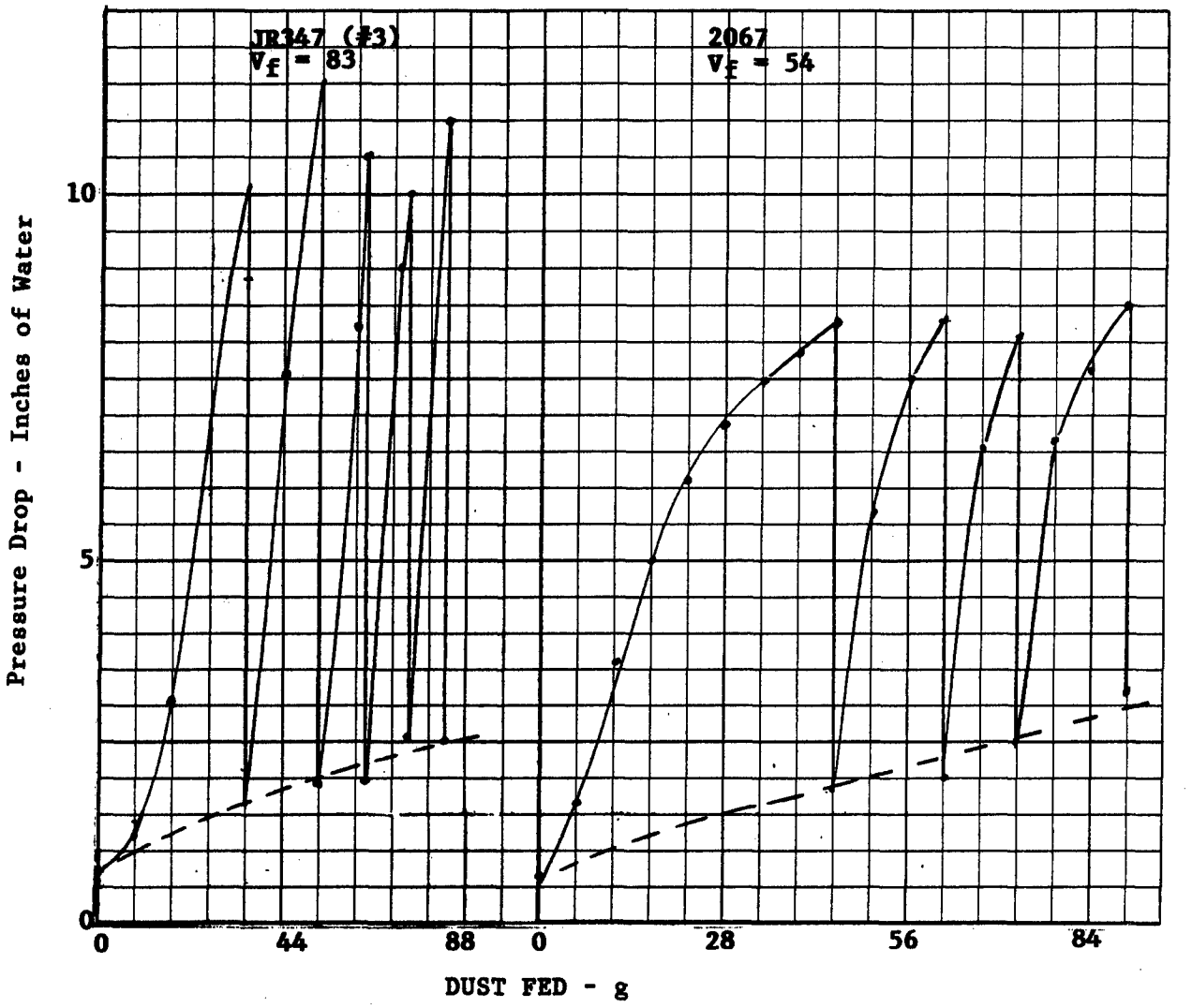

Figure B-14. Agglomerator Pressure Drop vs Dust Fed, JR347 (#3), V_f = 83, 2067, V_f = 54, AC Coarse dust.

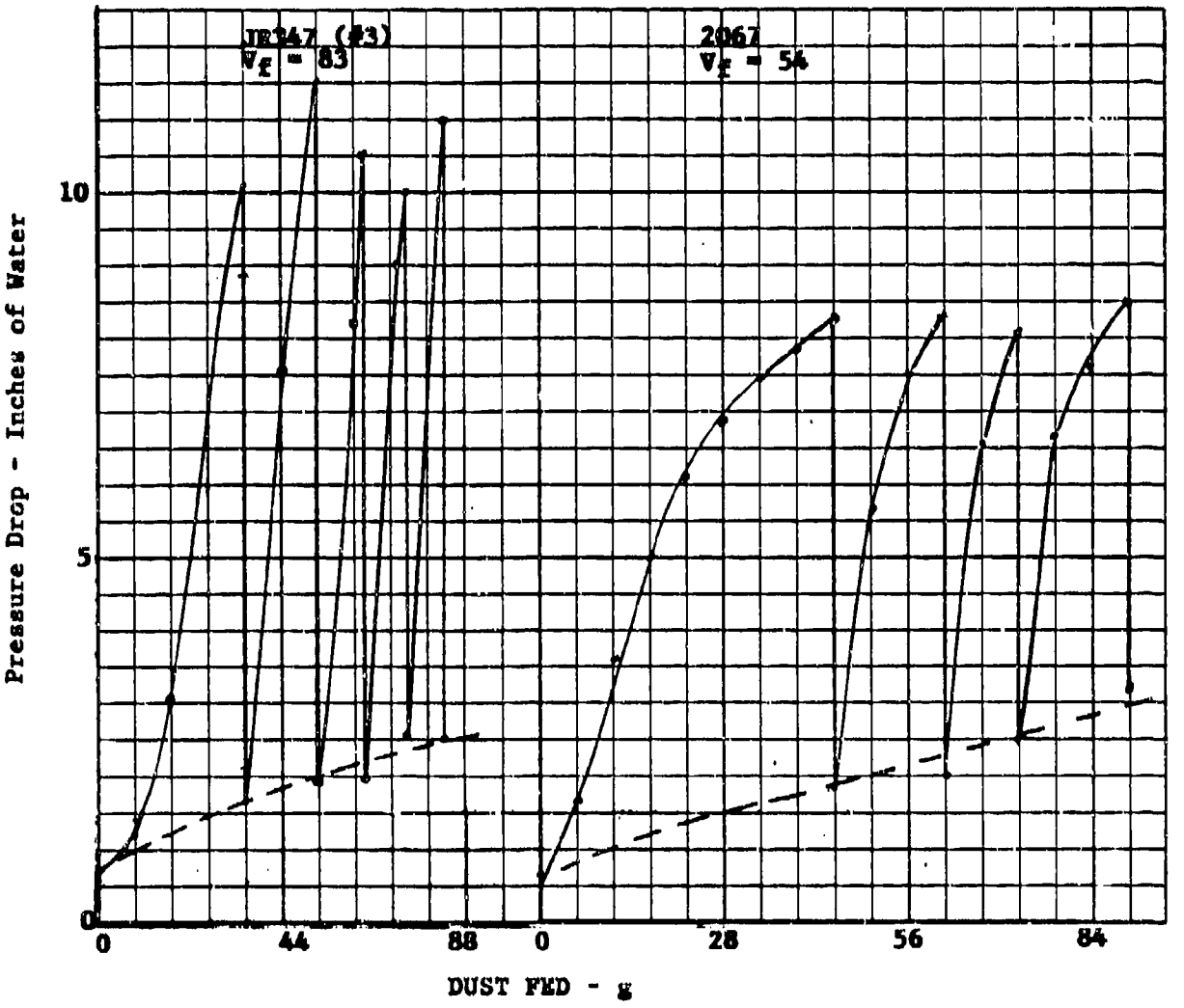

Figure B-14. Agglomerator Pressure Drop vs Dust Fed, JR347 (#3), V_f = 83, 2067, V_f = 54, AC Coarse dust.

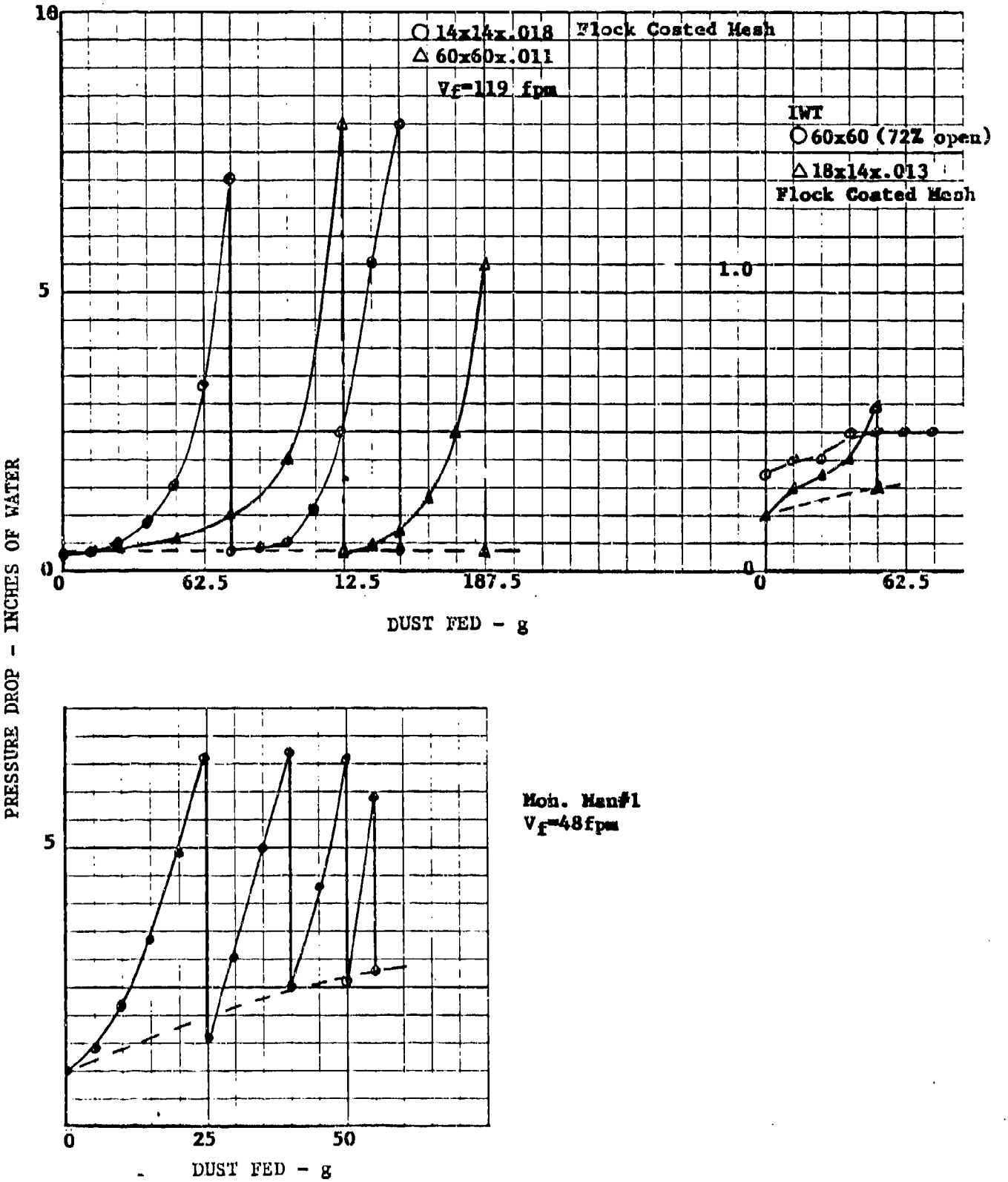

Figure B-15. Agglomerator Pressure Drop Vs. Dust Fed, 14x14x.018, 60x60x.011, 1WT 60x60 (72% open), 18x14x.013 Flock Coated Mesh, Mon. Man #1, AC Coarse Dust

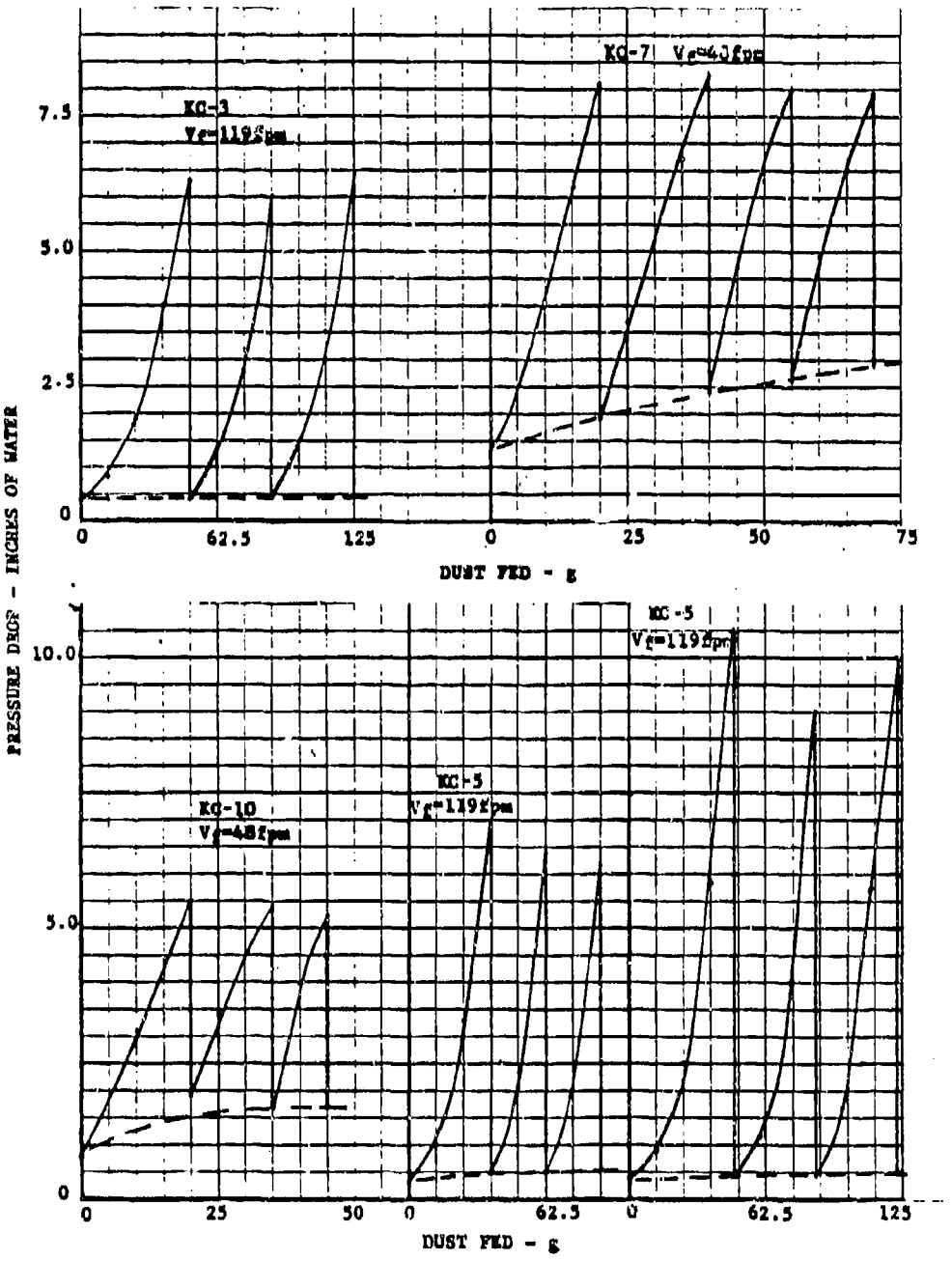

Figure B-16. Agglomerator Pressure Drop Vs. Dust Fed, KC-3, KC-5, KC-7, KC-10 Media, AC Coarse Dust

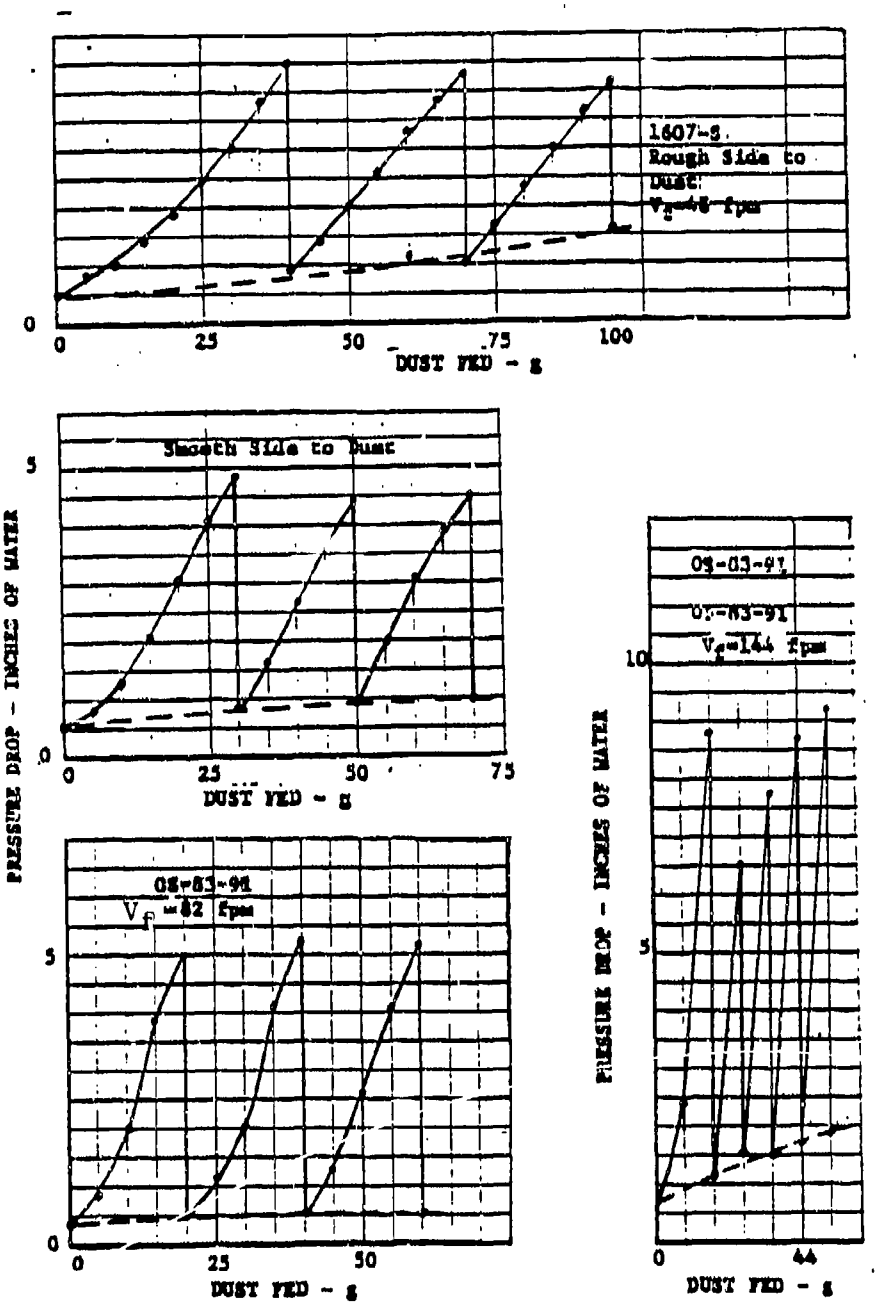

Figure B-17. Agglomerator Pressure Drop Vs. Dust Fed, 1607-S and OS-83-91 Media, AC Coarse Dust

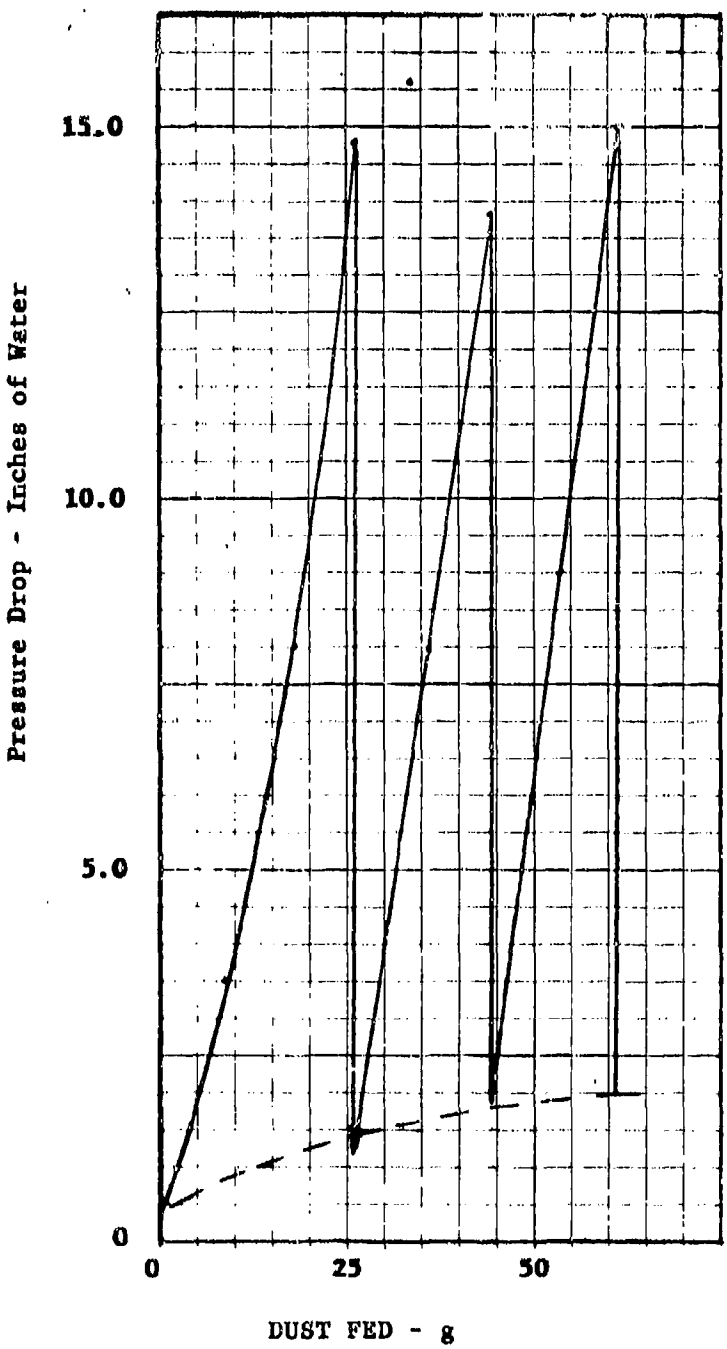

Figure B-18. Agglomerator Pressure Drop vs Dust Fed, KC-9 , V_f = 83 fpm, AC Coarse dust.

APPENDIX C

LIST OF CANDIDATE MEDIA

THIS PAGE LEFT BLANK INTENTIONALLY

List of Candidate Media

Media Code	Description	Manufacturer
KC-1	1.25 oz 5B sq pin	Kimberly-Clark
KC-2	3.5 oz 5B hopsack	Kimberly-Clark
KC-3	1.5 oz 5B sq pin	Kimberly-Clark
KC-4	1.5 oz 5B hopsack	Kimberly-Clark
KC-5	1.5 oz 5B RHT	Kimberly-Clark
KC-6	2.0 oz 5B sq pin	Kimberly-Clark
KC-7	2.5 oz SMS RHT	Kimberly-Clark
KC-8	1.5 oz SMS RHT	Kimberly-Clark
KC-9	1.5 oz SM RHT	Kimberly-Clark
KC-10	2.1 oz SM RHT	Kimberly-Clark
KC-11	4.2 oz SMS ex sq pin	Kimberly-Clark
BP-312	Starch bound pulp	Kimberly-Clark
BP-315	Latex saturated pulp	Kimberly-Clark
2067	HD Air Media, 95#/3k sq ft	Hollingsworth & Vose
JR-347		James River
JR-347FC	w/ fluorocarbon treatment	James River
1WT325X2300	Wire mesh laminate, 72% open, 2μm	Michigan Dynamics
1WT200X1400	Wire mesh laminate, 72% open, 5μm	Michigan Dynamics
1WT165X1400	Wire mesh laminate, 72% open, 10μm	Michigan Dynamics
1WT165X800	Wire mesh laminate, 72% open, 15μm	Michigan Dynamics
1WT30X250	Wire mesh laminate, 72% open, 69μm	Michigan Dynamics
1WT60X60	Wire mesh laminate, 72% open, 144 μm	Michigan Dynamics
T527C		Pallflex
TV20A45		Pallflex
R9230G		Pallflex
TX1040		Pallflex
74/64PE12		American Felt & Filter
74/64PE16		American Felt & Filter
PE1001	Polyester/surf coat, 16 oz/sq yd	Fiber-Taxis
PE1003	Polyester/surf coat, 8 oz/sq yd	Fiber-Taxis
HO1001	Homopolymer/surf coat, 16 oz/sq yd	Fiber-Taxis
S-1250-9517	Viskon II, 2.85 oz/sq yd, 12μm	Snow

List of Candidate Media (Continued)

Media Code	Description	Manufacturer
PE90K-12	Polyester	Tetko
PE76K-27	Polyester	Tetko
2F/777C	Polyester	Tetko
HD-7-10S	Nitex	Tetko
E35	Polypropylene	Technical Fabricators
681-C	Polyester w/acrylic coating, 5 oz/sq yd	Performance Media
1607-S	Fiberglass needle, 27 oz/sq yd	Huyck Felt
0805-S	Fiberglass needle, 16 oz/sq yd	Huyck Felt
U 2.5	2½-ton truck filter media	United Air Cleaner
GT3	Goretex membrane/3 oz SB	W.L. Gore & Associates
TFD 272X6	Dynalloy	Brunswick
TFD 272X13		Brunswick
GR 952		Dexter
GR3938		Dexter
14X14X.018	Flock-coated mesh	Robko
18X14X.0134		Robko
20X20X.011		Robko
MM1	1/8-inch foam media	Monitor Manufacturing
110-01-100-3675	10 μm porous metal sheet	Mott Metallurgical
0S-83-91		

Depth Media

Meshes	Kimre
Beads	PPG and Kaiser
Foam	Scott

DISTRIBUTION LIST

	Copies
Commander U.S. Army Tank-Automotive Command ATTN: DRSTA-RGT Warren, MI 48397-5000	10
Commander U.S. Army tank-Automotive Command ATTN: AMSTA-TSL (Technical Library) Warren, MI 48397-5000	2
Commander U.S. Army Tank-Automotive Command ATTN: AMSTA-CV (Col. Burke) Warren, MI 48397-5000	1
Commander Defense Technical Information Center Bldg. 5, Cameron Station ATTN: DDAC Alexandria, VA 22314	12
Manager Defense Logistics Studies Information Exchange ATTN: AMXMC-D Fort Lee, VA 23801-6044	2
Director Army Materiel systems Analysis Activity ATTN: AMXSY-MP Aberdeen Proving Ground, MD 21005-5071	1
DCASMA 615 East Houston Street San Antonio, TX 78294	1